Transport impacts on atmosphere and climate: Shipping

Veronika Eyring [a,*], Ivar S.A. Isaksen [b], Terje Berntsen [c], William J. Collins [d], James J. Corbett [e], Oyvind Endresen [f], Roy G. Grainger [g], Jana Moldanova [h], Hans Schlager [a], David S. Stevenson [i]

[a] Deutsches Zentrum für Luft- und Raumfahrt, Institut für Physik der Atmosphäre, Oberpfaffenhofen, 82234 Wessling, Germany
[b] University of Oslo, Department of Geosciences, Oslo, Norway
[c] Cicero, Oslo, Norway
[d] Met Office Hadley Centre, Exeter, UK
[e] College of Marine & Earth Studies, University of Delaware, Newark, DE, USA
[f] Det Norske Veritas, Høvik, Norway
[g] Atmospheric, Oceanic & Planetary Physics, Clarendon Laboratory, Oxford, UK
[h] IVL, Swedish Environmental Research Institute, Göteborg, Sweden
[i] University of Edinburgh, School of GeoSciences, Edinburgh, UK

ARTICLE INFO

ABSTRACT

Emissions of exhaust gases and particles from oceangoing ships are a significant and growing contributor to the total emissions from the transportation sector. We present an assessment of the contribution of gaseous and particulate emissions from oceangoing shipping to anthropogenic emissions and air quality. We also assess the degradation in human health and climate change created by these emissions. Regulating ship emissions requires comprehensive knowledge of current fuel consumption and emissions, understanding of their impact on atmospheric composition and climate, and projections of potential future evolutions and mitigation options. Nearly 70% of ship emissions occur within 400 km of coastlines, causing air quality problems through the formation of ground-level ozone, sulphur emissions and particulate matter in coastal areas and harbours with heavy traffic. Furthermore, ozone and aerosol precursor emissions as well as their derivative species from ships may be transported in the atmosphere over several hundreds of kilometres, and thus contribute to air quality problems further inland, even though they are emitted at sea. In addition, ship emissions impact climate. Recent studies indicate that the cooling due to altered clouds far outweighs the warming effects from greenhouse gases such as carbon dioxide (CO_2) or ozone from shipping, overall causing a negative present-day radiative forcing (RF). Current efforts to reduce sulphur and other pollutants from shipping may modify this. However, given the short residence time of sulphate compared to CO_2, the climate response from sulphate is of the order decades while that of CO_2 is centuries. The climatic trade-off between positive and negative radiative forcing is still a topic of scientific research, but from what is currently known, a simple cancellation of global mean forcing components is potentially inappropriate and a more comprehensive assessment metric is required. The CO_2 equivalent emissions using the global temperature change potential (GTP) metric indicate that after 50 years the net global mean effect of current emissions is close to zero through cancellation of warming by CO_2 and cooling by sulphate and nitrogen oxides.

© 2009 Elsevier Ltd. All rights reserved.

1. Introduction

This paper constitutes the shipping assessment component of the European 6th Framework project 'ATTICA', an assessment of transport impacts on atmosphere and climate. Partner assessments of climate metrics, aviation, and surface transportation are given by Fuglestvedt et al. (in this issue), Lee et al. (in this issue), and Uherek et al. (in this issue), respectively.

Emission of exhaust gases and particles from seagoing ships contribute significantly to the total emissions from the transportation sector (Corbett and Fischbeck, 1997; Eyring et al., 2005a), thereby affecting the chemical composition of the atmosphere, climate and regional air quality and health. Key compounds emitted are carbon dioxide (CO_2), nitrogen oxides (NO_x), carbon monoxide (CO), volatile organic compounds (VOC), sulphur dioxide (SO_2), black carbon (BC) and particulate organic matter (POM) (Lloyd's, 1995).

* Corresponding author. Tel.: +49 8153 28 2533; fax: +49 8153 28 1841.
E-mail address: veronika.eyring@dlr.de (V. Eyring).

Recent studies suggest that oceangoing ships consumed between 200 and 290 million metric tons (Mt)[1] fuel and emitted around 600–900 Tg CO_2 in 2000 (Corbett and Köhler, 2003; Endresen et al., 2003, 2007; Eyring et al., 2005a). These studies have estimated around 15% of all global anthropogenic NO_x emissions and 4–9% of SO_2 emissions are attributable to ships. Given nearly 70% of ship emissions occur within 400 km of land (Corbett et al., 1999; Endresen et al., 2003; Eyring et al., 2005a) ships have potential to contribute significant pollution in coastal communities.

Emissions of NO_x and other ozone precursors from shipping lead to tropospheric ozone (O_3) formation and perturb the hydroxyl radical (OH) concentrations, and hence the lifetime of methane (CH_4). The dominant aerosol component resulting from ship emissions is sulphate (SO_4^{2-}, hereafter SO_4), which is formed by the oxidation of SO_2. For some of the compounds (CO_2, O_3 and BC) the radiative forcing (RF) is positive while for others the forcing is negative (by the reflection of sunlight by sulphate particles (IPCC, 2007), and through reduced concentrations of atmospheric methane). The particles can also have an indirect effect on climate through their ability to alter the properties of clouds. The indirect aerosol effect contributes a negative forcing. In addition to impacts on the global scale, local and regional air quality problems in coastal areas and harbours with heavy traffic are of concern. It is therefore a major challenge to improve our understanding of the impact of oceangoing shipping on atmospheric composition and climate and come up with suggestions for mitigation options.

One of the challenges for society is to limit or reduce the emissions of greenhouse gases (GHG), in particular CO_2. Another key challenge is to reduce global anthropogenic NO_x and SO_2 emissions as these have health and ecosystem consequences and can be transported large distances from their sources. Shipping contributes an increasing proportion of these emissions. NO_x emissions from shipping are relatively high because most marine engines operate at high temperatures and pressures without effective reduction technologies. SO_2 emissions are high because of high average sulphur content (2.4–2.7%) in marine heavy fuels used by most oceangoing ships (EPA, 2006; Endresen et al., 2005). Importantly, future scenarios demonstrate that significant reductions are needed to offset increased emissions due to the predicted growth in seaborne trade (Eyring et al., 2005b).

For these reasons, shipping has been given increasing attention over the past few years and has been recognized as a growing problem by both policymakers and scientists. Since ship exhaust gases contribute to the worldwide pollution of air and sea, ships are facing an increasing number of rules and regulations as well as voluntary appeals from international, national and local legislators.

Merchant ships in international traffic are subject to International Maritime Organization (IMO) regulations. Emissions from ships in international trade are regulated by ANNEX VI of MARPOL 73/78 (the International Convention for the Prevention of Pollution from Ships) (IMO, 1998). IMO has declared the goal of a 30% NO_x reduction from internationally operating vessels and introduced a NO_x limiting curve in Annex VI, which depends on engine speed (IMO, 1998). From the 1st January 2000 all new marine diesel engines for new vessels should comply with this regulation (NO_x-optimized engines). Annex VI entered into force in May 2005, and sets limits on sulphur oxide and nitrogen oxide emissions from ship exhausts and prohibits deliberate emissions of ozone depleting substances. On the same day a global cap of maximum 4.5% on the sulphur content of fuel oil became mandatory for all ships. In addition, the first sulphur emission control area (SECA, with a maximum fuel sulphur content of only 1.5% sulphur content) in the Baltic Sea entered into force in May 2006, while the North Sea and English Channel SECAs entered into force in August–November 2007. Annex VI also prohibits deliberate emissions of ozone depleting substances, which include halons and chlorofluorocarbons (CFCs). New installations containing CFCs are prohibited on all ships, but new installations containing hydro-chlorofluorocarbons (HCFCs) are permitted until 1 January 2020.

Because of the increased pollution of harbour cities, the EU has agreed on the Directive 2005/33/EC, to limit the sulphur content to 0.1% in marine fuels for harbour regions in 2010. The United States Environmental Protection Agency (EPA) has adopted ship emissions standards for NO_x, CO and hydrocarbons (HC) for all US ships with engines manufactured on or after 1 January 2004 (EPA, 2002), and recently issued plans for new emission standards for diesel engines onboard large oceangoing vessels. The industrial countries have made commitments under the Kyoto Protocol to limit their GHG emissions, in particular CO_2. The Kyoto Protocol entered into force in February 2005. However, international shipping is currently excluded from emission targets under the Kyoto protocol and no decision has yet been taken on how to allocate the international GHG emissions from ships to the individual countries. Since no legislative action in this respect was agreed by the IMO in 2003, the EU is required to identify and take action to reduce the GHG emissions from shipping and is now discussing whether shipping is going to be included into the EU emission trading scheme (EU ETS).

The objective of this paper is to provide an assessment of the impact of oceangoing ships on atmosphere and climate. Inland shipping is discussed in the partner assessment on surface transportation (Uherek et al., in this issue). The paper assesses our current knowledge on ship emissions (Section 2) and their impact on atmospheric composition (Section 3), air quality, ecosystems and human health (Section 4). RF and impacts on climate are discussed in Section 5. This paper also examines how technological improvements and policy strategies might help reducing emissions from international shipping in the future (Section 6) and assesses the co-benefits and conflicts of possible future developments on air quality and climate (Section 7). A summary and conclusions are presented in Section 8.

2. Emissions

Before the impact of ship emissions on atmospheric composition and climate can be studied, emission inventories have to be developed. In this section we characterize the methodologies that are used to estimate fuel consumption and emissions from ships and present results for present-day (Section 2.1), trends and historical development (Section 2.2) and future estimates (Section 2.3).

2.1. Present-day fuel consumption and emissions

2.1.1. Methodologies
The principal existing approaches to produce spatially resolved ship emissions inventories for the key compounds can be characterised as either top-down (Section 2.1.1.1) or bottom-up (Section 2.1.1.2). One exception is the calculation of fugitive emissions, which are separately discussed in Section 2.1.1.3. Detailed methodologies for constructing ship emission inventories have been published by the Atmospheric Emission Inventory Guidebook (EMEP/CORINAIR, 2002; Woodfield and Rypdal, 2003).

2.1.1.1. Top-down approaches. In a top-down approach emissions are calculated without respect to location by means of quantifying the fuel consumption by power production first and then multiplying the consumption by emission factors. The resulting emission

---

[1] Million metric tons = 1 Mt = 1 Tg = 10^{12} g.

totals are distributed over the globe by using spatial proxies. There are mainly two different top-down approaches to calculate the fuel consumption.

One approach uses total fuel consumption from worldwide sales of bunker fuel by summing up by country. Bunker fuel sales figures require a combination of fuels reported under different categories (e.g. national or international bunker fuel). This can be challenging at a global scale because most energy inventories follow accounting methodologies intended to conform to International Energy Agency (IEA) energy allocation criteria (Thomas et al., 2002) and because not all statistical sources for marine fuels define international marine fuels the same way (Olivier and Peters, 1999).

The other approach models fleet activity and estimates fuel consumption resulting from this activity (summing up per ship/segment). The fuel consumption is often based on installed engine power for a ship, number of hours at sea, bunker fuel consumed per power unit (kW), and an assumed average engine load. Global ship emission totals are derived by combining the modelled fuel consumption with specific emission factors (Corbett et al., 1999; Corbett and Köhler, 2003; Endresen et al., 2003, 2007; Eyring et al., 2005a). Input data for these models is collected from different sources and maritime data bases. Detailed activity-based modelling has been defined as best practices for port and regional inventories (ICF Consulting, 2005), usually separating on different ship types and size categories, to establish categories with mostly the same characteristic of the input variables. On the global scale activity-based modelling is challenging. Uncertainties in the calculated emission totals in the activity-based approach arise from the use of average input parameters in the selected ship type classes, for example in input parameters like marine engine load factor, time in operation, fuel consumption rate, and emission factors, which vary by size, age, fuel type, and market situation.

Global inventory estimates for fuel use or emissions derived from a top-down approach are distributed according to a calculated ship traffic intensity proxy per grid cell referring to the relative ship reporting frequency or relative ship reporting frequency weighted by the ship size. Accuracy of top-down emission totals is limited by uncertainty in global estimates as discussed above and representative bias of spatial proxies limits the accuracy of emissions assignment (spatial precision). Differences exist among various global ship emission inventories (see Section 2.1.2).

2.1.1.2. Bottom-up approaches. In a bottom-up approach emissions are directly estimated within a spatial context so that spatially resolved emissions inventories are developed based on detailed activities associated to locations. Bottom-up approaches estimate ship- and route-specific emissions based on ship movements, ship attributes, and ship emissions factors. The locations of emissions are determined by the locations of the most probable navigation routes, often simplified to straight lines between ports or on pre-defined trades.

Although bottom-up approaches can be more precise, large-scale bottom-up inventories are also uncertain because they estimate engine workload, ship speed, and most importantly, the locations of the routes determining the spatial distribution of emissions. The quality of regional annual inventories in bottom-up approaches is also limited when selected periods within a calendar year studied are extrapolated to represent annual totals. Bottom-up approaches to date have been limited to smaller scale or regional emissions inventories due to the significant efforts associated with routing. Moreover, because they often use straight lines as routes between ports, they may overestimate ship emissions, as straight lines on a map usually are not the shortest path between two points on the globe. As such, locations of emissions may not be assigned correctly at larger scales.

A bottom-up inventory for Europe has been developed by Entec UK Limited (European Commission and Entec UK Limited, 2005). The inventory estimates emissions on the basis of kilometres travelled by individual vessels and uses weighted emission factors for each vessel type as opposed to fuel-based emission factors. The underlying vessel movement data for the year 2000 are taken from Lloyd's Marine Intelligence Unit (LMIU) and data on vessel characteristics by Lloyd's Register Fairplay. To enable separate fuel consumption estimates of residual oil and marine distillates to be made from total emissions, an assumption has been made that approximately 90% of fuel consumption is residual oil and that approximately 10% is marine distillate.

The Waterway Network Ship Traffic, Energy and Environment Model (STEEM) is the first network, that quantifies and geographically represents inter-port vessel traffic. STEEM applies advanced geographic information system (GIS) technology and solves routes automatically at a global scale, following actual shipping routes. The model has been applied with a focus for geographically characterization of ship emissions for North America, including the United States, Canada, and Mexico (Wang et al., 2008) and can be used to characterize ship traffic, estimate energy use and assess environmental impacts of shipping. Integrated approaches for assessing environmental impacts of shipping are also reported by Endresen et al. (2003) and Dalsøren et al. (2007).

2.1.1.3. Other approaches. Fugitive emissions from ship cargoes, e.g. VOCs from oil cargo handling are calculated by different approaches (McCulloch and Lindley, 2003; Endresen et al., 2003; Climate Mitigation Services, 2006; Dalsøren et al., 2007). These estimates are based on separate calculations of emissions in loading ports, on trade and at unloading ports, according to the number of voyages per year for specified sea routes. The number of voyages on each route is calculated based on vessel sizes and the oil (cargo) amounts transported.

2.1.2. Global fuel consumption and emissions in 2000/2001

Convergence is emerging on baseline estimates – at least in terms of major insights, through academic dialogue about uncertainty ranges in oceangoing fuel consumption and emissions. While it remains challenging to evaluate and quantify the impacts of ship emissions, greater uncertainty may be related to the technological and economic performance of strategies to implement effective regulations and incentives.

2.1.2.1. Input parameters. A profile of the oceangoing fleet of ships for the year 2001 is summarized in Table 1 (Lloyd's Maritime Information System (LMIS), 2002). The reason for choosing the year 2001 as a reference is because most of the emission inventories discussed in Section 2.1.2 are developed for this year or for 2000, and most of the impact studies (Section 3) also focus on the years between 2000 and 2002. According to the basic statistical information of LMIS (2002) the world merchant fleet greater than 100 gross tons (GT) at the end of the year 2001 consisted of 89,063 oceangoing ships (43,967 cargo ships and 45,096 non-cargo ships) of 100 GT and above. The non-cargo fleet included 971 fish factories, 22,141 fishing vessels, 12,209 tugs, and 9775 other ships (e.g. ferries, passenger ships, cruise ships, supply vessels, research vessels, dredgers, cable layers, etc.). Cargo ships account for around 49% of the ships but as much as 77% of main engine power installed in the fleet (not including military ships). Cargo ships are analogous to on-road trucking because they generally navigate well defined trade routes similar to a highway network. Other vessels are primarily engaged in extraction of resources (e.g. fishing, oil or other minerals) or as support vessels (vessel-assist tugs, supply vessels). Fishing vessels are the largest category of non-transport

Table 1
Fleet-average summary for 2001 and for ships of 100 GT and more. The table summarizes the number of ships and installed engine power (P_{MCR}) for the main ship classes from LMIS (2002).

Ship type	All vessels	Cargo vessels						Non-cargo vessels	Auxiliary engines (gensets)	Military vessels[a]
		All cargo ships	Tanker [b]	Container ships	Bulk and combined carriers	General cargo vessels	Passenger & fishing ships, tugboats, others			
Number of ships	90,363	43,967	11,156	2759	6457	23,595	45,096		–	1300
Number of ships[c] (%)		49	12	3	7	27	51			
P_{MCR} (MW)	343,384	218,733	54,514	46,461	46,297	71,461	67,051		40,000	17,600
P_{MCR}[c] (%)		77%	19%	16%	16%	25%	23%			

[a] About 300 GT and above (equals approximately 100 t standard displacement and more) including some 520 submarines, 190 of which are nuclear powered. The total navy fleet consist of almost 20,000 military ships (including 750 submarines) with 34,633 main engines and a total installed engine power (MCR) of 172,478 MW.

[b] Including 1301 crude oil carriers and 1153 gas carriers.

[c] Percent of civilian fleet main engines, excluding auxiliary engines.

vessels and account for more than one-quarter of the total fleet. Fishing vessels and other non-transport ships are more analogous to non-road vehicles, in that they do not generally operate along the waterway network of trade routes. Rather, they sail to fishing regions and operate within that region, often at low power, to extract the ocean resources. As a result, fishing vessels require much less energy per hour at sea for the same installed power as ships in transport service (e.g. supply ships).

The world fleet is powered mainly by diesel engines, and the emission profiles depend on engine type (slow, medium and high speed) more than on fuel type for some exhaust compounds (e.g. NO_x). The emissions factors for oceangoing vessels are derived from a variety of engine exhaust measurement studies and confirmed by several field plume measurements. At the stack, all measurements of emissions factors used in recent analyses in the U.S., Canada, and Europe are very similar (EPA, 2000; Skjølsvik et al., 2000; EMEP/CORINAIR, 2002; Cooper, 2002; European Commission and ENTEC UK Limited, 2002; Corbett and Köhler, 2003; Eyring et al., 2005a; ICF Consulting, 2005; California Air Resources Board, 2006; Levelton Consultants Ltd., 2006). Due to limited testing of ship-stacks and variability in fuel and combustion properties among engine types, some pollutant emissions factors, e.g. PM, are more uncertain on a fleet-average basis. Little is known on the actual split of PM, e.g. into BC, POM, sulphate, ash, and other particulate matter, and current emission estimates are based on a few measurements only (Petzold et al., 2007; Sinha et al., 2003). Emission factors for NO_x, SO_2, and particulates were also derived from aircraft measurements in exhaust plumes of known source ships (Williams et al., 2005; Petzold et al., 2007; Schlager et al., 2008), see Fig. 1 as an example. Emission indices (emitted mass per kg fuel burnt) were calculated using

$$EI(X) = EI(CO_2)M_X/M_{CO_2}\Delta[X]/\Delta[CO_2] \qquad (1)$$

where $EI(CO_2)$ denotes the CO_2 emission index, M_X and M_{CO_2} the mole masses of species X and CO_2 (44), respectively. $\Delta[X]$ and $\Delta[CO_2]$ are the observed enhancements of the mixing ratios in the plumes relative to ambient background concentrations. The CO_2 emission index is known with high accuracy (3070 ± 20 g CO_2/kg fuel) from the carbon mass fraction in ship fuel (85.1%), see, e.g. UNFCCC (2004), and the fraction of carbon that is converted to CO_2 for cruise conditions (98.5%). The emission factors for NO_x determined from the measurements were in good agreement with the values calculated with the emission models for the corresponding engine type and operation conditions (Table 2). Only the SO_2 emission factors were lower than expected from the fuel sulphur content indicating SO_2 loss from the gas phase in the young exhaust plumes. Fridell et al. (2006) compared emission of NO_x and CO_2 for cargo transported with a small ship and with a large ship, both with comparable parameters typical for ship transports in Europe. They

found that transport of a unit cargo with a small ship emits more CO_2 by factor 1.8 and slightly more NO_x by factor 1.2.

Units for emissions factors are translated from power-based (g k^{-1} Wh) to fuel-based (kg ton^{-1} fuel) using specific fuel oil consumption factors (g fuel k^{-1} Wh). Both units are reported in the literature, with fuel-based factors used where fuel records are the basis for estimates or where atmospheric field studies have derived emission indices from plume observations.

2.1.2.2. Fuel consumption. Several studies have modelled global emissions from oceangoing civil ships by combining estimates for marine fuel sales with their respective fuel-based emissions factors (top-down approach, see Section 2.1.1.1). These estimates based on energy statistics result in a total fuel consumption below 200 Mt in 2000 (e.g. Skjølsvik et al., 2000; Olivier et al., 2001; Endresen et al., 2003, 2007; Dentener et al., 2006).

Although emissions estimates and fuel consumption are related to the energy used by ships, recent studies call into question the validity of relying on the statistics of marine fuel sales. These studies have focused on activity-based estimation of energy and power demands from fundamental principles (Corbett and Köhler, 2003; Eyring et al., 2005a; Wang and Corbett, 2005; ICF Consulting, 2005). These approaches estimate fuel consumption for the world fleet of around 280 Mt year^{-1} in 2001 and have shown that fuel allocated to international fuel statistics is insufficient to describe total estimated energy demand of international shipping. Corbett and Köhler (2004) considered alternative input parameters in their activity-based fuel consumption and emission model. They conclude that alternative assumptions in the input parameters could reduce their fuel consumption estimate, but not more than 14–16%. However, other activity-based studies have reported lower estimates, considering alternative operation profile. They claim that the main reason for the large deviation between activity-based fuel consumption estimates is the number of days assumed at sea and that better activity data (per ship type and size categories) on a yearly basis is required when fleet modelling is used to determine the actual fuel consumption for the entire world fleet (Endresen et al., 2004, 2007).

Recent efforts to apply activity-based methods to regional inventories have begun to address the inherent undercounting bias in using international marine fuel sales statistics. The Core Inventory of Air Emissions in Europe (CORINAIR), under the Co-operative Programme for Monitoring and Evaluation of the Long-Range Transmission of Air Pollutants in Europe (EMEP) funded by the European Environmental Agency (EMEP/CORINAIR, 2002; Woodfield and Rypdal, 2003), adapted better criteria for labelling traffic as international or domestic that conforms to pollution-inventory guidance requirements rather than IEA energy allocation criteria (Thomas et al., 2002). Fuel used by ships is allocated for
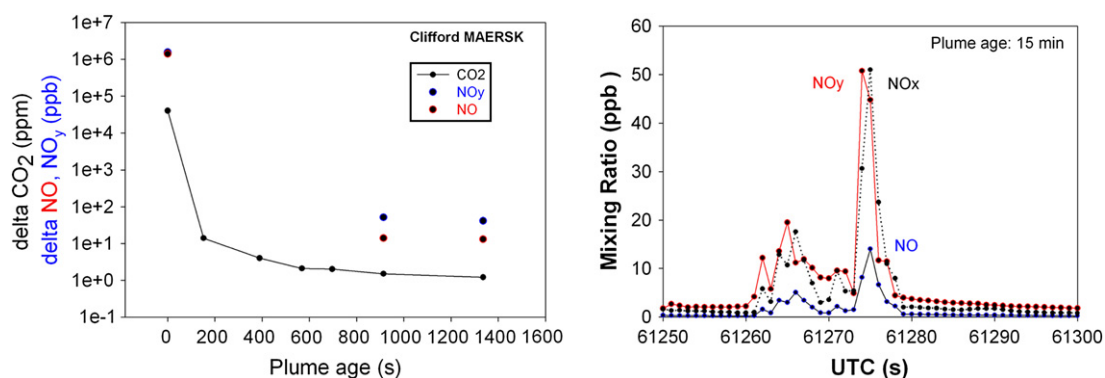
Fig. 1. Airborne emission measurements in the exhaust trail of a large container ship as a function of plume ages (left panel). Given are concentration enhancements of CO_2, NO, and NO_y (total reactive nitrogen). An individual exhaust plume transect is shown in the right panel for a plume age of 15 min.

emissions inventory purposes according to a simple but more accurate check list with regard to the voyage characteristics. This may still leave unresolved the problem of using energy statistics collected by OECD and IEA – especially with regard to the past.

Considering the different activity-based estimates reported, the lower estimates of fuel consumed by the oceangoing world fleet in 2000 is around 200 Mt, while estimates as great as 290 Mt of marine oil would include all internationally registered ships including fishing vessels, the military fleet and auxiliary engines. This does not account for growth in emissions that may be reflected in estimates for more recent years (discussed in Section 2.2.1). The latter is about 110 Mt higher than the reported total (i.e. sum IEA categories Internal Navigation and International marine bunkers) IEA marine sales (IEA, 2003). Despite the ongoing scientific debate regarding whether bunker fuel sale statistics are representative when estimating fuel-based emissions, and whether input data on engine operational profiles for different ship types and size categories are representative (Corbett and Köhler, 2003, 2004; Endresen et al., 2003, 2004, 2007; Eyring et al., 2005a), these estimates demonstrate some convergence in terms of uncertainty bounds (Fig. 2). More importantly, there is agreement among researchers that better input data on ship activity and improved means of allocating activity geospatially will reduce current differences among inventories.

2.1.2.3. Global emission totals. There is a correspondingly large range in ship emission totals estimated in different studies (see Fig. 2). However, all results support the finding that except for CO_2 ship emissions are significant compared to emissions from road traffic.

Shipping moved 80–90% of world trade by volume (European Commission and Entec UK Limited, 2005; U.S. Department of Transportation, 2003) within a bounded range of 540–1300 Tg CO_2 in 2000. Our best estimate plus upper and lower bound for fuel consumption and emissions from oceangoing shipping for the years 2000 and 2005 is given in Table 3. Fuel consumption and CO_2 are taken from the IMO GHG study (Buhaug et al., 2008). The 2000 mean is derived as mean from Corbett and Köhler (2003), Eyring et al. (2005a) and Endresen et al. (2007) for SO_2 and from the mean of Corbett and Köhler (2003), Eyring et al. (2005a) and Endresen et al. (2003) for all other species except for BC and refrigerants. For consistency, the resulting non-CO_2 emission totals are scaled with the factor 1.04, which is the ratio of the IMO CO_2 value and the mean CO_2 value from Corbett and Köhler (2003), Eyring et al. (2005a) and Endresen et al. (2007). According to our best estimate, oceangoing shipping emitted around 780 Tg CO_2 in the year 2000, which corresponds to a fuel consumption of 250 Mt and a contribution of around 2.7% to all anthropogenic CO_2 emissions in 2000. Our best estimate suggests that 5.4 Tg(N) of NO_x, 5.5 Tg(S) of SO_x, and 1.4 Tg PM have been released by the registered fleet in 2000, with a bounded range of 3–10 Tg(N), 3–10 Tg(S) and 0.4–3.4 Tg(PM), respectively. Uncertainty ranges are taken directly or are derived from the work of Corbett and Köhler (2003, 2004). Generally, uncertainty ranges are derived using Monte–Carlo simulation by varying each parameter according to distributions on the estimates for fuel consumption and emissions for each pollutant. For BC the current best estimate is the mean of the 5th and 95th percentile results from uncertainty analysis by Corbett and Köhler (2003). The best estimate of

Table 2
Emission factors of key compounds emitted by diesel powered ships reported in different studies.

Study	EI (CO_2)	EI(NO_x)	EI(SO_2)	EI(CO)	EI(HC)	EI(PM)
	Average all ships/cargo/non-cargo (g kg^{-1} fuel burnt)					
Lloyd's (1995)	3170	77/87/57	40/54/10	7.4	2.4	5.5/7.6/1.2
European Commission and ENTEC UK Limited (2005)	3190/3200/3050	67.9/71.9/60.3	52.8/52.9/50.4	–	2.26/2.43/1.96	5.19/6.14/3.79
Corbett and Köhler, 2003	3178/3179/3176	79/83/72	47/48/45	–	6/6/5.6	6/6/5.6
Endresen et al. (2003)	3170	87[a]/57[b]	54[c]/10[d]	7.4	2.4	7.6[e]/1.2[f]
Eyring et al. (2005a)	2905/2860/2930	76/86/50	43/45/40	4.7/4.7/4.7	7.0/6.6/6.6	6.0/5.9/6.6
New England measurements (Williams et al., 2005)	–	–/–/62	–/–/12	–	–	–
ICARTT-ITOP measurements (Schlager et al., 2008)[g]	–/3070/–	–/81/–	–/18/–	–	–	–

[a] Slow speed engines.
[b] Medium and high speed engines.
[c] Residual fuel: 2.7% sulphur content.
[d] Distillate fuel: 0.5% sulphur content.
[e] Slow speed engines.
[f] Medium and high speed engines.
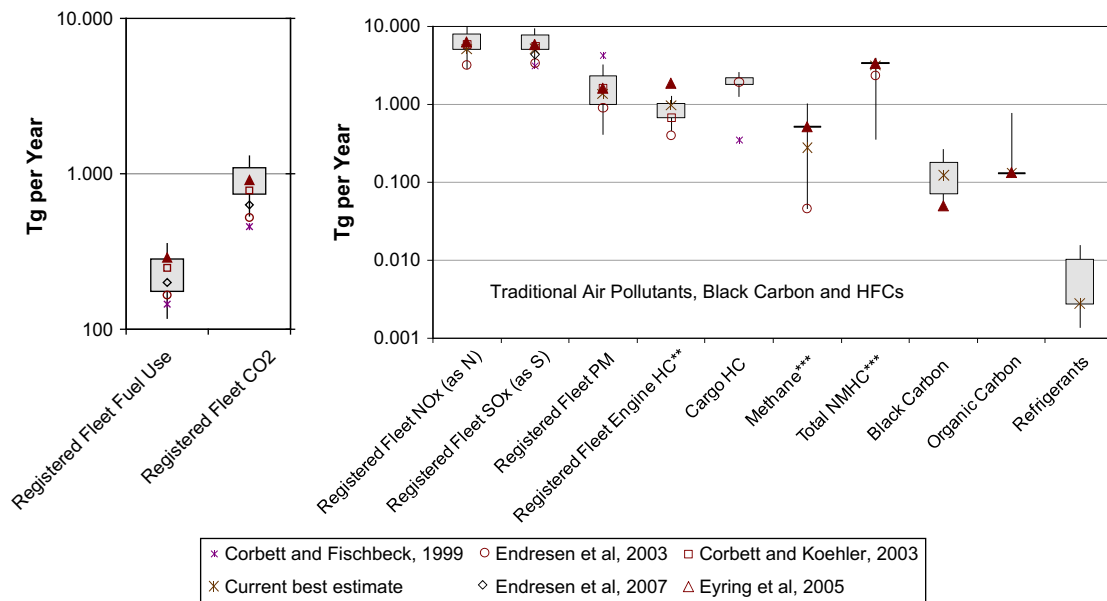[g] 47,000 kW engine, 2.45% fuel sulphur content.

Fig. 2. Summary of estimated ranges in global fuel consumption and emissions from maritime shipping for the year 2000. The current best estimate is derived as mean from Corbett and Köhler (2003), Eyring et al. (2005a) and Endresen et al. (2007) for fuel consumption, CO₂, and SO₂ or Endresen et al. (2003) for all other species except for BC and refrigerants. For BC the current best estimate is the mean of the 5th and 95th percentile results from uncertainty analysis and the source for refrigerants is Devotta et al. (2006). The Corbett and Köhler (2003) and Eyring et al. (2005a) results are for 2001 and have been scaled to 2000 fuel consumption and emissions by using the ratio of the total seaborne trade in 2000 and 2001 from Fearnleys (2007). Box-plots represent the 5th and 95th percentile results and whiskers extend to lower and upper bounds from explicit uncertainty analysis for fuel consumption, CO₂, NOₓ, SOₓ, and PM and from expert judgement for the rest. Uncertainty ranges are taken directly or are derived from the work of Corbett and Köhler (2003, 2004), with extensions for HFCs and cargo methane. Generally, uncertainty ranges are derived using Monte–Carlo simulation by varying each parameter according to distributions on the estimates for fuel consumption and emissions for each pollutant. Note: Emissions do not represent comparative climate impacts. *Registered fleet includes passenger vessels, fishing vessels plus cargo ships, but not military vessels. **Registered fleet engine HC does not include cargo evaporative HC. ***Total NMVOC (NMHC) includes tanker loading (see Table 3 of Eyring et al., 2005a).

0.13 Tg BC emitted by oceangoing shipping in 2000 agrees well with results from Lack et al. (2008). Emissions of N₂O from ships are very small (0.03 Tg in 2000; Buhaug et al., 2008).

While ship cargoes are not as recognized as a source of global emissions as ship propulsion, they are important sources of VOCs (methane and non-methane). Initially ship methane emissions were estimated to be quite low, together with rail at 0.09 Tg representing only 10% of light-duty vehicles (Piccot et al., 1996). VOCs emissions inventories were later produced using activity-based inventories designed for cargo activities (Endresen et al., 2003), speciating methane from engines to be about 11% and methane from cargoes to be about 15% of total hydrocarbons, respectively. Eyring et al. (2005a) characterized the methane fraction to be about 13% of total engine hydrocarbon emissions.

Table 3
Best estimate plus upper and lower bound for fuel consumption and emissions from oceangoing shipping for the years 2000 and 2005.

Year	Unit	2000 mean[a]	2000 lower bound[b]	2000 upper bound[b]	2005 mean[c]	2005 lower bound[c]	2005 upper bound[c]
Registered fleet fuel use[d]	[Mt]	250	120	370	300	150	450
Registered fleet CO₂	[Tg(CO₂)/a]	780	560	1360	960	450	1660
Registered fleet NOₓ	[Tg(N)/a]	5.4	3.0	10.4	6.6	3.7	12.7
Registered fleet SOₓ	[Tg(S)/a]	5.5	3.2	9.8	6.7	3.9	12.0
Registered fleet PM	[Tg PM/a]	1.4	0.4	3.4	1.8	0.5	4.1
Registered fleet CO	[Tg PM/a]	1.18	1.06	1.35	1.44	1.30	1.66
NMVOC[e,f]	[Tg NMVOC/a]	1.14	0.37	1.78	1.32	0.46	2.18
CH₄[e,f]	[Tg CH4/a]	0.14	0.05	0.23	0.17	0.06	0.28
BC	[Tg BC/a]	0.13	0.05	0.28	0.16	0.06	0.34
POM	[Tg POM/a]	0.14	0.12	0.82	0.17	0.15	1.00
Refrigerants	[Tg/a]	0.003	0.001	0.016	0.004	0.002	0.020

[a] Fuel consumption and CO₂ are taken from the IMO GHG study (Buhaug et al., 2008). The 2000 mean is derived as mean from Corbett and Köhler (2003), Eyring et al. (2005a) and Endresen et al. (2007) for SO₂ and from the mean of Corbett and Köhler (2003), Eyring et al. (2005a) and Endresen et al. (2003) for all other species except for BC and refrigerants. For consistency, the resulting non-CO₂ emission totals are scaled with the factor 1.04, which is the ratio of the IMO CO₂ value and the mean CO₂ value from Corbett and Köhler (2003), Eyring et al. (2005a) and Endresen et al. (2007). The Corbett and Köhler (2003) and Eyring et al. (2005a) results are for 2001 and have been scaled to 2000 fuel consumption and emissions by using the ratio of the total seaborne trade in 2000 and 2001 from Fearnleys (2007).

[b] Lower and upper bounds are derived from explicit uncertainty analysis for fuel consumption, CO₂, NOₓ, SOₓ, and PM and from expert judgement for the rest. Uncertainty ranges are taken directly or are derived from the work of Corbett and Köhler (2003, 2004), with extensions for HFCs and cargo methane. Generally, uncertainty ranges are derived using Monte–Carlo simulation by varying each parameter according to distributions on the estimates for fuel consumption and emissions for each pollutant.

[c] To calculate 2005 emissions, the 2000 emissions have been scaled with the ratio of the total seaborne trade (TST) in 2005 (29094) and TST in 2000 (23693) from Fearnleys (2007), see Fig. 4.

[d] Registered fleet includes passenger vessels, fishing vessels plus cargo ships, but not military vessels.

[e] Not including HC emissions from crude oil transport.

[f] NMVOC from crude oil transport (evaporation during loading, transport, and unloading) in 2000 is 1665 Tg and CH₄ is 0.294 Tg from Endresen et al. (2003).

According to the IPCC (Devotta et al., 2006), a small fraction, about 1100 of 35,000 commercial vessels, carry refrigerated cargoes. HCFC-22 is the common refrigerant in these systems. Nearly all other commercial ships also use HCFC-22 to refrigerate their crew food supplies, and operate air conditioning systems. Ammonia refrigerants are also used in shipping. Devotta et al. (2006) estimate ship refrigerant emissions to be less than 3000 tons annually. Emissions of CFCs from the world shipping fleet were estimated at 3000–6000 tons for the year 1990 – equivalent to around 1–3% of annual global emissions. Halon emissions from shipping for the same year were estimated to be 300–400 tons, or around 10% of world total. More recent figures are not readily available. It is anticipated that these would show a significant reduction in CFC and halon emissions on account of the phase out of these substances as a consequence of the Montreal Protocol on Substances that Deplete the Ozone Layer and subsequent amendments (Reynolds and Endresen, 2002).

Fig. 2 presents summary estimates and bounding ranges of pollutant emissions discussed above, including NO_x (as elemental nitrogen), SO_x (as elemental sulphur), and particulate matter (PM_{10}), hydrocarbons and methane (from both engines and cargoes), BC and POM (constituents of PM with climate implications), and refrigerants. The figure shows estimated ranges of fuel use and CO_2 alongside the other emissions using a log-scale. The most important insight from Fig. 2 is that nearly all previous estimates fall within bounded ranges, and that point estimates using activity-based methods are consistently higher than estimates based on fuel sales statistics. A second insight is that some emissions are much more uncertain than others (e.g. PM, CH_4, POM, HFCs). A third important point for policy decisions is that for most pollutants, the action level for policy decisions may fall below the range of current "disagreement" among point estimates. For example, action to create SO_x Emission Control Areas under IMO Annex VI was justified using estimates based on fuel sales, which falls near the lower bound for SO_x estimates. Moreover, these point estimates are based on in-year estimates, and must be adjusted for growth to compare using a more recent or common year (discussed in Section 2.2.1). Lastly, recent estimates using activity-based methods are converging on a narrower range than represented by these bounded box-whisker plot.

2.1.2.4. Spatial proxies of global ship traffic. Scientific research also improved the geographical distributions of ship emissions so they more accurately represent world fleet traffic (Corbett and Köhler, 2003; Endresen et al., 2003; Dalsøren et al., 2007; Wang et al., 2007).

The spatial distribution of emissions used in Environmental Database for Global Atmospheric Research (EDGAR; Olivier et al., 1999; Dentener et al., 2006) was derived from the world's main shipping routes and their traffic intensity (Times Books, 1992; IMO, 1992; Fig. 3 upper panel) and was one of the first top-down shipping inventories. However, EDGAR is now considered to be unrealistic and more comprehensive inventories represent more realistic shipping patterns. Corbett et al. (1999) produced one of the first global spatial representations of ship emissions using a shipping traffic intensity proxy derived from the Comprehensive Ocean-Atmosphere Data Set (COADS), a data set of voluntarily reported ocean and atmosphere observations with ship locations which is freely available. Endresen et al. (2003) improved the global spatial representation of ship emissions by using ship size (gross tonnage) weighted reporting frequencies from the Automated Mutual-Assistance Vessel Rescue system (AMVER) data set (Fig. 3 middle panel). AMVER, sponsored by the United Coast States Guard (USCG), holds detailed voyage information based on daily reports for different ship types. Participation in AMVER was, until very recently, limited to merchant ships over 1000 GT on a voyage for 24

or more hours and data are strictly confidential. The participation in AMVER is 12,550 ships but only around 7100 ships have actually reported. Endresen et al. (2003) observed that COADS and AMVER lead to highly different regional distributions. Wang et al. (2007) addressed the potential statistical and geographical sampling bias of the International Comprehensive Ocean-Atmosphere Data Set (ICOADS, current version of COADS; Fig. 3 lower panel) and AMVER datasets, the two most appropriate global ship traffic intensity proxies, and demonstrate (using ICOADS) a method to improve global proxy representativeness by trimming over-reporting vessels that mitigates sampling bias, augment the sample data set, and account for ship heterogeneity. Apparent underreporting to ICOADS and AMVER by ships near coastlines, perhaps engaged in coastwise (short sea) shipping especially in Europe, indicates that bottom-up regional inventories may be more representative locally. The three different shipping traffic intensity proxies discussed above are shown in Fig. 3.

All recent studies report that the majority of the ship emissions occur in the Northern Hemisphere within a fairly well defined system of international sea routes (Skjølsvik et al., 2000; Endresen et al., 2003; Corbett and Köhler, 2003; Wang et al., 2007). The best estimate is that 80% of the traffic is in the Northern Hemisphere, and distributed with 32% in the Atlantic, 29% in the Pacific, 14% in the Indian Ocean and 5% in the Mediterranean. The remaining 20% of the traffic in the Southern Hemisphere is approximately equally distributed between the Atlantic, the Pacific, and the Indian Ocean. Across all regions, some 70% of ship emissions occur within 400 km of coastlines, conforming to major trade routes (Corbett et al., 1999). It is important to recognize that the significant growth in ship activity in Asian waters over recent years will change the above distribution.

Ship activity patterns depicted by ICOADS, AMVER and their combination demonstrate different spatial and statistical sampling biases. None can be judged to represent global ship traffic and emissions better than any other by cross-comparison alone. These differences could significantly affect the accuracy of ship emissions inventories and atmospheric modelling, and can be used together to perform uncertainty analyses of ship air emissions impacts on a global scale. Researchers have improved the global proxy representativeness by adjusting the data to mitigate sampling bias, augment sample data set, and account for ship heterogeneity (Endresen et al., 2003; Wang et al., 2007). Even with these improvements, global proxy data has limitations. National inventories covering coastal shipping may have to be added to these global data – especially where short sea shipping is substantial, as outlined by Dalsøren et al. (2007). Endresen et al. (2007) also pointed out that this is important, as ships less than 100 GT typically in coastal operations are not included in the geographical distribution (e.g. today some 1.3 million fishing vessels).

Effective monitoring and reliable emission modelling on an individual ship basis is expected to improve if data from the long-range identification and tracking (LRIT) technology and the automatic identification system (AIS) are used. LRIT is a satellite-based system with planned global cover of maritime traffic from 2008. AIS transponders automatically broadcast information, such as their position, speed, and navigational status, at regular intervals. Since 2004, all ships greater than 300 GT on international voyages are required by the IMO to transmit data on their position using AIS. The LRIT information ships will be required to transmit the ship's identity, location and date and time of the position. One of the more important distinctions between LRIT and AIS, apart from the obvious one of range, is that, whereas AIS is a broadcast system, data derived through LRIT will be available only to the recipients who are entitled to receive such information and safeguards concerning the confidentiality of those data have been built into the regulatory provisions. Because no interface is planned for LRIT and AIS data, these
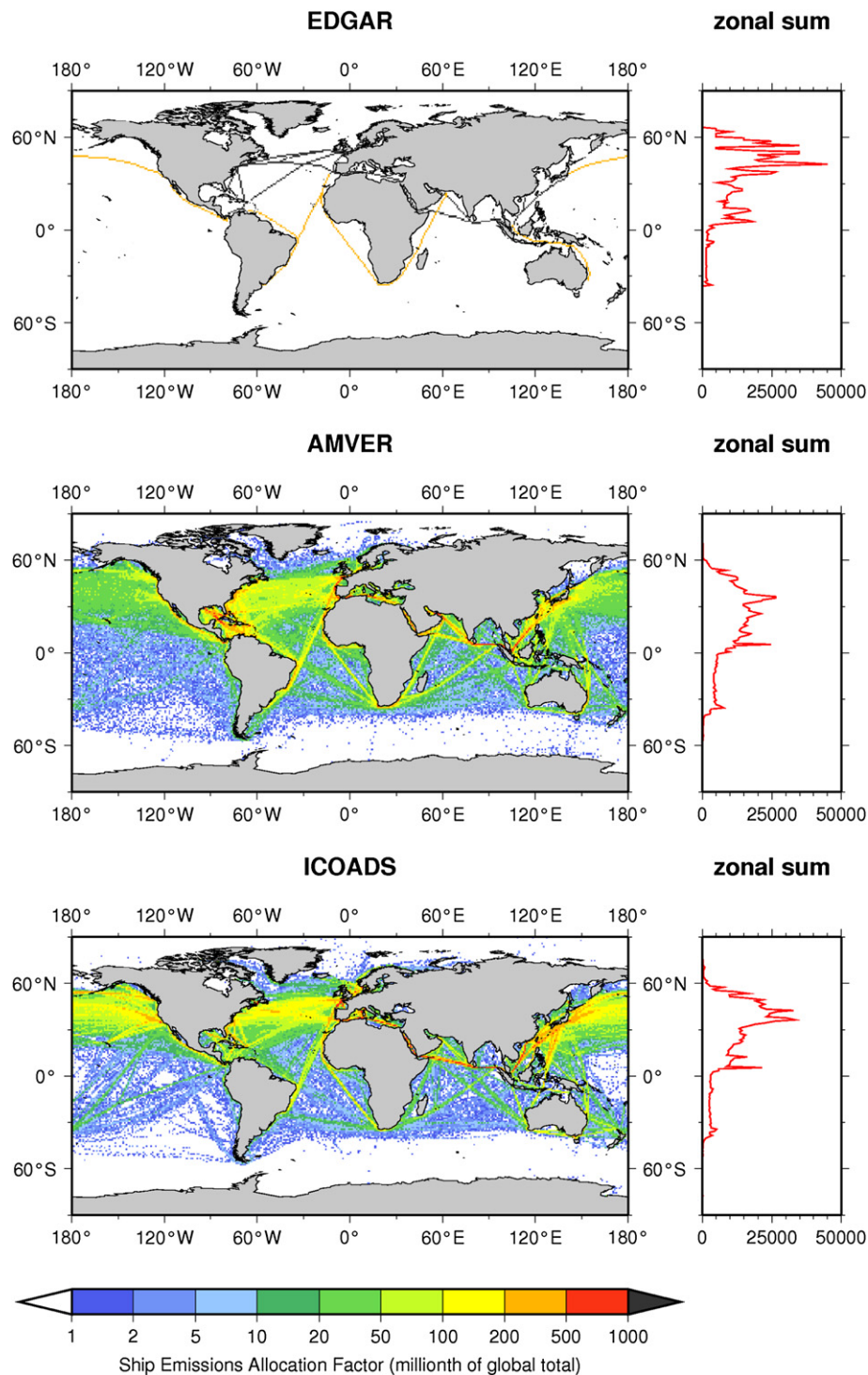
Fig. 3. Ship Emissions Allocation Factors (SEAF) from EDGAR (Dentener et al., 2006), AMVER (Endresen et al., 2003), and ICOADS (Wang et al., 2007). SEAF in each grid cell is defined as the fraction of ship emissions in that grid cell of the global total (expressed in millionth of the global total).

sources will independently describe common ship activities that should help improve the global proxy data and enable better development of global networks like STEEM (Wang et al., 2008).

2.2. Shipping growth trends and historical development

This section presents trend indicators corresponding to global trade volumes, and discusses some of the specific details characterizing historical fleet characteristics.

2.2.1. Growth rates since 2001

Over the last 30 years a clear and well understood correspondence is observed between fuel consumption and seaborne trade in ton-miles, because the work done in global trade is proportional to the energy required. The IMO greenhouse gas study chose a linear trend extrapolation of 3% year^{-1} for trade to represent the energy and CO_2 emissions trend (Skjølsvik et al., 2000). More recent studies have revealed that the growth in trade over recent decades is non-linear and that it is higher than 3% year^{-1} (e.g. Corbett et al.,

2007a). Similarly, Endresen et al. (2007) illustrated strong correlation between the world fleet fuel consumption and total seaborne trade in ton-miles ($r = 0.97$). Recent annual growth rates in total seaborne trade in ton-miles have been 5.2% on average from 2002 to 2007, a lot higher than in past decades (Fearnleys, 2007, see also Fig. 4). Accordingly, the fuel consumption from 2001 to 2006 has increased significantly as the total installed power increased by about 25% (Lloyd's Register Fairplay, 2006). Fig. 5 shows the fuel consumption from 1950 to 2007 as reported in the literature in addition to the back- and forecast calculated from the time evolution of freight ton-miles.

It is reported that estimated container trade, measured in cargo tons, to have grown in 2006 by 11.2%, reaching 1.13 billion tons by 2006. Over the last two decades, global container trade (in tons) is estimated to have increased at an average annual rate of 9.8%, while the share of containerized cargo in the world's total dry cargo is estimated to have increased from 7.4% in 1985 to 24% in 2006. In this context, it is important to note that over 70% of the value of world international seaborne trade is being moved in containers. Chinese ports (including Taiwan Province of China and Hong Kong, China) accounted for 102.1 million TEUs[2] in 2005, representing some 26.6% of the world container port throughput. In 2006 preliminary figures show that throughput has increased to 118.6 million TEUs, a rise of 16% in 2005 (UNCTAD, 2007). Clearly, the increase in recent years in shipping particular in Asian waters (see also Fig. 5) needs to be taken into account in future studies.

2.2.2. Historical fuel consumption and emissions

Over the last 100 years the fleet expanded by 72,000 motor ships to a total of 88,000, with a corresponding increase in tonnage from 22.4 to 553 GT (Lloyd's Register of Shipping, statistical tables, 1964 (year 1900), and world fleet statistics and statistical tables, 2000). This growth has been driven by increased demand for passenger and cargo transport, with 300 Mt cargo transported in 1920 (Stopford, 1997) and 5400 Mt in 2000 (Fearnleys, 2003). In 1950 the civilian fleet consisted of 30,844 vessels of 100 GT and above with a total of 84.6 million GT (ISL, 1994; Lloyd's, 2002). Starting around 1960, the world merchant fleet increased rapidly and the ship number more than doubled in the period between 1960 and 1980. Part of this ship boom was the tanker business, which reached its peak around 1973–1975, and the introduction of a new type of cargo ship, the container vessel. In general, little information on the historical development of fuel consumption is available, with little data published pre-1950 and large deviations reported for estimates covering the last three decades (see Fig. 5).

Eyring et al. (2005a) produced one of the first estimates for fuel usage over a historical period from 1950 to 2001. They have reported simplified activity-based inventories from 1950 up to 1995 using ship number statistics and average engine statistics, while the estimate for 2001 is based on detailed fleet modelling (see Section 2.1.2.2). The results suggest that fuel consumption from oceangoing ships has increased by a factor of 4.3 from 1950 (64.5 Mt) to 2001 (280 Mt). Uncertainties in this estimate arise from the fact that reliable input data such as detailed shipping and engine as well as engine performance statistics, activity data and the detailed fleet structures before 1976 are not available. Endresen et al. (2007) reported more detailed activity estimates from 1970 to 2000 per year. They suggested that activity-based estimates for past fuel consumption and emissions must take into account variation in the demand for sea transport and operational and technical changes over the years, to better represent the real fuel
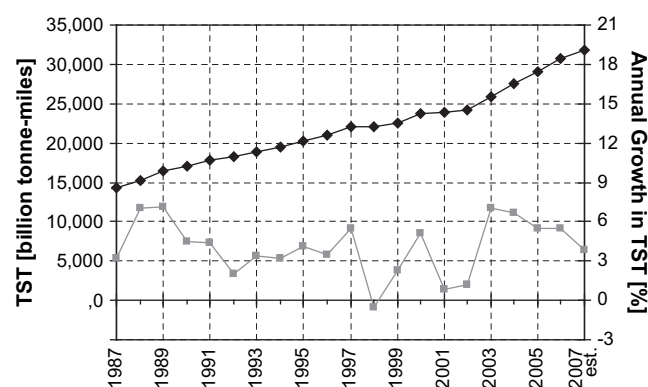
consumption and corresponding emissions. Their results suggest that the fleet growth is not necessarily followed by increased fuel consumption, as technical and operational characteristics have changed. They also reported annual fuel consumption before the First World War, and detailed fuel-based estimates (based on sales) from 1925 up to 2000 (Fig. 5). The results indicated that oceangoing ships had a yearly fuel consumption of about 80 Mt of coal (corresponding to 56.5 Mt heavy fuel oil) before the First World War. This increased to a sale of about 200 Mt of marine fuel oils in 2000 (including the fishing fleet), i.e. about a 3.5-fold increase in fuel consumption. Ships emitted around 229 Tg (CO_2) in 1925 (Endresen et al., 2007) and grew to 638–800 Tg (CO_2) in 2000/2001 (Endresen et al., 2007; Corbett and Köhler, 2003; Eyring et al., 2005a). The corresponding SO_2 emissions are about 2.5 Tg (SO_2) in 1925 and between 8.7 and 12.03 Tg (SO_2) in 2001. The CO_2 emissions per ton transported by sea have been significantly reduced as a result of larger and more energy efficient ships. For comparison, the tonnage increased from 22.4 million GT in 1900 to 84.6 million GT in 1950, and 553 million GT in 2000.

2.3. Future scenarios compliant with current international legislation

Merchant ships in international traffic are subject to IMO regulations and emissions from ships in international trade are regulated by ANNEX VI of MARPOL 73/78. Here we discuss only those future scenarios that are compliant with present-day IMO regulations. These scenarios are subsequently used in this study to assess the impacts on atmospheric chemistry, climate and human health. National or regional regulations call for even more stringent NO_x and SO_x limits than those given by IMO (e.g. EPA, 2002). As a result, compliance with emission regulations through technological improvements will impact ship operators and the technology in use, and will thus impact on the emissions. Those other future scenarios that consider possible emission reductions and improvements of fuel efficiency are presented in Section 6.

Ship activity has increased steadily over the last two decades and is predicted to continue growing for the foreseeable future. Most studies on future scenarios take historic trends for some recent period and extrapolate with adjustment for expected change in trends, e.g. the response to economic and population drivers affecting global trade or consumption.

The TREMOVE maritime model (Ceuster et al., 2006; Zeebroeck et al., 2006) estimates fuel consumption and emissions trends derived from forecast changes in ship voyage distances (maritime movements in km) and the number of port calls. It includes every year from the base year 1995 until 2020. According to the TREMOVE

Fig. 4. World seaborne trade (TST) in billion ton-miles and corresponding annual growth rate from 1987 to 2007. Source: Fearnleys (2007).

---

[2] TEU (20-foot equivalent unit). An equivalent unit is a measure of containerized cargo capacity equal to one standard 20 ft (length) × 8 ft (width) container.
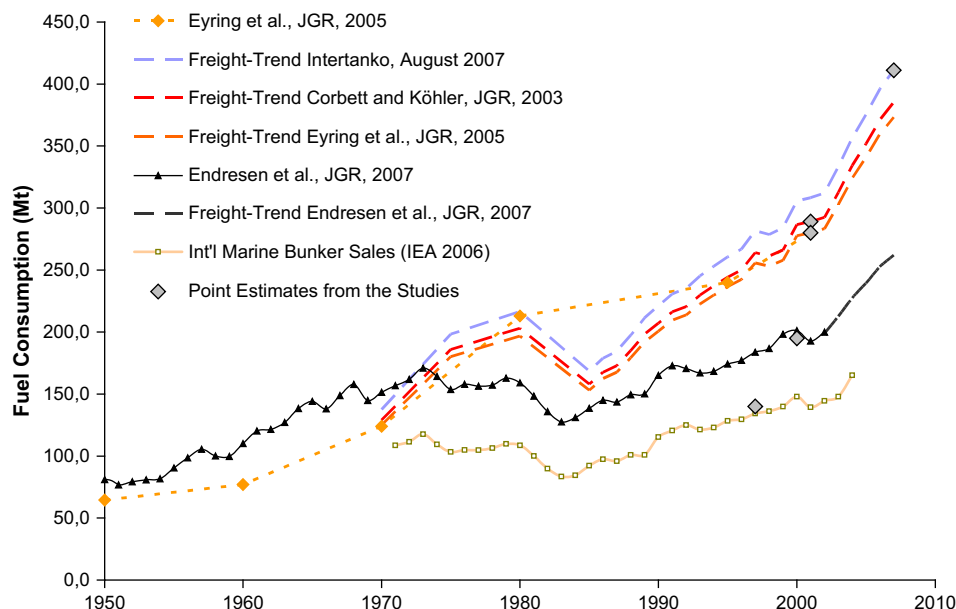
Fig. 5. World fleet fuel consumption (civilian, military, and auxiliary) and international marine bunker fuel statistics in Mt from different estimates. The symbols indicate the original estimates for individual years and the solid lines show the original trend estimates from these studies. The dashed lines show the back- and forecast calculated from the time evolution of freight ton-miles with the point estimates from 2001 (Corbett and Köhler, 2003; Eyring et al., 2005a), 2000 (Endresen et al., 2007), 2007 (Gunner, 2007), and 1997 (IEA, 2006) taken as the reference year.

report, maritime fleet and vehicle kilometres grow annually by 2.5% for freight and 3.9% for passengers, while port callings grew by 8% compared to the previously used input figures. Other estimates that are published outside of the journal literature also confirm the general importance and sometimes suggest higher growth rates (e.g. Meszler Engineering Services analysis, ICCT, 2007).

The IMO study on greenhouse gas emissions from ships (Skjølsvik et al., 2000) used fleet growth rates based on two market forecast principles, validated by historical seaborne trade patterns: (1) world economic growth will continue; and (2) demand for shipping services will follow the general economic growth. The IMO study correctly described that growth in demand for shipping services was driven by both increased cargo (tonnage) and increased cargo movements (ton-miles), and considered that these combined factors make extrapolation from historic data difficult. Nonetheless, their forecast for future seaborne trade (combined cargoes in terms of tonnage) was between 1.5 and 3% annually. The IMO study applied these rates of growth in trade to represent growth in energy requirements. The ENTEC study (European Commission and ENTEC UK Limited, 2002) adopted growth rates from the IMO study.

However, a constant annual growth of the world's real gross domestic product (GDP) does not necessarily mean the same increase in seaborne trade. During the past two decades real GDP according to the statistics of the International Monetary Fund (IMF, 2004) grew by 2.8% p.a. on average, whereas international trade experienced an average annual growth rate of 6.2% (IMF, 2004). Since 1985 the world seaborne trade gained 3.3% in terms of volumes and 3.6% p.a. in terms of ton-miles on average (Fearnleys, 2004; Clarkson, 2004). The lower growth rate of seaborne trade compared to international trade results from the fact that international trade is measured in monetary values while seaborne trade is measured in weight. Based on the historical correlation between the total seaborne trade and GDP over the time period 1985–2001, Eyring et al. (2005b) estimated future world seaborne trade in terms of volume in million tons for a specific ship traffic scenario in a future year, using a linear fit to historical GDP data.

This represents one of the only studies to forecast growth in seaborne trade for energy and emissions purposes at rates faster than GDP. Following the annual growth rate in GDP of the four IPCC SRES storylines (2.3–3.6%), seaborne trade in the four future ship traffic demand scenarios increased by 2.6–4.0% p.a. According to this study, fuel consumption by the oceangoing fleet could increase from 280 Mt in 2001 to 409 Mt by 2020 and 725 Mt by 2050. These scenario calculations demonstrate that significant technological improvements are needed to offset increased emissions due to growth in seaborne trade and cargo energy intensity. Without stringent emission reduction strategies, CO_2 and SO_2 emissions from ships would more than double present-day values by 2050 and NO_x emissions could exceed the values from present-day global road transport (Fig. 6, technology scenario 4).

It is important to note that the future in the scenario calculations from Eyring et al. (2005b) starts in 2002 and thus does not include the recent unexpected high growth rates between 2002 and 2007 (see Section 2.2.1). Further work is currently underway with respect to the latest growth rates and with respect to the likely updated technology pathways.

3. Impact on atmospheric composition

The majority of emissions from shipping are injected into the atmosphere in the form of coherent plumes, often in relatively pristine parts of the atmosphere. To assess the impact of shipping on the atmospheric composition with the help of global models the emission totals are distributed over the globe with spatial proxies of global ship traffic derived in various ways (see Sections 2.1.2.3 and 2.1.2.4) and are instantaneously spread onto large inventory grid boxes, usually 1° longitude × 1° degree latitude, without accounting for dispersion, transformation and loss processes on the subgrid scale. Ship emissions occur locally at relatively high concentrations in relation to the atmospheric background concentrations. The emissions are diluted by mixing with the ambient air. During the dilution process the emitted species are chemically transformed, secondary species (e.g. ozone) are formed
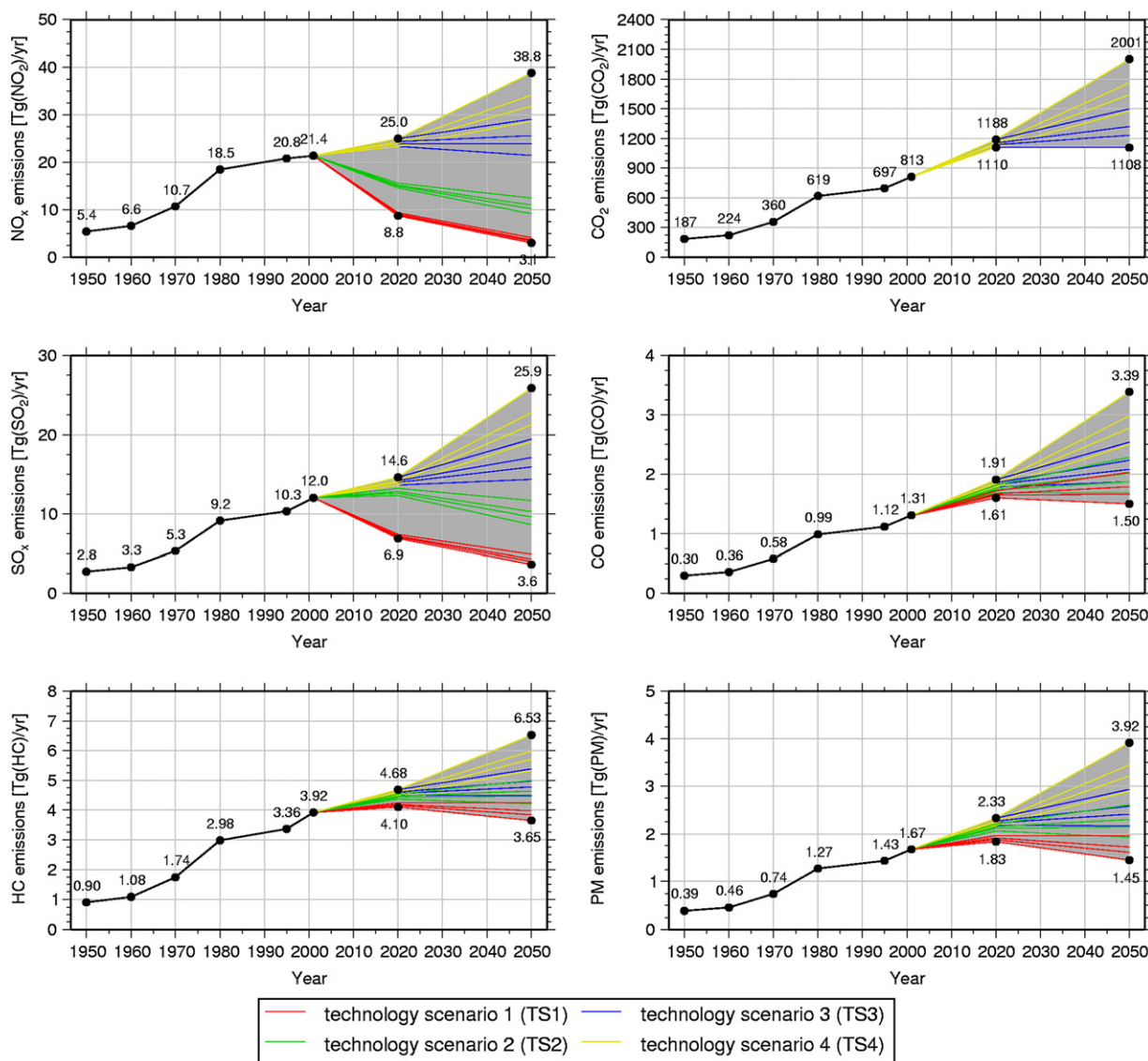
Fig. 6. Possible range of future NO_x emissions in $Tg(NO_2)$, CO_2 in $Tg(CO_2)$, SO_x in $Tg(SO_2)$, CO in $Tg(CO)$, HC in $Tg(HC)$, and PM in $Tg(PM)$ according to four different technology scenarios (TS1–4) and four different ship traffic demand scenarios (DS1–4). Results for the technology scenario 1 (TS1) are shown for different ship traffic demand scenarios (DS1–4) with solid lines in black, those for TS2 with long dashed lines, for TS3 with short dashed lines, and for TS4 with dotted lines (from Eyring et al., 2005b, their Fig. 4; Copyright, 2005; American Geophysical Union; Reproduced by permission of American Geophysical Union).

and they are already partially removed from the atmosphere by wet and dry deposition. These processes non-linearly depend on the concentrations of the primary emissions, the atmospheric background concentrations and on the actual meteorological state of the atmosphere such as height and stability of the marine boundary layer, vertical wind profile or the presence of clouds. Other important factors involve the insolation depending on latitude and time of the day. The chemistry and transport in the marine boundary layer (MBL) is discussed in Section 3.1, while near–field processes and impacts of shipping on the large-scale are assessed in Sections 3.2 and 3.3, respectively.

3.1. Chemistry and transport in the marine boundary layer

3.1.1. Chemistry in the marine boundary layer

To a large extent the chemistry of the MBL, as with the rest of the troposphere, is determined by the oxidation of primary emitted species and their subsequent reactions (Seinfeld and Pandis, 1998).

The main reaction pathways of relevance for the climate active compounds (e.g. CH_4, O_3 and sulphate particles) are the NO_x-catalysed formation of ozone, the gaseous and aqueous oxidation of SO_2 to sulphate aerosol, and the destruction of methane by OH. The halogen-catalysed destruction of ozone can also be significant in the MBL.

The main oxidising agent in the troposphere is the OH radical. This is produced through the ultra-violet photolysis of ozone (R1; see Table 4) followed by reaction of the $O(^1D)$ radical with water vapour (R2) and through conversion of the HO_2 radical to OH by nitric oxide (NO) (R7). Thus NO_x emissions from shipping increase the OH radical through two routes, directly by reaction with HO_2, and indirectly by generating ozone (see below). This extra OH removes methane and other hydrocarbons from the atmosphere.

The formation of ozone is initiated by the reaction of OH with species such as CO and CH_4 forming hydroperoxyl radical (HO_2) and methyl peroxy radical (CH_3O_2), respectively (R3–R6). OH reactions with more complex hydrocarbons are analogous to CH_4, generating

the related organic peroxy radicals. Net ozone formation in the MBL is then a result of competition between ozone formation and sink reaction cycles. In the presence of NO_x, reaction of peroxy radicals with NO leads to formation of NO_2 which photolyses to give ozone (R7–R10). However, at low concentrations of NO_x, peroxy radicals primarily react through peroxy–peroxy self- and cross reactions yielding hydrogen and organic peroxides (R11 and R12). Ozone is mainly destroyed by photolysis (R1 and R2), reaction with HO_2 (R13) and deposition to the ocean surface. Ozone chemistry in the MBL is thus very sensitive to changes in concentrations of NO_x. Fleming et al. (2006) performed calculations of ozone formation in the MBL during the NAMBLEX experiment and found a linear dependency of ozone production rate on NO concentration. Emissions far away from land in relatively clean environment are particularly important from the point of view of the formation of tropospheric ozone. The efficiency of ozone production from NO_x emissions is much greater in cleaner environments (Liu et al., 1987; Lin et al., 1988). There are few NO_x sources over the oceans other than ships. NO_x itself has a short lifetime in the atmosphere but continental emissions of NO_x are often collocated with significant concentrations of the acetyl peroxy radical (either from anthropogenic or biogenic sources). The reaction with NO_x (R14) forms peroxy acetyl nitrate (PAN) which is longer lived than NO_x. PAN formed over the continents can be transported to the marine atmosphere where it can decompose to release NO_x thus providing an additional NO_x source.

The ozone chemistry in the MBL can also be significantly affected by reactive halogen species (Dickerson et al., 1999; Carpenter et al., 2003). The sources of these are autocatalytic

Table 4
Important chemical reactions in the marine boundary layer.

[R1]	$O_3 + h\nu\ (\lambda < 290\ nm) \rightarrow O_2 + O(^1D)$
[R2]	$O(^1D) + H_2O \rightarrow 2\ OH$
[R3]	$OH + CO \rightarrow H + CO_2$
[R4]	$H + O_2 \rightarrow HO_2$
[R5]	$OH + CH_4 \rightarrow H_2O + CH_3$
[R6]	$CH_3 + O_2 \rightarrow CH_3O_2$
[R7]	$HO_2 + NO \rightarrow OH + NO_2$
[R8]	$CH_3O_2 + NO \rightarrow CH_3O + NO_2$
[R9]	$NO_2 + h\nu \rightarrow O(^3P) + NO$
[R10]	$O(^3P) + O_2 + M \rightarrow O_3 + M$
[R11]	$RO_2 + HO_2 \rightarrow ROOH + O_2$
[R12]	$HO_2 + HO_2 \rightarrow H_2O_2 + O_2$
[R13]	$HO_2 + O_3 \rightarrow OH + 2\ O_2$
[R14]	$NO_2 + CH_3COO_2 \Leftrightarrow PAN$
[R15]	$NO_2 + OH + M \rightarrow HNO_3 + M$
[R16]	$X_2 + h\nu \rightarrow 2X\ (X = Cl\ or\ Br)$
[R17]	$X + O_3 \rightarrow XO + O_2$
[R18]	$XO + HO_2 \rightarrow HOX + O_2$
[R19]	$HOX + h\nu \rightarrow OH + X$
[R20]	$HOX \Leftrightarrow HOX(aq)$
[R21]	$HX \Leftrightarrow X^- + H^+$
[R22]	$HOX(aq) + X^- + H^+ \Leftrightarrow X_2 + H_2O$
[R23]	$NO_2 + XO \rightarrow XNO_3$
[R24]	$XNO_3 + H_2O(aq) \rightarrow HOX(aq) + HNO_3(aq)$
[R25]	$XNO_3 + X^-(aq) \rightarrow X_2(aq) + HNO_3(aq)$
[R26]	$N_2O_5 + H_2O(aq) \rightarrow HNO_3(aq) + HNO_3(aq)$
[R27]	$N_2O_5 + X^-(aq) \rightarrow XNO_2 + HNO_3(aq)$
[R28]	$SO_2 + OH + H_2O \rightarrow H_2SO_4$
[R29]	$SO_2 \Leftrightarrow SO_2(aq)$
[R30]	$SO_2(aq) \Leftrightarrow HSO_3^-(aq) + H^+(aq)$
[R31]	$HSO_3^-(aq) \Leftrightarrow SO_3^{2-}(aq) + H^+(aq)$
[R32]	$HSO_3^-(aq) + H_2O_2(aq) \rightarrow SO_4^{2-}(aq) + H^+(aq)$
[R33]	$HSO_3^-(aq) + O_3(aq) \rightarrow SO_4^{2-}(aq) + H^+(aq) + O_2$
[R34]	$SO_3^{2-}(aq) + O_3(aq) \rightarrow SO_4^{2-}(aq) + O_2$
[R35]	$DMS + OH \rightarrow CH_3S(OH)CH_3$
[R36]	$DMS + OH + O_2 \rightarrow CH_3SO_2 + HCHO + H_2O$
[R37]	$DMS + NO_3 + O_2 \rightarrow CH_3SO_2 + HCHO + HNO_3$
[R38]	$CH_3S(OH)CH_3 \rightarrow MSA\ or\ SO_2$
[R39]	$CH_3SO_2 \rightarrow MSA\ or\ SO_2$

halogen activation mechanisms (Vogt et al., 1996) and photolysis of I-containing organic compounds emitted by macroalgae in coastal regions (O'Dowd et al., 2002). In the halogen activation mechanism, gaseous HOBr and HOCl are scavenged on sea-salt aerosol where they form only slightly soluble BrCl and Br_2 that are released back to the gas phase (R16–R18, R20, R22). Halogen atoms formed by photolysis of the dihalogens or the I-containing organic compounds react with ozone to form halogen monoxides. These recycle in the gas phase via reaction sequences involving HOX ($X = Br$, Cl or I; reactions R17–R19) that catalytically destroy ozone analogously to atomic chlorine and bromine cycling in the stratosphere. The halogen activation mechanism also acts as a sink for HO_2 (HO_2 consumed in R18 is transferred to $H_2O_{(aq)}$ by R20 and R22). Formation of halogen nitrates XNO_3 in R23 and their heterogeneous reactions on sea-salt and in particular on acidic sulphate particles (R24, R25) can significantly decrease the lifetime of NO_x in the MBL. In box model simulations supported by measurements of gas phase and aerosol composition in the tropical MBL, Pszenny et al. (2004) showed that heterogeneous reactions of halogen nitrates on sulphate particles were responsible for approximately 25% of the total sink of NO_x in the MBL. Importance of these reactions on sea-salt particles varied with sea-salt concentrations from 5% of the total NO_x sink at moderate sea-salt concentrations to as much as 60% at high sea-salt concentrations. Heterogeneous reactions of dinitrogen pentoxide (N_2O_5) (R26, R27) can also influence the NO_x lifetime, however, these reactions were not found to be important in the MBL.

The MBL is important for production of aerosol particles. Primary aerosol in the form of sea-salt particles is produced from bursting bubbles and by direct release of sea-spray from the wave crests. Oxidation of dimethyl sulfide (DMS) released by phytoplankton produces sulphate aerosol that is active as cloud condensation nuclei (CCN) (Charlson et al., 1987), and methyl sulphonic acid (MSA) aerosol that does not act as CCN (R35–R39). Most DMS oxidation is initialized by the OH radical (R35 and R36), with a contribution from the nitrate radical (NO_3) at night (R37). Shipping will therefore increase the DMS oxidation rate, particularly in winter. This means that more DMS is oxidised over the ocean, which may increase CCNs.

SO_2 emissions from shipping are oxidized to sulphate primarily in the aqueous phase (in cloud droplets and sea-salt particles) by hydrogen peroxide (H_2O_2) and ozone (R29–R34) and also in the gas phase by the OH radical (R28). The largest impact of shipping on sulphate chemistry is through the direct emissions of SO_2. However, increases in the OH radical due to NO_x emissions will enhance the gaseous oxidation pathway. This pathway is important since it leads to new particle generation which is important for the climate forcing whereas aqueous oxidation adds mass to existing particles.

Dry deposition to the ocean surface occurs for many of the reactive species discussed here (O_3, NO_2, SO_2, sulphate). This is generally at a lower rate than to the continental surface, and the deposition velocity is typically 1 mms^{-1} for ozone. Even so, deposition to the ocean is still an appreciable loss rate for ozone since the photochemical loss is slower in the cleaner environment. Collins et al. (2009) showed that around a third of the ozone generated by shipping was lost to deposition, the majority of which was over the ocean. It might be expected that dry deposition is more rapid in rougher seas. Fairall et al. (2007) calculated an enhancement in ozone deposition of up to a factor of 3 due to ocean turbulence. This is not generally taken into account in modelling studies.

3.1.2. Transport in the marine boundary layer

A major part of ship emissions (excluding emissions in ports and in the vicinity of coastlines) are emitted in or transported to the

MBL. As mixing and transport in the MBL has specificities that substantially differ from conditions that determine mixing and transport of the land-based emissions, and since these conditions impact on the effect of these emissions on chemistry, this section discusses micrometeorological properties of the MBL.

The large heat capacity of water and efficient mixing processes in the upper oceanic mixed layer makes the distinguished property of the MBL the remarkable spatial and temporal homogeneity in temperature. The air–sea temperature differences tend to be small, except close to the coasts. If the air temperature is much lower than the sea surface temperature (SST), vigorous convection will reduce the temperature difference, and, except for areas with large horizontal gradients in SST, horizontal advection can not maintain the imbalance. Hence the surface layer is nearly neutral over almost all of the oceans (Pasquill stability class D) (Arya, 1988). When warm air moves over cooler water, the 'very stable' condition corresponding Pasquill stability class F occurs and movement of cold air over warmer water leads to 'unstable' condition corresponding Pasquill stability class B (Song et al., 2003).

Due to the small air–sea temperature difference the major component of the energy balance at the sea surface is the latent heat of evaporation, which is typically 50–200 W m^{-2}, an order of magnitude larger than the sensible heat flux, typically 0–30 W m^{-2}. Only during episodes of cold air outbreaks over warmer seas the sensible heat becomes an important part of the energy balance (Arya, 1988).

The transfer of momentum from the atmosphere to the ocean partly generates surface waves and partly drifts currents and turbulences in the upper layers of the ocean. Relation between these two modes is complex and not easy to determine. Near the water surface (few wave heights) a downwelling–upwelling pattern of wave motion generates both positive and negative vertical momentum flux (Sullivan et al., 2004). The wind profile measurements above few wave heights show validity of the Monin–Obukhov relation

$$U/u^* = (1/k) \times \ln(z/z_0 - \Psi_m(z/L)), \tag{2}$$

where u^* is the friction velocity, κ the von Karman's constant taken as 0.4, z_0 the roughness length and $\psi_m(z/L)$ the stability function for momentum that describes deviation from the neutral wind profile and depends on stability index z/L where z is the height above the surface and L is the Monin–Obukhov length (Edson and Fairall, 1998). The roughness length z_0 of the sea surface has a range between around 10^{-4} and 10^{-3} m (Arya, 1988) and depends on the wind and wave fields. The simplest and widely used relation between z_0 and u^* is described by Charnock's formula based on dimensional arguments (Charnock, 1955) $z_0 = a \times (u^{*2}/g)$, where a is an empirical Charnock's constant, also called dimensionless roughness, and g is the gravitational acceleration. The value of a derived from block-averaged datasets from many different observation sites at open sea is 0.01–0.02 (Charnock, 1955: 0.012, Garratt, 1977: 0.0144, Wu, 1980: 0.0185). The underlying wave field (the wave age) also affects the Charnock's constant (Johnsson et al., 1998) and it varies largely when the water surface is affected by the coast (Arya, 1988).

Most often the MBL is perceived as being well mixed between the surface layer and the capping inversion (this layer is also called 'mixed layer'). When cumulus clouds are forming near the top of this layer, where the latent heat from condensation allows the newly formed clouds to penetrate the capping inversion and transport fluid to the overlaying layer, the concept of MBL has sometimes been extended to this overlaying layer (Cotton et al., 1995).

The MBL is frequently covered with clouds. It is cloud free in areas where warm air is transported over colder air and a stable and shear-driven BL is formed. The tropical MBL is associated with deep convection and formation of cumulus clouds. The mixed layer height z_{mbl} extends from a few hundred meters up to over 1000 m and the overlaying layer extends typically up to 2 km in Pacific and Atlantic ocean and up to 4.5 km in Indian ocean (Ramana et al., 2004 and references there in). Variation of thickness of the MBL results in exchange between the MBL and the free troposphere. Russell et al. (1998) determined the bi-directional entrainment rates during the ACE-1 experiment. The thickness of the MBL z_{mbl} at mid latitudes extends typically between 500 and 1000 m. During the daytime the subcloud layer of the MBL can be decoupled from the overlaying stratocumulus layer due to the shortwave radiation heating of the cloud. In the afternoon the mixing throughout the whole MBL will reoccur. This process occurs especially in the MBL topped with a thick cloud layer and is of importance for the air–sea exchange and dispersion of pollutants in the MBL.

Expansion of the ship plume in the MBL is often described by expansion coefficient F. If we assume expansion in the direction perpendicular to the main plume axes only, neglecting concentration differences in neighbouring volumes of the plume, we obtain:

$$\frac{\partial \overline{c}_{pl}}{\partial t}\Big|_{mix} = \left(\overline{c}_{bg} - \overline{c}_{pl}\right) \times F(t) = \left(\overline{c}_{bg} - \overline{c}_{pl}\right) * \frac{1}{A_{pl}}\frac{dA_{pl}}{dt}, \tag{3}$$

where $\overline{c}_{bg}$ and $\overline{c}_{pl}$ are mean concentrations in background air and in plume respectively and A_{pl} is the plume area. The vertical expansion is usually limited by the capping inversion layer. Song et al. (2003) parameterised the expansion by a Gaussian plume taken from the offshore and coastal dispersion (OCD) model (Hanna et al., 1985). The area of the expanding plume is defined as $A_{pl} = \pi\sigma_y\sigma_z$, where σ_y and σ_z are the time dependent standard deviations for the horizontal and vertical distribution of the concentration in a Gaussian shaped plume, which are parameterized for three stability classes and for downwind distances <10 and >10 km (Table 5). The plume is not allowed to exceed $\sqrt{2/\pi}*z_{mbl}$. von Glasow et al. (2003) formulated the plume dispersion coefficient with time-independent horizontal and vertical expansion coefficients α and β, $F = (\alpha + \beta)/t$, and restricted the vertical plume expansion to $z = z_{mbl}$. They estimated the values of $\alpha = 0.75$ and $\beta = 0.6$ based on observations during the MAST experiment (Durkee et al., 2000a). Both approaches neglect the inhomogeneity perpendicular to the main plume axes. Hooper and James (2000) analysed lidar measurements of a ship spray plume in convective MBL and found maximum values of the vertical mixing velocity of 0.54 m s^{-1}. When the plume was released outside the updraft regions of the convective cells, much lower values of vertical mixing were found as the plume was first transported laterally into the updraft regions (the corresponding mean vertical mixing velocity calculated for an MBL of 750 m thickness and $\beta = 0.6$ according to von Glasow et al. (2003) is 0.21 m s^{-1}). This phenomenon can be only simulated by large eddy simulation (LES) model coupled with a Lagrangian particle dispersion model. Schlager et al. (2008) present a comparison of such a simulation within situ aircraft measurements, where a ship plume is released in a stable MBL on 23 July 2004 in the English Channel. Fig. 7 shows a rather complex pattern of the plume expansion simulated by the model compared to CO_2, NO and total reactive nitrogen (NO_y) peak concentrations measured in the plume from a research aircraft. The concentrations shown in the figure are normalized by plume concentration at $t = 3000$ s. The LES and Lagrangian particle dispersion model simulation shows very good agreement with the measurements.

Table 5
Formulas for lateral and vertical dispersion coefficients, σ_y and σ_z for downwind distances $\times$ as a function of time t after the plume release for moving ships[a] (reformulated for $t = x/u_r$ from Song et al., 2003).

Over-water stability class		σ_y, m[b]	σ_z, m
B (unstable)	$x < 10$ km	$0.08tu(1 + 0.0001tu)^{-1/2}$	$0.06tu$
	$x > 10$ km	$0.08tu(1 + u/u_r)^{-1/2}$	$0.06tu$
D (neutral)	$x < 10$ km	$0.04tu(1 + 0.0001tu)^{-1/2}$	$0.03tu(1 + 0.0015tu)^{-1/2}$
	$x > 10$ km	$0.04tu(1 + u/u_r)^{-1/2}$	$0.03tu(1 + 0.0015tu)^{-1/2}$
F (stable)	$x < 10$ km	$0.02tu(1 + 0.0001tu)^{-1/2}$	$0.008tu(1 + 0.0003tu)^{-1}$
	$x > 10$ km	$0.02tu(1 + u/u_r)^{-1/2}$	$0.008tu(1 + 0.0003tu)^{-1}$

[a] Here, the wind speed is u and u_r defines the magnitude of the resultant vector of the wind speed and ship speed.
[b] The minimum value of the leading constant in the σ_y formulas is $0.5/u$, where u is the wind speed.

3.2. Near-field processes

It is recognised now that subgrid-scale processes should be accounted for in global models with a resolution of several hundred kilometres because of non-linearities in atmospheric processes. In plume processes that need to be considered include oxidation of NO_x, scavenging of HNO_3, ozone formation, oxidation and heterogeneous removal of SO_2, impact of ship-emitted and background particles on plume chemistry and processing of particles affecting their physical properties.

3.2.1. Nitrogen compounds and ozone

Davis et al. (2001) proposed that in the plume the reaction of NO with HO_2 (R7) leads to enhanced OH mixing ratios and thus to an enhanced rate of the main sink reaction for NO_x (R15). Fast oxidation of NO_x in concentrated plumes due to elevated OH levels could lead to a substantial decrease in lifetime of NO_x compared to the background. Additional chemical loss of NO_x can be through PAN formation, through nighttime formation of NO_3 and N_2O_5, followed by their heterogeneous oxidation on aerosol, and through NO_2 oxidation by halogen oxides (R23) yielding halogen nitrates. In highly concentrated parts of the plume and in cases when the plume is emitted to a NO_x pre-polluted background with already enhanced OH levels, reaction R15, being also a sink for OH, can cause OH depletion in the plume, which leads on contrary to increased NO_x lifetime in the plume.

Chen et al. (2005) inferred from measurements in a ship plume a chemical NO_x lifetime of about 2 h, almost four times shorter than calculated for background air. Ship plume modelling studies of Song et al. (2003) and von Glasow et al. (2003) showed NO_x lifetimes of a factor of 2.5–10 and 4, respectively, shorter in the ship plume than in the background. Photo-stationary calculations with a box model in Chen et al. (2005) showed that 80% of the loss was due to R15 and a remainder due to PAN formation. Song et al. (2003) found that elevated levels of NO_3 and N_2O_5 shortened the NO_x lifetime during the nights. The observed NO_x loss rates in the ship plume measured by Chen et al. (2005) were 30% larger than those estimated with the model. Measured HNO_3 levels in the plume were only about 20% of the mixing ratios estimated by the model simulations indicating a rapid HNO_3 loss in the plume not included in the model, possibly uptake of HNO_3 on particles. NO_y/CO_2 measurements in a ship plume aged 0.5 h by Schlager et al. (2008) also indicate a loss of 50% gas phase NO_y. A modelling study by Franke et al. (2008) found an increased NO_x lifetime compared to NO_x lifetime in the background during the first hours of the simulation, which was only slightly reduced later on. The NO_x emission source strength in the Franke et al. (2008) study was much higher than in previous studies (a large container ship emitting 145 g NO_x/s, compared to an average ship emitting 47 g NO_x/s) leading to much higher NO_x mixing ratios at the initial stage of the plume. Also model simulations of the ship plume measured by Schlager et al. (2008) showed increased lifetime of NO_x during

1–2 h after the emission. A sensitivity study has shown that at high NO_x background concentrations, when the ozone formation is in peroxy radical limited regime, the increased lifetime would persist over the entire lifetime of the plume. The chemical lifetimes of NO_x in the ship plumes from different studies are summarised in Table 6.

Neglecting the plume processes in global models may lead to an overestimation of O_3 formation. In early stages of the plume the main reason of this overestimate is that the plume becomes limited in peroxy radicals that would react with NO in the ozone-forming NO_x cycle (R7–R10). Later, in more diluted stages of the plume the decreased NO_x mixing ratios in plume caused by its reduced lifetime have further effect on ozone formation. von Glasow et al. (2003) quantified the effect of neglecting the plume processes in a grid of a global model by comparing a box model including multiple plumes with a box model including continuous homogeneous emissions of a same magnitude. They found 50% lower O_3 mixing ratios when the plume dispersion was considered. Franke et al. (2008) compared box model simulations of a single plume entraining background air using the Gaussian plume model parameterization (PD case) with a box model where the same ship emissions were instantaneously dispersed into a large grid box (ID case). The ozone formation in the PD case was found to be 70% lower than in the ID case.

3.2.2. Sulphur compounds

In contrast to NO_x, Davis et al. (2001) and Eyring et al. (2007) found significant underestimation of the SO_2 mixing ratios in the MBL simulated by the global models compared to observations. Model simulations in Davis et al. (2001) produced significant increase of SO_2 mixing ratios in MBL from ship emissions. The ensemble mean increase of SO_2 from shipping in Eyring et al. (2007) was small, so the authors questioned whether the underestimation of SO_2 in the marine boundary layer in the models is due to the ship emission inventory or due to the underestimation of another source (e.g. DMS), overestimation of a sink (e.g. oxidation), errors associated with simulating specific events (e.g. horizontal/vertical transport and mixing), or a combination of several factors, opened. Davis et al. (2001) put forward a hypothesis that in contrary to oxidation of NO_x, where its increased concentration in ship plumes and ship lanes leads to shortening of NO_x lifetime through increased OH concentrations, the SO_2 oxidation by OH is only a minor oxidation pathway and the pH sensitive oxidation by heterogeneous reactions, the dominant oxidation pathway for SO_2, may be significantly inhibited by H_2SO_4 produced in oxidation. This theory was, however not confirmed with measurements in plumes. On contrary, the SO_2 concentrations measured in aged ship plumes were significantly lower than values expected from the sulphur fuel content and the dilution as given by the plume excess CO_2 in all studies (Chen et al., 2005; Williams et al., 2005; Schlager et al., 2008). The reason for this discrepancy is still to be investigated.
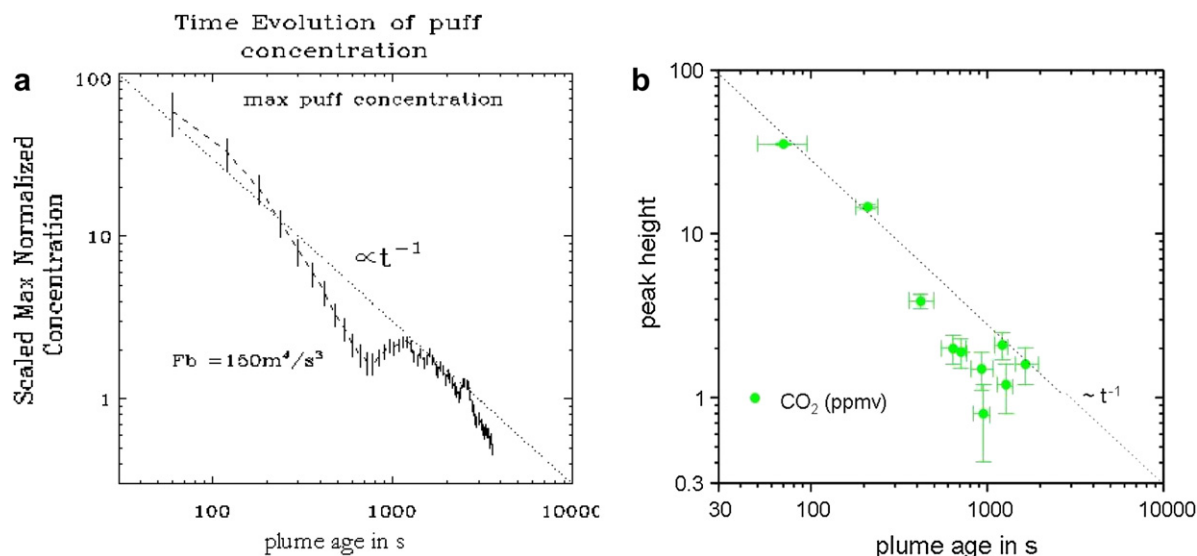
Fig. 7. (a) Plume concentrations normalised by concentrations at plume age $t = 3000$ s, $(c_{pl} - c_{bg})/(c_{lp} - c_{bg})_{t=3000}$ plotted against the age of the plume. Maximum normalised concentrations in LES and Lagrangian particle dispersion coupled model (dashed line) and (b) measured peak normalised concentrations. The dotted line on both panels is a mean concentration development in a plume described by normalised concentration $C = 3000/t$, t in s (Schlager et al., 2008).

3.2.3. Particles

von Glasow et al. (2003) studied the effect of processes on heterogeneous particles emitted from the ship and on the background sea-salt and sulphate particles in plume. They found that the partly soluble particles emitted from the ship (sulphate-coated particles) have the potential to substantially decrease the NO_x lifetime and ozone formation in the plume only under extremely high particle emissions due to reactions of NO_3, N_2O_5, $BrNO_3$ and $ClNO_3$. Heterogeneous processes on ship-emitted soot were found to be negligible. Background sea-salt and sulphate aerosol may have a larger effect on the plume chemistry than ship-emitted particles. This effect may well be caused by changes of NO_x, O_3, and OH mixing ratios in the background air in the two sensitivity runs.

Petzold et al. (2007) measured the transformations of aerosols in a plume of a large container ship. An extensive change in the size-distribution was observed from a count median diameter of 52 nm of the raw exhaust to 70 nm in the young plume and 100 nm in the plume aged 0.5 h. The strong nucleation mode measured in the raw exhaust was completely depleted in the aged plume. The mass of BC and the associated number of non-volatile combustion particles were well correlated with the excess CO_2 in the plume. From the decay of the non-volatile particle concentration in the aging plume a maximum plume lifetime of about 24 h was estimated by Petzold et al. (2007) for a well mixed MBL.

3.2.4. Effective emissions

Several approaches to parameterise the non-linear plume effects in global models have been suggested. Petry et al. (1998) defined effective emission indices (EEI) for aviation, an approach where the emissions are modified in a way that after being dispersed into a global model grid cell, the effective emissions approach at a certain time horizon the same mixing ratios as if they had undergone plume dispersion. Esler (2003) introduced a more general concept of equivalent emissions where the modification of emissions is calculated from the mixing history of the plume and applied it on a simplified NO_x–CO–O_3–HO_x system. Franke et al. (2008) further developed and applied the EEI concept of Petry et al. (1998) on ship plume emissions, however only for a limited set of conditions. They presented variation of the EEI of NO_x, O_3 and H_2O_2 with time of the day of the emission and with the source strength of NO_x. The EEI are expressed as $\delta_{rel}X = \delta X/\Delta NO_x$, where δX is the effective emission of NO_x, O_3 and H_2O_2 (in mol or mol s^{-1}) and ΔNO_x is the actual emission of NO_x. The EEI of ozone varied between -20% for emission at nighttime to -750% for emissions in the middle of the day. The EEI of NO_x were also negative with largest absolute values at nighttime (-7%) and smallest around noon (-1%). The EEI of H_2O_2 showed similar pattern of diurnal variation as EEI of NO_x with values of -20% at night and $+5\%$ at noon. If this concept should be used in a global model, extensive

Table 6

Chemical lifetimes of NO_x in observed and model-simulated ship plumes and ratios of the background air to plume lifetimes. The source strength of NO_x (emitted as NO), Q_{NO} (in g(NO)/s) is given in column 3. Notes in the last column indicate how the NO_x lifetimes were derived: The measured lifetime is inverse value of the first order loss rate coefficient of measured NO_x enhancement due to ship emissions relative to the enhancement of a non-reactive plume tracer as derived in Chen et al. (2005). The modelled lifetime is the photochemical lifetime of NO_x defined by first order loss rates $L_{NO_x} = k1[OH][NO_2] + k2[NO_3][DMS] + k3[NO_3] + 2^*k4[N_2O_5]$, where $k1$–$k4$ are the appropriate reaction rate constants.

	Fuel type	Q_{NO} g s^{-1}	τ_{NO_x} in plume h	$\tau_{NO_x}(bg)/\tau_{NO_x}(pl)$ d.l.	Note to τ_{NO_x}
Chen et al. (2005)	Residual	13.4	1.7/2.4	3.8/2.7	Measured/modelled
d.t.t.o.	Residual	–	1.9/2.25	3.4/2.9	Measured/modelled
Schlager et al. (2008)	Residual	184	128/6.3	0.15/0.99	Model, early plume/average
d.t.t.o. ship corridor					
Song et al. (2003)	Residual	4	10.5–25.4	1.3–1.8	Model, tropics – mid. lat.
d.t.t.o.	Residual	20	5.1–14.5	2.4–3.2	Model, tropics – mid. lat.
von Glasow et al. (2003)	Residual	16.5	2.8/7.5	5.3/3.6	Model, early plume/average
Franke et al. (2008)	Residual	145	5/8	0.6/1.01	Model, early plume/average

calculations of EEI for combinations of meteorological and chemical conditions and larger set of different source strengths would be necessary.

3.3. Large-scale effects on atmospheric composition

Global modelling studies (Lawrence and Crutzen, 1999; Capaldo et al., 1999; Kasibhatla et al., 2000; Davis et al., 2001; Endresen et al., 2003; Eyring et al., 2007; Dalsøren et al., 2007; Collins et al., 2009) have generally used similar global totals for NO_x and SO_2 emissions from ships, about 3 Tg (N) year^{-1} and 4 Tg (SO_x) year^{-1}. The distributions used have been more variable. The EDGAR2.0 distribution contains narrow shipping lanes (Fig. 3, upper panel), while the COADS distribution uses data from ship position reports and is more widespread (similar to ICOADS, Fig. 3, lower panel). Endresen et al. (2003) used AMVER as their preferred distribution (Fig. 3, middle panel) and compared the ozone response to the simulated response using COADS and PF (Purple Finder). The COADS distribution is more concentrated at higher latitudes and over the North Atlantic than AMVER. The PF distribution is similar to AMVER but more concentrated towards the coasts. Lauer et al. (2007) applied the three emission inventories displayed in Fig. 3 in a global aerosol climate model to address uncertainties in emission totals and global distributions on the impact of oceangoing shipping on aerosols, clouds and the radiation budget.

3.3.1. Large-scale chemistry effects of ozone precursor emissions

Being a short-lived chemical compound, NO_x enhancement from ship emissions is closely dependent on the routes. NO_x increases of 200 to more than 1000 ppt in the shipping lanes were simulated by Lawrence and Crutzen (1999), and increases of 200–500 ppt derived from the multi-model mean of ten state of the art atmospheric chemistry models have been reported by Eyring et al. (2007). Both studies used the EDGAR dataset (Fig. 3, upper panel). The other emissions datasets (COADS, AMVER, PF) are more realistic and more spread out. Using one of the latter emission distributions, NO_x increases of over 200 ppt were calculated in Kasibhatla et al. (2000) over the northern Atlantic and Pacific oceans. Increases of 100–150 ppt over the same regions were calculated by Dalsøren et al. (2007), Endresen et al. (2003) and Davis et al. (2001). Estimated background concentrations vary considerably between models, with the earlier models that included little or no NMVOCs (non-methane VOCs) and PAN chemistry (e.g. Lawrence and Crutzen, 1999) having very low background NO_x levels, around 10 ppt or less. A model that did include higher hydrocarbons (Endresen et al., 2003) simulated July north Atlantic background values of 20–50 ppt in the continental outflow, compared to below 5 ppt inside the Azores anticyclonic circulation. In the coastal regions of North America and Europe, NO_x enhancements from shipping can be 200–300 ppt in a higher resolution model (Dalsøren et al., 2007). Using the EDGAR emissions database (Eyring et al., 2007; Collins et al., 2009) gives particular high NO_x values in the Baltic due to an overestimate of emissions from this area in the inventory.

The lifetime of shipping NO_x (defined as the burden divided by the emission rate) can be calculated from Fig. 9 of Eyring et al. (2007). Total troposphere NO_x burden increased by about 0.012 Tg for emissions of 3.1 Tg year^{-1} (excluding two outlier models), resulting in a lifetime of shipping NO_x of around 1.5 days.

Some comparisons of shipping generated NO_x in large-scale models with observations have shown significant overestimates (Kasibhatla et al., 2000; Davis et al., 2001; Endresen et al., 2003). These studies suggested that subgrid-scale processes not included in the global models rapidly convert NO_x to total reactive nitrogen (NO_y) in ship plumes. However these models overestimated the NO_x concentrations even without shipping. The amount of observational data available to compare to is very limited and comparisons are very sensitive to the choice of the dataset. Eyring et al. (2007) found disagreement between their multi-model average NO_2 simulations and the observations used in Davis et al. (2001), but agreement with a larger observational dataset from Emmons et al. (2000).

Observations from satellite have confirmed the existence of high NO_2 concentrations along shipping lanes (Beirle et al., 2004; Richter et al., 2004, see Fig. 8). The implications for the larger scale of neglecting small-scale plume chemistry depend on the resolution of the models, and the size of the tracks. From the point of view of large-scale composition impacts, there is not enough observational data to confirm or refute the various emission datasets used by global models. There are sound chemical reasons why spreading shipping plumes over the size of grid squares used by global models could overestimate the NO_x, OH and ozone responses (see Sections 3.1 and 3.2). Plume model studies have not yet come up with a simple reduction factor for the NO_x emissions that could be applied to global models. Thus in a crude attempt to compensate for plume effects, global models tend to use a lower NO_x emission total of ∼3 Tg(N) year^{-1} rather than the estimate of ∼5 Tg(N) year^{-1} recommended in Table 3.

Modelling studies generally simulate increases in ozone due to shipping NO_x emissions of up to 12 ppb in the central North Atlantic, and central North Pacific in July. Ozone enhancements tend to peak in mid-ocean, and not in the coastal regions, due to the higher NO_x levels there from continental sources. Eyring et al. (2007) found much smaller increases over the Pacific due to the smaller and more concentrated emissions in the EDGAR dataset used. In January, ozone increases of 2–4 ppb are found in the tropical and sub-tropical oceans except in the Eyring et al. (2007) study, which has lower tropical emissions. In winter, Eyring et al. (2007) found shipping NO_x leads to ozone destruction in northern Europe. This is strongest over the Baltic and countries bordering it and is due to the removal of HO_x through the reaction R15. In the high-latitude winter where there is little insolation, HO_x levels are already low so the OH + hydrocarbon oxidation is the rate determining step for ozone production (R3 and R5). This ozone destruction is not found in other studies and may be exacerbated due to the high level of shipping emissions in the Baltic in the EDGAR distribution.

To identify changes in coastal ozone production requires a high (by global modelling standards) resolution model. The Dalsøren et al. (2007) study with a 1.8° × 1.8° resolution identifies regions of high ozone production from shipping in smaller seas with busy shipping, such as the North Sea, Baltic, Mediterranean, Red Sea and Persian Gulf where enhancements exceed 14 ppb (see Fig. 9).

The climate impact of the extra ozone generated by emissions of NO_x from shipping largely depends on the change to the total ozone column. The distribution and magnitude are quite sensitive to the emissions distribution used. In Dalsøren et al. (2007) these changes are generally concentrated in a band from the equator to 45°N (2–3 DU) with a local maximum over the Persian Gulf and Arabian Sea (up to 5 DU). The Eyring et al. (2007) simulations do not show this zonal band. They have a maximum south of India of 1.2 DU, otherwise increased ozone columns of up to 1.0 DU are found over the North Atlantic. Again, the lack of ozone changes at lower latitudes is likely to be due to the EDGAR shipping distribution and will have a significant effect on the calculated radiative forcing from shipping (Section 5.2).

None of the studies listed here included any of the halogen chemistry described in Section 3.1.1 in their models. As a result they are likely to slightly overestimate the marine boundary layer ozone concentrations. The impact of CO, VOCs and direct methane from
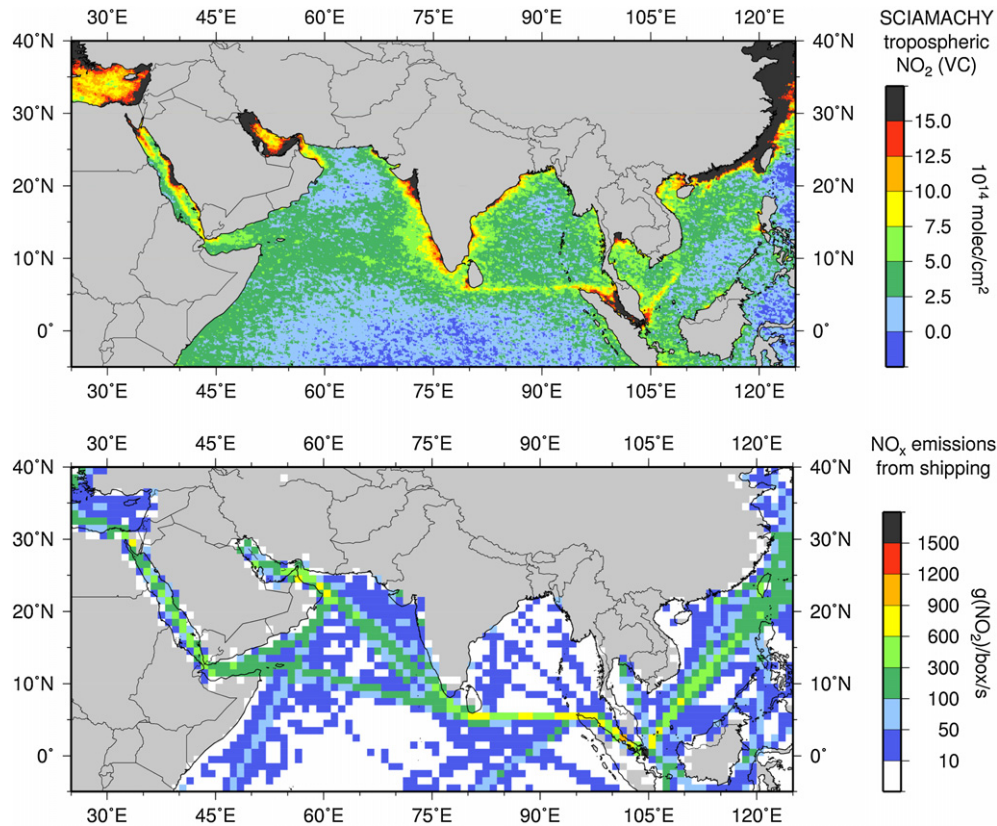
Fig. 8. NO$_x$ signature of shipping in the Indian Ocean. Upper panel: Tropospheric NO$_2$ columns derived from SCIAMACHY data from August 2002 to April 2004. Lower panel: Corresponding distribution of NO$_x$ emissions from shipping taken from an emission inventory (from Richter et al., 2004, their Fig. 3; Copyright, 2004; American Geophysical Union; Reproduced by permission of American Geophysical Union).
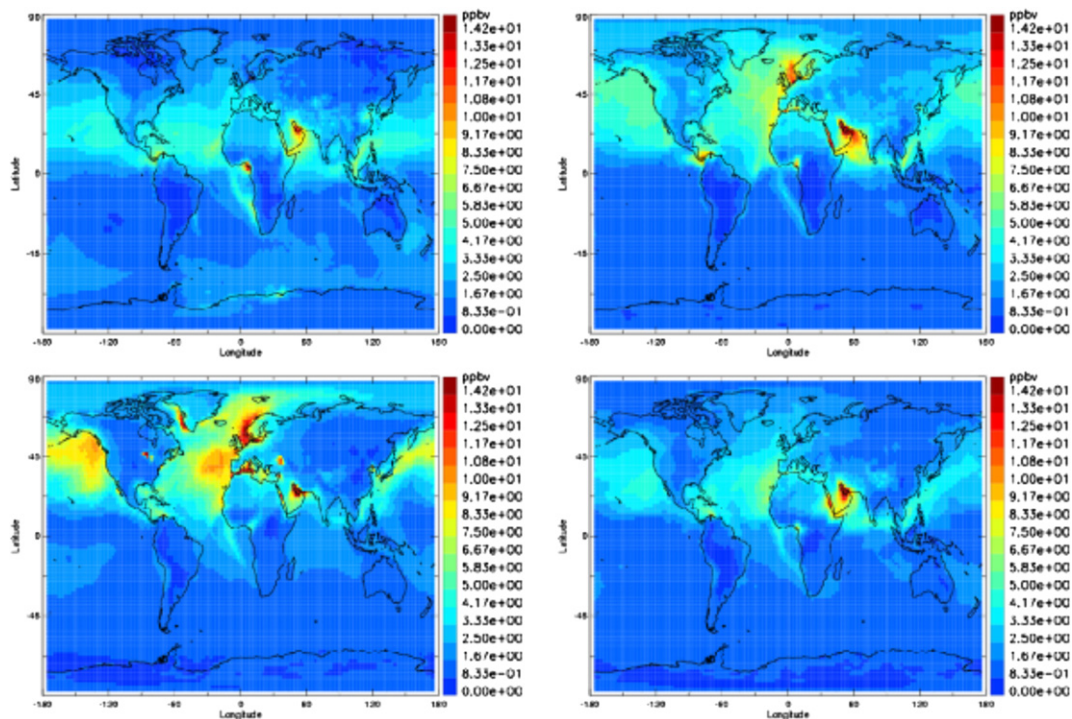

Fig. 9. Ozone change at the surface due to year 2000 ship emissions simulated by the OsloCTM2 for the months (top left) January, (top right) April, (bottom left) July and (bottom right) October (from Dalsøren et al., 2007, their Fig. 5; Copyright, 2007; American Geophysical Union; Reproduced by permission of American Geophysical Union).

shipping on ozone is very small, generally less than 0.1 ppb (Endresen et al., 2003; Eyring et al., 2007).

3.3.2. Methane lifetime

Emissions of NO_x increase the concentrations of the OH radical and hence reduce the methane lifetime. Reductions in methane lifetime due to shipping NO_x vary between 1.5% (Dalsøren et al., 2007; Eyring et al., 2007) to 0.4 years ($\sim$5%) (Lawrence and Crutzen, 1999; Endresen et al., 2003). The reaction between methane and the OH radical is very temperature dependent. Hence methane is oxidised principally in the tropics in the lower troposphere. Thus it might be expected that the models using the EDGAR distribution, which has little NO_x enhancement in the tropics, would show the least effect on methane lifetime. However, there seems little obvious relationship between the methane impact in the model results published so far and the emission distribution used. It is likely that other aspects of the model formulations are more important. Four of the five models reporting methane lifetimes in Eyring et al. (2007) calculated decreases of 0.13 years (1.56%) with the fifth model calculating nearly twice this amount.

Hoor et al. (2008) show that compared to other forms of transport, shipping has the greatest effect on the methane lifetime. This is because the NO_x emissions are released into a cleaner, environment and have larger contributions in the tropics than land-based transport. Aircrafts have a smaller effect as their emissions are away from the lower troposphere where most methane oxidation occurs.

The decrease in methane lifetime and consequent decrease in the methane concentrations leads to a longer term decline in the ozone concentrations that may offset some or all of the direct ozone production from the NO_x emissions. Derwent et al. (2008) found that the ozone response to the methane decrease due to land-based NO_x emissions from Asia cancelled out about half of the direct ozone production as a global average. The ozone decrease is much more globally homogenous than the increase thus it is important for climate forcing (Section 5.2) but less important for air quality.

3.3.3. Large-scale chemistry effects of aerosol emissions and their precursors

Ship emissions are responsible for up to 60% of the July surface SO_2 concentrations over large areas of the North Atlantic and North Pacific, and for more than 30% of the concentrations of the rest of the Northern Hemisphere oceans (Capaldo et al., 1999). The chemistry-transport model (CTM) results also revealed that shipping contributes up to 5–20% of the non-sea-salt sulphate concentrations in coastal regions over land, demonstrating the importance of including ship emissions in regional air quality studies. These findings are confirmed in an independent study by Lauer et al. (2007). Generally oceanic SO_2 observations are underestimated by models (Davis et al., 2001; Eyring et al., 2007) even when shipping emissions are included. Thus shipping SO_2 emissions may be underestimated if anything. As SO_2 is primarily controlled by aqueous processes, unlike NO_x it is expected that SO_2 is largely independent of enhanced OH in the plume (Davis et al., 2001).

Ship emissions contribute 10–40% to sulphate concentrations over most of the Northern Hemisphere oceans (Lauer et al., 2007). The fractional increases depend on the assumed background. Over the remote oceans sulphate comes mainly from DMS and is a function of the DMS emission rates and chemistry in the models (R35–R39). Shipping at 2000 levels contributes about 3% to the global sulphate loading (Endresen et al., 2007; Eyring et al., 2007). Sulphur emissions might reduce air quality over land, e.g. by contributing to sulphate aerosol concentration or sulphate deposition. Globally shipping contributes 5% of the total sulphur

deposition, and around 3% to the deposition over land (Collins et al., 2009). Ships contribute 5–10% of the sulphate deposition over coasts of Europe, North America and China (Endresen et al., 2003; Collins et al., 2009; Dalsøren et al., 2007). The precise numbers vary with distance from the coasts. These calculations have been undertaken with global models that are not able to resolve coastal areas well enough to give more than approximate estimates. Contributions of shipping to aerosol components other than sulphate are small. Lauer et al. (2007) calculate contributions to BC of 0.4–1.4%, to POM of 0.1–1.1%, and to nitrate aerosol of 0.1–2.3%. The large ranges in these estimates reflect the very large uncertainty due to the three different emission inventories used.

4. Impacts on air quality, ecosystems and human health

About 70% of the emissions from oceangoing shipping occur within 400 km of the coastlines along the main trade routes (Corbett et al., 1999). Thereby, ship emissions can have an impact on the air quality in coastal regions and may partly offset the decline of land-based sources and coastal pollution due to national control measures (Schlager and Pacyna, 2004). The addition of NO_x and SO_2 from ships also contributes to acidification of the ocean (Doney et al., 2007). On the global scale these effects are small, but could be more significant in shallower coastal waters where shipping is concentrated.

4.1. Regional impact on atmospheric composition

Regional impacts of ship emissions include enhancements of NO_x, CO, VOCs, and SO_2 boundary layer gas concentrations and subsequent perturbations of ozone and other photochemical products, increase of the concentration of particulates (sulphate aerosol, POM, BC), and enhanced deposition of acidifying and eutrophying sulphur and nitrogen compounds. In addition, there is a significant local impact on pollution in the vicinity of major harbours (Canepa and Georgieva, 2005).

Model studies of the regional impact of ship emissions have been performed for the Atlantic Ocean seaboard of Europe (Jonson et al., 2000; Derwent et al., 2005; Collins et al., 2009) the Pacific Basin (Davis et al., 2001), the United Kingdom (Dore et al., 2006), the Scandinavian countries (Dalsøren et al., 2007), and the Mediterranean region (Marmer and Langmann, 2005). Note that these models are of varying resolution. Derwent et al. (2005), Collins et al. (2009), Davis et al. (2001), and Dalsøren et al. (2007) used global models with resolutions of $\sim$500, $\sim$250, 265, and $\sim$200 km respectively. Jonson et al. (2000), Dore et al. (2006) and Marmer and Langmann (2005) used regional models with resolutions of 50 , 5 and $\sim$50 km. The resolution of the models affects their ability to simulate coastal regions, although the finest resolution model uses statistical meteorology with winds from wind roses and deposition according to constant drizzle, which may affect its ability to simulate the transport of pollutants near coast. For Europe, the modelled contribution of shipping to summertime mean surface ozone concentrations from emissions of NO_x and VOC precursors vary from 2 to 4 ppb (5–15%) over the coasts of north-western Europe (Derwent et al., 2005; Collins et al., 2009). Additional regional ozone impacts are simulated for the Mediterranean region and the Baltic Sea.

The conditions in the Mediterranean region during summer (slow transport and mixing, high solar radiation intensity, limited wash out) favour in particular the accumulation of primary ship emissions and production of secondary emissions (Marmer and Langmann, 2005). According to model simulations, secondary sulphate aerosols from shipping account for 54% of the mean

sulphate aerosol concentration in this region during the summer season (Fig. 10).

Coastal areas of north-western Europe and north-western North America are substantially impacted by nitrate and sulphate deposition from shipping. In Europe the modelled maximum annual sulphate deposition from ship emissions of 400 mg S m^2 year^{-1} occurs over the North Sea and Baltic Sea (Derwent et al., 2005). This is about 50% of the total sulphur deposition in these regions. Along the western coasts of the UK and Scandinavia, the calculated percentage of total sulphur deposition from shipping range between 10 and 25% (Dore et al., 2006; Dalsøren et al., 2007; Collins et al. 2009).

There are only a few measurement studies on the regional impact of ship emissions. Satellite measurements from the GOME and SCIAMACHY instrument clearly detected enhanced NO_2 tropospheric vertical column densities along international shipping routes in the Indian Ocean (Beirle et al., 2004; Richter et al., 2004; see Fig. 8). Aircraft survey flights across the ship corridors off the coast of Brittany revealed very inhomogeneous concentration fields of shipping-related trace species (Schlager et al., 2008). A multitude of ship plumes were detected in the vicinity of the main shipping routes, aged between minutes and up to 5 h (Fig. 11). The measured ship plumes of different ages were often superimposed on each other and showed concentration enhancements in NO, NO_y, SO_2, CO and CO_2. Also ship engine combustion aerosol particles were detected in the aged plumes (Petzold et al., 2007). Along the shipping lanes, the measured ozone concentrations were up to 5 ppb lower compared to values observed outside the corridors as expected from the reaction of fresh NO ship emissions with ozone to NO_2. These observations are in accordance with results from a regional model for the experimental conditions.

There is also a considerable local impact of shipping-related emissions on air quality in the vicinity of major harbours, in particular, from NO_x, SO_2, PM, and VOCs emissions. Ship manoeuvring in harbours contributes about 6% of NO_x and 10% of SO_2 to total shipping emissions (Corbett and Fischbeck, 1997). Besides manoeuvring, loading and unloading of tankers also contribute substantially to harbour emissions since this is a highly energy consuming process (Wismann and Oxbol, 2005). The harbour emissions often occur near major residential areas and can be transported far inland due to local land–sea breeze winds. For example, near the waterways of the port of Rotterdam shipping causes an enhancement of the surface NO_2 mixing ratio of 5–7 ppb (Keuken et al., 2005).

4.2. Impact on ecosystems and human health

Local and regional air quality problems in coastal areas and harbours with heavy traffic are of concern because of their impact on human health. Furthermore, emissions from ships are transported in the atmosphere over several hundreds of kilometres, and thus can contribute to air quality problems on land, even if they are emitted over the sea. This pathway is especially relevant for ozone and the deposition of sulphur and nitrogen compounds, which cause acidification of natural ecosystems and freshwater bodies and threaten biodiversity through excessive nitrogen input (Cofala et al., 2007).

Due to the non-linear nature of ozone chemistry, the effects of shipping depend on the magnitude of the emission change, and on the choice of scenario for the land-based emissions. Ozone is toxic to plants (Ashmore, 2005), affecting growth (e.g. crop yield) and appearance. The potential for sulphate and nitrate deposition to cause ecosystem change can be defined by the critical loads. The effects on sulphate aerosol levels and deposition fluxes of sulphate aerosols and oxidised nitrogen species are larger, and are significant compared to expected changes in land-based emissions. On average shipping increases current sulphate aerosol, and sulphate and nitrate deposition over Europe by about 15% (Collins et al., 2009). Sulphate deposition increases the acidity of soils, rivers and lakes. This harms ecosystem growth. Nitrate deposition increases the available nitrogen of soils (eutrophication; Stevens et al., 2004; Galloway et al., 2003; Cofala et al., 2007). This can harm ecosystems through asymmetric growth in nitrogen poor regions (e.g. algae in rivers and lakes, and lichens and mosses in hillsides), in some regions encouraging invasive alien species.

Shipping impacts on human health through the formation of ground-level ozone and particulate matter. Cofala et al. (2007) provided an assessment of the health and environmental impacts of shipping scenarios in Europe for the year 2020. They find that compared to land-based sources, at least some of the maritime emissions have less health and environmental impacts since they are released sometimes far from populated areas or sensitive ecosystems. However, they also find that in harbour cities ship emissions are in many cases a dominant source of urban pollution and need to be addressed when compliance with EU air quality limit values for, e.g. fine particulate matter is an issue. An increase in ship emissions will counteract the envisaged benefits of the costly efforts to control the remaining emissions from land-based sources in Europe. Technologies exist to reduce emissions from
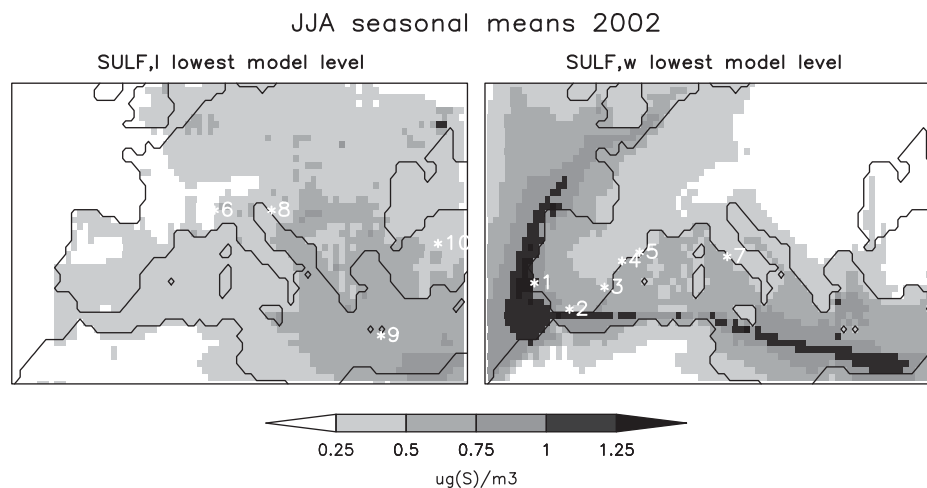

Fig. 10. Calculated seasonal mean (June/July/Aug.) of sulphate concentration (μg S m^{-3}) at lowest model level over Europe from land-based emissions (left panel) and ship emissions (right panel). From Marmer and Langmann, 2005, their Fig. 6. Copyright 2005 Elsevier.
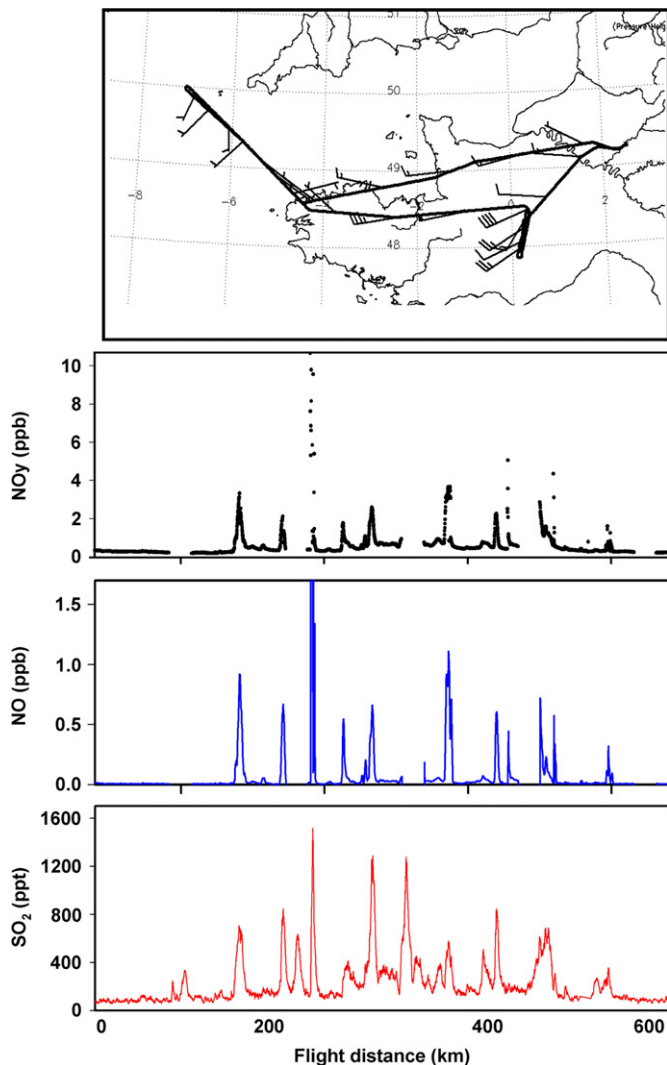
Fig. 11. Mixing ratios of NO_y, NO, and SO_2 measured during two ship corridor transects across the English Channel (Schlager et al., 2008).

shipping beyond what is currently legally required. Epidemiological studies also consistently link ambient concentrations of particulate matter to negative health impacts, including asthma, heart attacks, hospital admissions, and premature mortality. Mortality resulting from PM emission from ships has been estimated by either estimating loss of life expectancy in months (Cofala et al., 2007) or by using total number of premature deaths (Corbett et al., 2007b). Previous assessments of regional shipping-related health impacts focused on European or Western US regions, but ignored long-range and hemispheric pollutant transport (California Air Resources Board, 2006; Cofala et al., 2007). This undercounts oceangoing shipping impacts within local and regional jurisdictions. Recent results by Corbett et al. (2007b) indicate that shipping-related PM emissions are responsible for around 60,000 cardiopulmonary and lung cancer deaths annually, with most deaths occurring near coastlines in Europe, East Asia, and South Asia. This number is bounded by a range of 20,000–104,000 premature deaths when considering the uncertainties due to emission inventories and models used in this study. Based on previous estimates of global $PM_{2.5}$-related mortalities (Cohen et al., 2005), the Corbett et al. (2007b) estimates indicate that 3–8% of these mortalities are attributable to marine shipping. Cohen et al.

(2005) estimate that approximately 712,000 cardiopulmonary deaths are attributable to urban outdoor $PM_{2.5}$ pollution annually. Thus, the relationship between concentrations and mortality appears nearly proportional within reasonable percentage uncertainty bounds. Uncertainties of the results are detailed in the Supporting Information of Corbett et al. (2007b).

5. Radiative forcing and impact on climate

In addition to the impact on atmospheric composition and human health, ship emissions have an impact on climate through changes in clouds (Section 5.1) and RF (Section 5.2). RF is a common metric to quantify climate impacts from different sources in units of W m^{-2}, since there is an approximately linear relationship between global mean radiative forcing and change in global mean surface temperature (Forster et al., 2007). Other climate metrics are discussed in Section 5.3.

5.1. Impact on clouds

The perturbation of a cloud layer by ship-generated aerosol potentially changes the cloud reflectivity. This can be identified by elongated structures in satellite images known as ship tracks (Section 5.1.1). In addition to ship tracks, aerosol emissions from shipping can also affect clouds on a larger scale after dispersion. The impact of shipping on aerosol properties and on large-scale clouds is assessed in Section 5.1.2.

5.1.1. Ship tracks

Of all anthropogenic sources, ship-stack effluents provide the clearest demonstration of the indirect aerosol effect on cloud albedo. Curves of larger reflectance in cloud fields are observed in satellite imagery and identified as ship tracks. The first observations of ship tracks were presented by Conover (1966) and the many subsequent observations confirm they are a recurrent phenomenon (e.g. Coakley et al., 1987; Durkee et al., 2000a; Segrin et al., 2007). Such perturbations of the marine stratiform cloud field are characterised as long-lived, narrow, curvilinear regions of enhanced cloud reflectivity which occur downwind of ships. An example of ship tracks appearing as bright features in satellite data is given in Fig. 12.

The brightness of a cloud observed from space is determined primarily by its visible optical thickness τ, which for drops large compared to wavelength can be approximated as

$$\tau = \frac{3LWP}{2\rho r} \qquad (4)$$

where LWP is the liquid water path, ρ is density of water and r is the particle effective radius. Using this approach Twomey et al. (1968) concluded that observed increased optical thickness in ship tracks was consistent with the addition of CCN to a cloud layer with drop concentrations of about 1–10 drops cm^{-3}, i.e. a clean maritime boundary layer. This simple description captures the essence of ship track formation and is widely accepted.

Airborne measurements in a cloud free environment above a cargo ship showed that approximately 12% of exhaust particles act as CCN (Hobbs et al., 2000). Several studies have shown that the droplet concentration in the ship tracks was enhanced significantly over the ambient cloud and that the effective radius was reduced (Albrecht, 1989; Radke et al., 1989; Durkee et al., 2000b; Ferek et al., 2000; Schreier et al., 2006). Taylor et al. (2000) summarised the results of 11 aircraft flights off the west coast of North America during the Monterey Area Ship Track (MAST) experiment. The impact of the aerosol emitted from the ships was found to be very

dependent on the background cloud microphysics. If the ambient or background cloud was of continental influence (and thus contained a higher typical CCN concentration than clean maritime air) the cloud was found to be relatively insensitive to further aerosol emissions, with only a weak microphysics signature in the ship tracks. However, if the background clouds were pristine maritime stratiform then increases in droplet concentration of a factor of 2, and reduction in droplet size of up to 50%, were measured.

A detailed description of the average or composite ship track characteristics for the entire MAST observation period is given in Durkee et al. (2000a). The set of ship tracks examined during the MAST experiment formed in marine boundary layers that were between 300 and 750 m deep, and no tracks formed in boundary layers above 800 m. The tracks form in regions of high relative humidity, small air–sea temperature differences, and moderate winds (average of 7.7 ± 3.1 ms^{-1}). The composite ship track is 296 ± 233 km long, 7.3 ± 6 h old, and 9 ± 5 km wide. The ship is, on the average, 16 ± 8 km from the head of the ship track along the relative wind vector and corresponds to a time of 25 ± 15 min. The experiment showed a high dependence of ship track development on the amount of sulphur in the shipping fuel.

Ship emissions can increase the concentration of CCN to over 10 times that of clean air, to about 1000 CCN per cm^3 (Durkee et al., 2000c). As the total amount of water in polluted and unpolluted clouds at a particular height is about the same, the water in polluted clouds is distributed over a much larger number of smaller droplets. The precipitation process is therefore highly sensitive to the size of the initial cloud droplets (e.g. Rogers and Yau, 1989). These smaller water droplets are then less likely to grow into larger drops of precipitation size, extending the lifetime of the cloud and increasing reflectivity. Ackerman et al. (1995) used numerical simulations to show that ship track lifetimes could be in excess of a day. Ship track measurements have yielded strong hints, but not clear evidence, that precipitation is affected by exhaust from ships. Albrecht (1989) showed that for ship tracks measured off the coast of California on 13 June 1976, the droplet size-distributions were narrower and the droplet count was lower, which directly corresponded to a notable reduction in drizzle. During an aircraft campaign off southern California, Radke et al. (1989) observed an increase in cloud liquid water and a decrease in drizzle-size drops in ship tracks. Ferek et al. (2000) also noticed a reduction in drizzle drops in ship tracks off Washington but no associated increase in cloud liquid water. During the MAST experiment Ferek et al. (2000) used aircraft measurements to report that significant changes in cloud droplet size-distribution, as well as reductions in drizzle flux and concentrations of drops larger than 50 μm radius, were observed in ship tracks when drizzle was more uniformly present in the ambient cloud.

A satellite study of clouds forming in the region of the English Channel showed a trend of increasing cloud albedo and decreasing cloud top temperature (Devasthale et al., 2006), which may be related to the impact of ship emissions. The global distribution of ship tracks from 1 year of AATSR data has been reported by Schreier et al. (2007) and from ATSR/2 data by Campmany et al. (2009). Fig. 13 shows the percent coverage of ship tracks derived from AATSR measurements in 2004. It shows the predominant area for ship track occurrence is a latitude band between 30° and 60° N in both the North Atlantic and the Pacific Ocean. In the Southern Hemisphere ship tracks are much less frequent and are concentrated between 10° and 30° S off the west coasts of southern Africa and Australia.

5.1.2. Large-scale impact on clouds

Ship plumes mix with the ambient air and are able to affect the surrounding clouds on a larger scale than visible ship tracks. To quantify the overall effect, global aerosol model studies or satellite trend analyses are needed. The model simulations by Lauer et al. (2007) reveal that the effect of changes in particle number concentration, aerosol size-distribution and particle composition due to ship emissions on clouds is mainly confined to the lower troposphere, from the surface up to about 1.5 km. This implies that regions with a frequent high amount of low clouds above the oceans are most susceptible to ship emissions. Such regions coincide with dense ship traffic over the Pacific Ocean west of North America, and over the Atlantic Ocean west of southern Africa and in the North eastern Atlantic Ocean. In particular, accumulation mode particles act as efficient condensation nuclei for cloud formation.

Whereas the cloud liquid water content is only slightly increased in these simulations, effective radii of cloud droplets decrease, leading to cloud optical thickness increase up to 5–10% depending on geographic region and ship emission inventory used. The sensitivity of the results is estimated by using three different emission inventories for present-day conditions. According to these studies, shipping increases the aerosol number concentration, e.g. up to 40% in the size range of the Aitken mode (typically <0.1 μm) in the near surface layer over the Northern Atlantic.

Above the main shipping routes in the Atlantic Ocean the modal mean diameter of the Aitken mode decreases from 0.05 to 0.04 μm. Due to subsequent growth processes such as condensation of sulphuric acid vapour onto pre-existing particles or coagulation, some particles emitted by shipping grow into the next larger size range of the accumulation mode (typically >0.1 μm). Accumulation mode particles can act as additional cloud condensation nuclei. The changes in chemical composition (Section 3.3.3), particle number concentration, and size-distribution cause an increase in aerosol optical thickness above the oceans, which is related particularly to enhanced scattering of incoming solar radiation by sulphate, nitrate, ammonium, and associated aerosol liquid water. Increases in total aerosol optical thickness up to 8–10% are found over the Indian Ocean, the Gulf of Mexico and the North eastern Pacific, depending on the ship emission inventory.

5.2. Radiative forcing

Ship emissions of CO_2, SO_2, NO_x and other O_3 precursors perturb atmospheric concentrations of greenhouse gases (CO_2, CH_4 and O_3), and aerosols (mainly sulphate, SO_4), causing both positive and
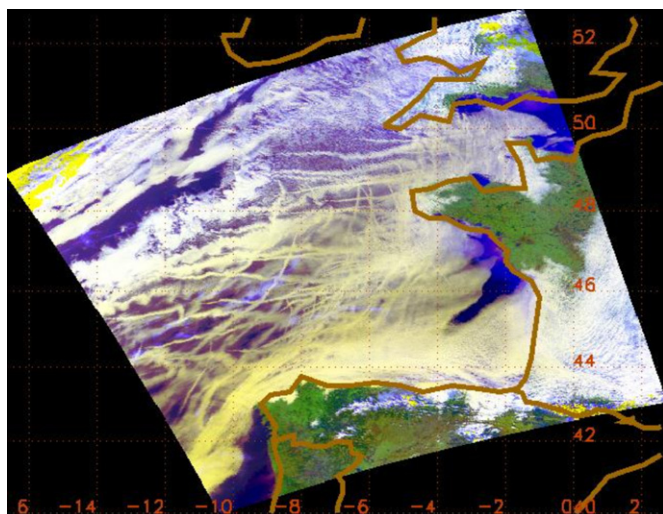

Fig. 12. Ship tracks over the Gulf of Biscay (colour composition from AVHRR on 27 January 2003).
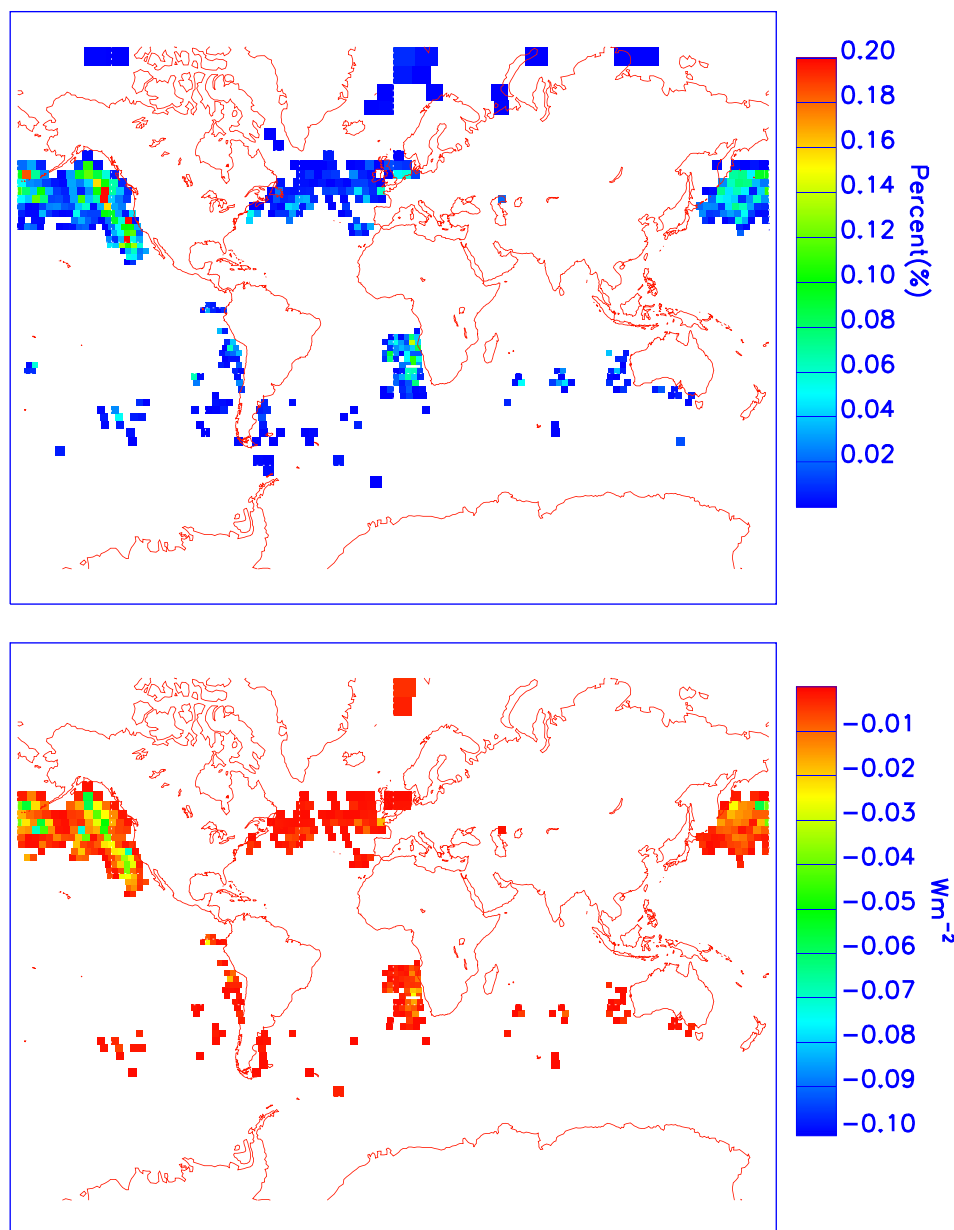
Fig. 13. Annual mean coverage distribution of ship tracks (left panel) and resulting RF distribution due to ship tracks in W m^{-2} (right panel) in 2004. From Schreier et al. (2007), their Fig. 3. Copyright 2007 American Geophysical Union; Reproduced by permission of American Geophysical Union.

negative contributions to direct radiative forcing (RF) of climate. In addition, ship-derived aerosols cause a significant indirect RF, via changes in cloud microphysics (see Section 5.1). As CO_2 is a well mixed greenhouse gas, its atmospheric lifetime (>100 year) is much longer than global atmospheric mixing timescales, so ship CO_2 emissions generate a RF in just the same way as any other CO_2 source. SO_2 and NO_x are reactive species with much shorter lifetimes (days). Emissions of these species generate SO_4 and O_3, which themselves have lifetimes of days to weeks in the troposphere. Perturbations to SO_4 and O_3, and hence their RFs, have regional-scale structure, and are closely related to their precursor source distributions. Emissions of NO_x, and the O_3 they form, lead to enhanced levels of the hydroxyl radical (OH), increasing removal rates of CH_4, generating a negative RF (Wild et al., 2001). Because of the decadal CH_4 lifetime, this RF has a global signature.

Table 7 summarises estimates of the present-day contribution of ship emissions to these different RF components from several

studies (Capaldo et al., 1999; Endresen et al., 2003; Eyring et al., 2007; Lee et al., 2007; Lauer et al., 2007; Dalsøren et al., 2007; Fuglestvedt et al., 2007). These studies used a variety of ship emission inventories and different models. Some studies only focussed on specific RFs. Three studies estimated uncertainties: Eyring et al. (2007) used a multi-model ensemble to assess inter-model differences; Fuglestvedt et al. (2007) used the OsloCTM2 model to carry out an uncertainty analysis based on uncertainties in fuel use, emission factors, modelling atmospheric dispersal and removal, and RF; and Lauer et al. (2007) used three different inventories to study the direct and indirect aerosol RFs due to shipping. Further uncertainties arise due to plume processes, which are so far not resolved in the models.

The last row of Table 7 summarises the range of values for each RF from the literature. We take this range as a useful indicator of uncertainty, with the caveat that a small range in the literature does not necessarily reflect a narrow uncertainty range, but may just be

due to the use of common methodologies or emissions between studies. A summary of RF literature ranges for the years 2000 and 2005 is displayed in Fig. 14. Except for CO_2, the 2005 RF are calculated from the RF values in 2000 by linearly scaling them with the increase in emissions from 2000 to 2005 (see Section 2.2.1 and Fig. 4). The RF due to CO_2 emissions is calculated from the actual evolution of CO_2 emissions up to 2005 using the climate response model described in Lee et al. (in this issue). Table 7 also includes a comparison with the total anthropogenic RFs 2005 for the various components reported in Forster et al. (2007). In the following text we discuss the 2005 RF values.

The RF from shipping generated CO_2 for 2005 in Table 7 is 37 mW m^{-2}. The IPCC Fourth Assessment Report estimated that the total RF from CO_2 (all sources) was 1.66 W m^{-2}, so that shipping according to this estimate contributed approximately 2.2% to the total anthropogenic CO_2 RF in 2005. The CO_2 RF is the least uncertain (37 mW m^{-2} ± 25%), with the main sources of uncertainty being the present-day magnitude and historical evolution of ship CO_2 emissions. The CO_2 RF of 43 mW m^{-2} calculated for the year 2000 by Lee et al. (2007) is thought to be more accurate than the lower values of 26–30 mW m^{-2} calculated by Eyring et al. (2007) and Endresen et al. (2003), as the former study took into account the historical evolution of ship CO_2 emissions. This evolution differs from other anthropogenic emissions, so a simple scaling, as performed in the latter two studies, is less appropriate.

The RFs related to ship NO_x emissions, associated with the increase in tropospheric O_3 (26 mW m^{-2}) and the decrease in CH_4 lifetime (−33 mW m^{-2}), compare to values of 60 and −170 mW m^{-2} given by Forster et al. (2007; Table 2.13) for the total anthropogenic tropospheric O_3 and CH_4 RFs, respectively, associated with all anthropogenic NO_x emissions. It should be noted that these total RFs come from a single model study (Shindell et al., 2005), and carry significant uncertainties, and direct comparison with the ship RFs, which come from a range of different models, should be treated with caution. Both the ship RFs have literature ranges of ±67%. These ranges derive from uncertainties in the magnitude and spatial distribution of NO_x emissions, and also how models simulate the tropospheric chemistry of NO_x, O_3 and OH. No study to date has explicitly estimated the contribution of ship NO_x emissions to changes in nitrate aerosol, although Lauer et al. (2007) found that sulphur emissions accounted for about 75% of the total

ship-derived aerosol RFs, indicating that 25% is associated with other aerosol or aerosol precursor emissions. The impact of NO_x emissions on OH, and hence CH_4 lifetime (Section 3.3.2), strongly depends on the latitudinal distribution of emissions (Fig. 3), which varies significantly between the studies reported in Table 7. This is a major contributing factor to the differences in CH_4 RFs between different studies. Ships also directly emit methane: Eyring et al. (2005a) estimate emissions of ∼0.5 Tg CH_4 year^{-1}. The IPCC Fourth Assessment Report estimates a total present-day anthropogenic CH_4 source of 341 Tg CH_4 year^{-1} (range 264–428 Tg CH_4 year^{-1} – see Denman et al. (2007), Table 7.6), and the CH_4 RF from pre-industrial to present-day as 0.48 W m^{-2} (Forster et al., 2007). Assuming a simple scaling, ship emissions of CH_4 contribute about 0.7 mW m^{-2} to this total, so direct CH_4 emissions only slightly offset the negative RF related to NO_x emissions. The overall effect of NO_x (and CH_4) emissions is probably a net negative RF, as more weight should be placed on the multi-model ensemble results of Eyring et al. (2007) and the multi-simulation ensemble results of Fuglestvedt et al. (2007); both these studies indicate a net negative RF. It should be reiterated that the positive O_3 RF will be regional in structure, whilst the negative CH_4 RF will be more global.

The direct RF from ship-derived SO_4 (−31 mW m^{-2}; about 8% of the total anthropogenic direct RF from SO_4 of −0.4 W m^{-2}) has a range of about ±52% and the RF from POM which has been estimated only by one study (−0.4 mW m^{-2}) has a range of about ±67%. Sulphur emissions, together with other aerosol precursor and direct aerosol emissions, also perturb cloud microphysics, producing an indirect RF. The best known manifestation of the indirect RF is the production of 'ship tracks' (Section 5.1.1). However, while enhanced backscattering with values between 10 and 100 W m^{-2} has been reported for some areas and regions (Fig. 13), the global RF due to ship tracks is thought to be small (−0.4 to −0.6 mW m^{-2} ± 40%; Schreier et al., 2007) and negligible compared to global model estimates of the total indirect aerosol RF and the RF contributions from other ship emissions. The reported indirect RF range exceeds nearly an order of magnitude, extending from −66 mW m^{-2} (Fuglestvedt et al., 2007) to as large as −600 mW m^{-2}, or up to 39% of the total indirect RF from anthropogenic aerosols (Lauer et al., 2007). Lauer et al. (2007) included contributions to the indirect effect from several aerosols (SO_4, NO_3, NH_4, BC, POM and aerosol liquid water), whereas all the other

Table 7

Global total emissions (Tg(CO_2, S, N, BC, POM) year^{-1}) and radiative forcings (mW m^{-2}) for the year 2000 (and extrapolated values for 2005) from different studies estimating the impacts of oceangoing ship emissions; 2005 total anthropogenic RFs and the estimated contribution of ships towards them are also included.

Study	CO_2 Tg(CO_2)	SO_2 Tg(S)	NO_x Tg(N)	BC Tg(BC)	POM Tg(POM)	CO_2 RF	SO_4 RF direct	Aerosol RF indirect	CH_4 RF indirect	O_3 RF	BCRF	POM RF
Capaldo et al. (1999)		4.2	3.1					−110 (−60 to −210)				
Endresen et al. (2003)	501	3.4	3.6			30	−20		−28	29		
Eyring et al. (2007)	501	3.9	3.1			26	−14		−14	9.8 ± 2.0		
Lee et al. (2007)	812	6.0	6.5			43	∼−22	∼−110 from CA99	−11	28		
Lauer et al. (2007)		3.8–5.9	2.9–6.5	0.05–0.13	0.06–0.71		−12 to −38	−190 to −600				
Dalsøren et al. (2007)									−14			
Fuglestvedt et al. (2007)	577	4.2	4.4	0.2	0.06	35 [−6, +7]	−31 [−16, +15]	−66 [−48, +28]	−43 ± 13	32 ± 9	2.0 ± 0.9	−0.3 ± 0.2
Range[a]	501–812	3.4–6.0	2.9–6.5	0.05–0.2	0.06–0.71	26–43	−47 to −12	−600 to −38	−56 to −11	8 to 41	1.1 to 2.9	−0.5 to −0.1
Mean[b] (2000)	780	5.5	5.4	0.13	0.14	34	−25	−333	−27	21	2	−0.3
Mean[c] (2005)	960	6.7	6.6	0.16	0.17	37	−31	−409	−33	26	2	−0.4
Total anth.[d] (2005)						1660 ± 170	−400 ± 170	−700 [−1100, +400]	−170 ± 85	60 ± 30	340 ± 250	−190 ± 200

[a] Range spans the maximum and minimum literature values used by modellers; where individual studies quote an uncertainty, this has also been included. These ranges are depicted by whiskers in Fig. 14.

[b] Mean for emissions taken from Table 3. Mean for RFs is the average of the maximum and minimum literature values; where individual studies quote a range, this has not been included, except in the case of Lauer et al. (2007). These means are depicted by boxes in Fig. 14.

[c] Apart from CO_2, 2005 values are calculated from extrapolation of 2000 values (see Section 5.2 for details).

[d] Total anthropogenic RFs and uncertainties from Forster et al. (2007), Table 2.12 (CO_2, SO_4 direct, and aerosol indirect) and Table 2.13 (effect of NO_x emissions on O_3 and CH_4; BC and POM).
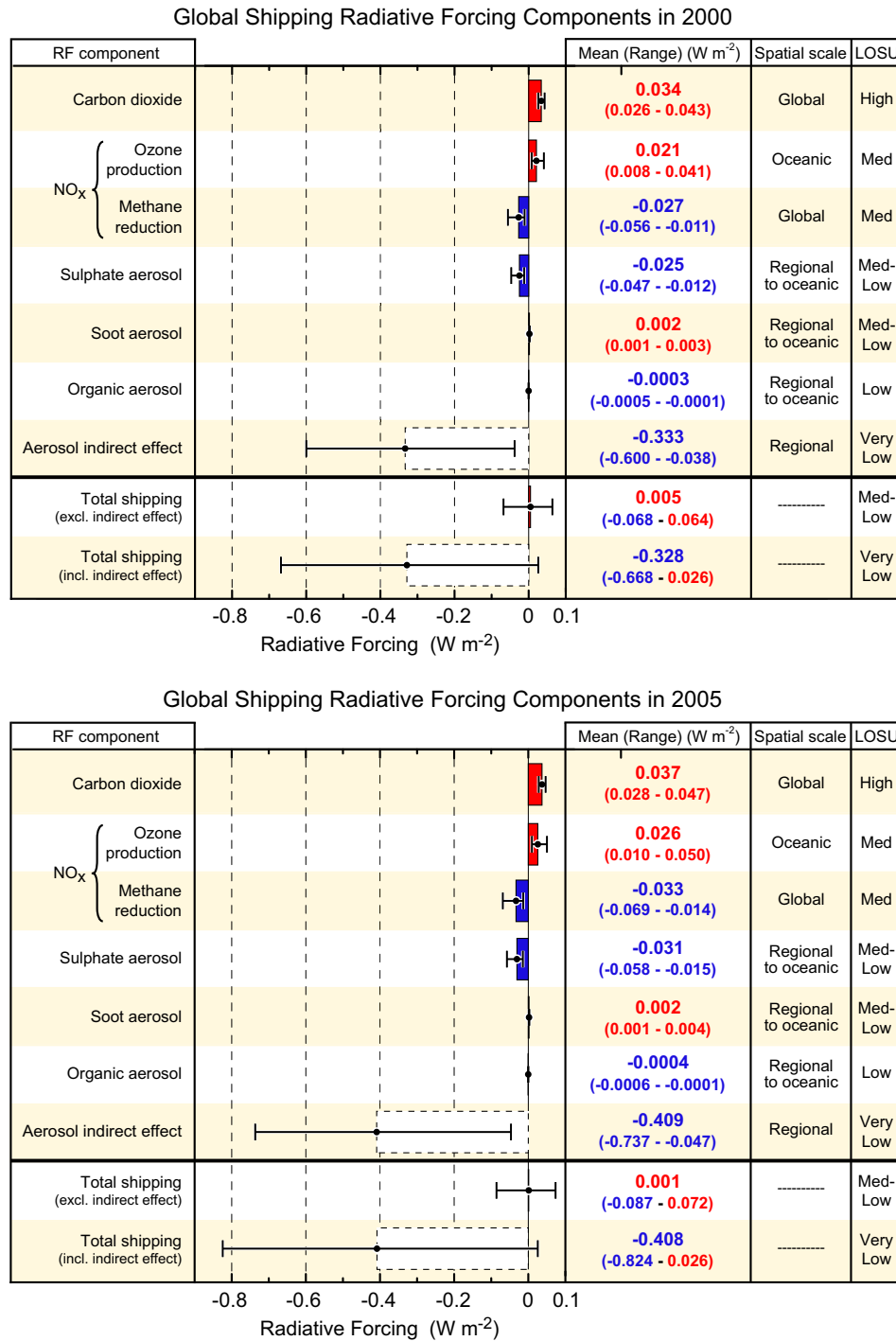
Fig. 14. Global average annual mean radiative forcing (RF) and literature ranges due to emissions from oceangoing shipping in W m^{-2} for 2000 (upper panel) and for 2005 (lower panel). The boxes show the mean of the lower and upper estimate reported in the literature and the whiskers show the range of literature values given by the highest and lowest estimate (see Table 7). The typical geographical extent (spatial scale) of the RF and the level of scientific understanding (LOSU) is given in addition. The RF contributions with very low LOSU are displayed in dashed lines. The figure does not include the positive RF that could possibly occur from the interaction of BC with snow which has so far not been investigated for ships.

studies only considered the indirect effect related to changes in SO$_4$. In a sensitivity study, Lauer et al. (2007) removed all ship sulphur emissions, and found that the total ship aerosol RF fell by 75%, indicating that ship sulphur emissions are responsible for 75% of the ship aerosol RF. This should be taken into account when comparing with the other studies. Lauer et al. (2007) used three different emission inventories, with significantly different spatial distributions (Fig. 3); these produce a wide range for the indirect RF (−190 to −600 mW m^{-2}) due to the differing coincidence of ship-derived aerosol and low marine cloud. The lower boundary of −66 mW m^{-2} is the result of Fuglestvedt et al. (2007), who used the ratio of the indirect and direct RF over the ocean from Kvalevåg and Myhre (2007) to estimate the indirect aerosol RF. In this way they accounted for the land–ocean differences. However, the global

model results of Lauer et al. (2007) indicate that a simple scaling of the total anthropogenic indirect aerosol RF to the contribution of an individual source to the total aerosol burden, even if this is done only over the ocean, is questionable, because the large values they calculate mainly stem from those regions where ship emissions coincide with frequent occurrence of low clouds, which are highly susceptible to the enhanced aerosol number concentration in an otherwise clean marine environment (Fig. 15). The only other study that also used a global model to estimate the indirect aerosol effect was carried out by Capaldo et al. (1999). They estimated the indirect aerosol RF of ship-derived sulphate particles from model studies without detailed aerosol microphysics and aerosol–cloud interaction, and found a value of -110 mW m^{-2}. As Lauer et al. (2007) considered a wider range of aerosols, and found that sulphate contributed about 75% to the total ship-derived aerosol RF, the Capaldo et al. (1999) estimate is close to the lowest estimate given in Lauer et al. (2007). Fuglestvedt et al. (2007) estimate the RF due to BC emissions from ships at 2.0 ± 0.9 mW m^{-2}.

Despite the wide range of RF values reported, all studies agree that the present-day net RF due to shipping is negative (see Fig. 14), in contrast to, for instance, estimates of RF from aircraft (Sausen et al., 2005). However, none of the studies on RF from shipping so far investigated the positive RF that could possibly occur from the interaction of BC with snow (Hansen and Nazarenko, 2004; Hansen et al., 2005; Koch and Hansen, 2005; Flanner et al., 2007). Flanner et al. (2007) applied a snow, ice, and aerosol radiative model coupled to a GCM with prognostic aerosol transport and studied the climate forcing from fossil fuel, biofuel, and biomass-burning BC emissions deposited to snow. They find that global annual mean equilibrium warming resulting from inclusion of BC in snow is 0.1–0.15 K depending on the set of present-day emissions used, but that the annual Arctic warming is significantly larger (0.5–1.6 K). The results indicate that the interaction between snow and BC could be an important component of the carbon aerosol climate forcing, in particular in the Arctic. A similar positive BC/snow forcing from ships could potentially play a role in the Arctic in the future (see Section 7.2).

5.3. Temperature response and other climate metrics

While the present-day radiative forcing of the different components of the shipping emissions are useful to evaluate the impact of historical emissions on climate (up until present), they are not directly useful to evaluate impacts of present and future emissions on the future climate. As discussed in Fuglestvedt et al. (in this issue) there is not a unique correct way to do this, but it depends on how the long-term goals of a climate policy are determined. In the Kyoto Protocol to the UNFCCC it was decided to use the global warming potential with a 100 year time horizon (GWP$_{100}$) for this purpose (see Fuglestvedt et al. (in this issue) for definition and discussion of the GWP and other metrics). Recently Shine et al. (2005, 2007) have proposed a new emission metric, the global temperature change potential (GTP), that is designed to serve a policy consistent with a long-term climate target of constraining the global mean surface temperature increase below a threshold (e.g. the EU's target of keeping it below 2 °C above pre-industrial levels).

Due to the short-lived nature of many of the key components of shipping emissions there are several fundamental problems of applying global and annual averaged metric values to these components. However, they can be readily calculated from the global model simulations (Endresen et al., 2003; Eyring et al., 2007; Lauer et al., 2007). Table 8 shows the GWP$_{100}$, GTP$_{20}$, GTP$_{50}$, GTP$_{100}$ and CO$_2$ equivalent emissions for these metrics for the various components of the ship emissions and the range caused by

uncertainties in emissions and metric values. The time horizon of 50 years for the GTP metrics is used as that may be consistent with a time horizon of stabilizing global temperature increase. Details on input data and how the metrics are calculated are given in Fuglestvedt et al. (in this issue).

Both SO$_2$ and NO$_x$ emissions from shipping are found to cause cooling. Using the GWP$_{100}$ metric and including the large indirect effects on clouds found by Lauer et al. (2007) present-day ship emissions have negative CO$_2$ equivalent emissions. Note that this is supposed to represent an integrated effect between the time of emissions and the time horizon and does not imply that current ship emissions will have a cooling effect after 100 years. Indeed the CO$_2$ equivalent emissions using the GTP$_{50}$ metric indicate that after 50 years the net effect of current emissions is nearly neutral through cancellation of warming by CO$_2$ and cooling by sulphate and NO$_x$ (see Fuglestvedt et al. (in this issue) for further details on transport metrics). Berntsen and Fuglestvedt (2008) use a simple analytical climate model to calculate the time dependent contributions to global mean temperature change for current emissions from the different transport sectors. In the case of shipping their results for a 1 year emission pulse are consistent with the results from simple analysis using GTPs, in that NO$_x$ and SO$_2$ contribute to cooling, and that the long-term warming caused by CO$_2$ leads to a net warming after about 35 years.

6. Mitigation

The potential for emission reductions through technological improvements, alternative fuels and ship modifications is significant (Eyring et al., 2005b; ICCT, 2007). Several technologies and alternative fuels summarized in Section 6.1 could reduce ship emissions for both new and existing engines. Emissions control strategies for the shipping fleet have not been widely adopted in the absence of policy measures, making their ultimate performance across the fleet less certain. Policymakers are debating the trade-off between regulations that are technology-based (e.g. mandating emission reduction systems) or performance-based (e.g. requiring a level of control that may be achieved through alternate control measures; see Section 6.2). Another consideration is whether local mitigation policies (e.g. requiring emissions control in ports only) will result in behaviours that also meet regional and global pollution reduction objectives. While current legislation scenarios have already been discussed in Section 2.3, Section 6.3 assesses how possible improvements in technology or the use of alternative energies and fuels could impact on the future evolution of ship emissions.

6.1. Technology options, alternative fuels and energy

Here we provide a summary on technology options, alternative fuels and energy. More detailed reports, including how the various techniques reduce the emission indices and specific fuel consumption rates can be found in Corbett and Fischbeck (2002), Eyring et al. (2005b), and ICCT (2007).

6.1.1. Reduction of NO$_x$ emissions

NO$_x$ emissions are directly related to compression-ignition (diesel) combustion in marine engines. Marine diesel engines operate at low revolutions per minute (rpm), and therefore have very large cylinder volumes with diameters that routinely range from 20 to 90 cm and piston speeds as slow as 7 m per second (m s^{-1}) (Heywood, 1988; Harrington, 1992). Over the past 25 years, the power output per cylinder has more than doubled while specific fuel consumption has decreased by 25%, mainly through increased maximum firing pressure and better fuel injection
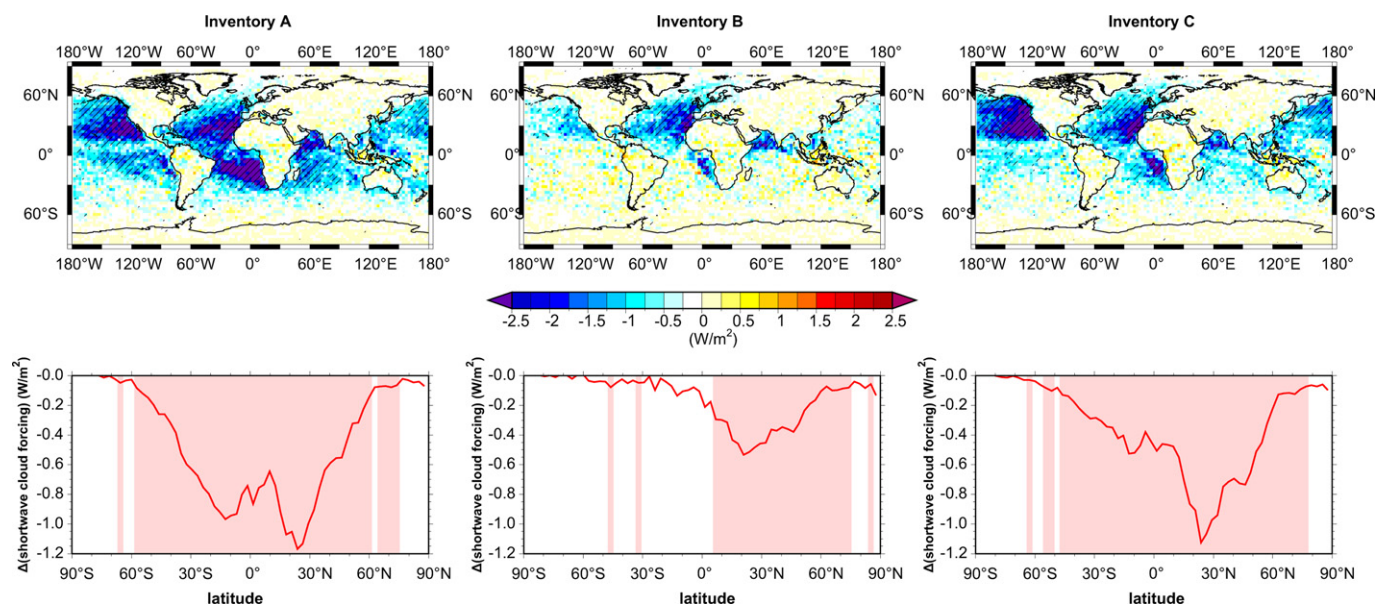
Fig. 15. Multi-year average of simulated changes in shortwave cloud forcing due to shipping at the top of the atmosphere (ToA) in W m^{-2}. Upper row shows the geographical distribution, lower row zonal averages. Hatched areas (upper row) and light-red shaded areas (lower row) show differences which are significant at the 99% confidence level compared to the inter-annual variability (from Lauer et al., 2007, their Fig. 11).

control, supercharging, and scavenging (Heywood, 1988). To be efficient, the fuel injected into large cylinders has to atomize and be well mixed with air before the long-duration power strokes. This combustion leads to higher peak temperatures and longer residence times, which cause marine engines to have typically higher NO_x emissions than other diesel engines (Carlton et al., 1995). The NO_x resulting from nitrogen bound in the heavy residual fuel used by oceangoing ships can also lead to higher NO_x emissions.

Technologies that reduce NO_x emissions can be divided into three groups (MAN B&W, 1996; European Commission and Entec UK Limited, 2005): those that require engine modifications (in engine controls), those that are implemented in the fuel or air system (pre-engine technologies), and those that are on the exhaust system (post-engine technologies). Pre-Engine technologies, e.g. include the addition of water to the diesel combustion process, which is a promising approach to reduce emissions, primarily NO_x. Any method of introducing water into the combustion space reduces the formation of NO_x by cutting temperature peaks in the engine cylinder. Techniques under this category include fuel water emulsification (FWE), humid air motor (HAM), and combustion air saturation system (CASS). In engine NO_x control strategies include aftercooler upgrades, engine derating, injection timing delays, fuel system modifications to increase supply pressure, diesel-electric propulsion and marine gas turbine propulsion. Post-engine technologies, e.g. include the selective catalytic reduction (SCR) for NO_x controls.

6.1.2. Reduction of SO_x and particulate matter emissions

SO_x emissions from ships are important precursors for aerosols and are determined by the sulphur content of the fuel. The most effective measure to reduce SO_x and particulate matter emissions from ships therefore is to lower the sulphur content in marine fuels. Due to predicted low sulphur fuel supply limitations and the high price premium of low sulphur marine fuel other options are considered. The scrubber option is receiving increasing attention as a cost-effective alternative (European Commission and Entec UK Limited, 2005). Due to seawater's natural alkalinity and the large quantities of sulphur already in it, seawater scrubbing is a versatile, readily available and cost-effective process. SO_2 reduction rates by seawater scrubber demonstrations show similar SO_2 reduction rates (between 65 and 94%) with 75–80% being sustainably achieved when operating the system within the existing design parameters. A diesel particulate filter system in the exhaust stream collects and stores particles, usually equipped with a means to burn off accumulated particulate with or without catalysts. Rated efficiencies in service with on-road distillate fuels range from 80% to more than 90% control of PM. The diesel oxidation catalyst (DOC) is designed to convert particulate matter that contains liquid hydrocarbons or soluble organic fractions through post-combustion oxidation. The reduction in overall PM emissions with a DOC is a function of the fraction of total PM that can be oxidized, generally 20–50% using on-road diesel fuels, probably 10–30% in marine applications.

Table 8
Emission metrics (GWP$_{100}$, GTP$_{20}$, GTP$_{50}$, GTP$_{100}$) and corresponding CO_2 equivalent emissions (in Tg (CO_2)/year for all metrics) for the various components of ship emissions. The range in the brackets represent the range caused by uncertainties in emissions and metric values. The metric values for SO_2 is given on SO_2 basis, while for NO_x it is given on N-basis (cf. Fuglestvedt et al., in this issue). Ranges for CO_2 emissions are taken from Table 7.

	GWP$_{100}$	GTP$_{20}$	GTP$_{50}$	GTP$_{100}$	CO_2-eq emissions (GWP$_{100}$-based)	CO_2-eq emissions (GTP$_{20}$-based)	CO_2-eq emissions (GTP$_{50}$-based)	CO_2-eq emissions (GTP$_{100}$-based)
CO_2	1	1	1	1	[501, 812]	[501, 812]	[501, 812]	[501, 812]
SO_2 (direct)	[−43, −11]	[−44, −11]	[−7.3, −1.8]	[−6.1, −1.5]	[−520, −75]	[−530, −75]	[−88, −12]	[−73, −10]
SO_2 (total)	[−480, −230]	[−380, −180]	[−63, −30]	[−53, −25]	[−5800, −1600]	[−4600, −1200]	[−760, −200]	[−640, −170]
NO_x	[−36, −25]	[−190, −130]	[−35, −30]	[−6.1, −4.2]	[−230, −73]	[−1240, −380]	[−230, −87]	[−40, −12]

6.1.3. Alternative fuels

There are a number of alternative fuels that can be used in marine service (National Research Council, 1980). Primary fuel sources are fossil fuels, petroleum, goal, and gas. Fuels derived from petroleum are commonly considered alternate marine fuels to heavy residual oil (marine bunkers). These include low sulphur residual fuels, marine distillates and blends (ISO, 1987). Coal-derived and gaseous fuels can be used in marine engines. Gaseous fuels can also be used in marine internal combustion engines (ICEs). The use of hydrogen diesel in large-bore diesel engines has been developed for high power densities and low exhaust gas emissions (Vogel, 1999). NO_x is the only pollutant of such an engine, but slightly more is produced than with marine distillate oil (MDO) or heavy fuel oil (HFO). This means NO_x reduction methods have to be applied, which, due to the relatively clean exhaust gas, work more efficiently. CO_2 is less than 2% of the CO_2 emission of a conventional diesel engine.

Bio-oils, such as palm oil, coconut oil, rapeseed oil, soya oil and others have been suggested as fuel for small low power combustion engines for many years. Within the last few years, the first tests with biofuels have been made with land-based medium-speed diesel engines in the power range of several MW, and the first few commercial biofuel engines have been sold already by manufacturers (Gros, 2002). Bio-diesel, defined as the mono alkyl esters of long-chain fatty acids derived from renewable lipid sources, offer some potential to reduce particulate matter and are being evaluated for their potential to reduce CO_2 emissions on a life-cycle basis (including carbon uptake during plant growth). However, only in recent years have bio-diesel gained commercial attention, primarily in land-based installations.

However, efforts to introduce alternative fuels in marine vessels have raised questions about the energy use and environmental impacts of such fuels. Understanding the true emissions from marine transportation requires a total fuel cycle analysis (TFCA). TFCA involves consideration of energy use and emissions from the extraction of raw fuel (e.g. oil from the ground) to the use of the processed fuel in the vessel itself. Each stage in the fuel cycle includes activities that produce GHG and criteria pollutant emissions. These emissions are typically caused by fuel combustion during a particular stage, although some non-combustion emissions occur (e.g. natural gas emissions from pipeline leaks, evaporative losses in refueling). The goal of a TFCA is to account for each of the emissions events along the entire fuel cycle. One approach to compare these multistage energy and emissions for ships is the Total Energy & Emissions Analysis for Marine Systems (TEAMS) model (Winebrake et al., 2007; Corbett and Winebrake, 2008). TEAMS captures "well-to-hull" emissions—that is, emissions along the entire fuel pathway, including extraction, processing, distribution, and use in vessels. TEAMS produces emissions estimates directly, not full impacts analyses; however, emissions estimated by TEAMS (or similar tools that are not intrinsically geospatial) at various stages in the fuel cycle can be geographically located, allowing impacts to be evaluated according to local environmental or social conditions.

6.1.4. Reduction of fuel consumption and CO_2

Optimization of various ship systems other than the engines such as propeller, rudder, and hull are promising options to reduce fuel consumption rates and, with them, GHG emissions (Maeda et al., 1998). The energy-reduction potential, and therefore the emission reduction potential, of an optimized hull shape and a better propeller for a new ship are estimated to be up to 30% (MARINTEK, 2000). Proper ship maintenance can ensure that the vessel operates efficiently (ICCT, 2007). The most effective way to reduce fuel consumption and GHG emissions from ships is reducing

and optimizing the vessel speed and adjust ship routes to avoid heavy wind (Skjølsvik et al., 2000).

In addition, alternative power systems or the combination of those with the traditional ship energy source could reduce GHG emissions from ships. A few commercial installations of fuel cells (FC) onboard very small ships are currently in use. Wind can be used as propellant for ships in two ways, as a power producer by wind turbines or as a thruster producer by sails or similar devices. Solar cells, as fuel cells, are the type of prime movers that produce energy without torque. They deliver voltage and the electrical current drives the motor which in turn drives the propeller of a ship. The advantages are no fuel consumption and no emission (Ahlqvist, 1999). Although already in use today for demonstration purposes on a few small boats, the disadvantage of solar panels today is their enormous price level and their size in order to provide an appropriate power density, but ongoing research and development might change this situation.

6.2. Policy strategies

Future emissions are influenced by the application of emission control measures. The maritime industry is at the centre of international attention due to increasing pressure to reduce emissions from marine vessels and port operations. Policymakers responded to these concerns by considering emissions reduction programs specifically for vessel and port activities. Policy instruments for achieving environmental objectives can be categorized into *command-and-control* approaches and *market-based* or *incentive-based* approaches. Policy measures to reduce ship emissions are briefly discussed here and detailed in Cofala et al. (2007) and ICCT (2007).

Command-and-control regulations achieve environmental management goals by setting uniform standards for sources of pollutants (Stavins, 2002). In market-based approaches, policy makers use market signals and economic incentives to encourage desired behaviour (Seik, 1996; Stavins, 2002; UNEP, 2002). These approaches are defined broadly by the U.S. EPA as instruments that use financial means to motivate polluters to reduce the health and environmental risks posed by their facilities, processes, or products (U.S. Environmental Protection Agency, 2001). There have been several studies conducted to evaluate the cost-effectiveness of different approaches for reducing ship emissions (Farrell et al., 2003; Kågeson, 1999; Swedish Shipowners' Association, 2002). These studies have largely argued that the regulatory approach on the shipping industry had not been very successful until 2002 (Swedish Shipowners' Association, 2002). In particular, there was no incentive for ships to invest in pollution control equipment – shipowners who invested in environmentally friendly equipment were at an economic disadvantage compared to those who did nothing (Volk et al., 2000). But now a number of direct and indirect incentives that support emissions reduction on ships are available (Coalition Clean Baltic et al., 2001; Volk et al., 2000). There are various types of regulatory instruments considered command-and-control, and the most prevalent regulatory instruments are technology and performance-based standards (Stavins, 2002). *Technology-based standards* specify the method, and sometimes the actual equipment, that firms must use to comply with a particular regulation. A *performance-based standard* sets a uniform control target for firms, while allowing some latitude in how this target is met. For example, the MARPOL Annex VI SECA requirements can be categorized as a performance-based regulation because ships can either switch to low sulphur fuel or use approved technology to reduce an equivalent amount of SO_2 emissions.

Market-based instruments encompass a range of policy tools from pollution taxes, charges, to marketable permits, to

government subsidies – all of which change poor environmental behaviour by changing the incentive structure for polluters (Panayotou, 1994; Stavins, 2002; UNEP, 2002). If well designed and implemented, market-based instruments have the potential to be more cost-effective than command-and-control regulations, because command-and-control measures set emissions targets/ limits for which cost-reducing measures apply where economic instruments often incentivize both cost-reducing and emissions reducing innovations (Harrington and Morgenstern, 2004). Economic incentives can also encourage polluters to control pollution above and beyond the level required by regulation, as well as spur technological innovation for pollution control technologies. Market-based instruments, e.g. include environmental differentiation of fairway and port fees, ship environment index system and differentiated tonnage tax (green tax), the green award foundation (GAF), and emission trading. Overall, there is increasing support for market-based instruments. For example, Europe is currently discussing whether shipping is going to be included into the EU emission trading scheme (EU ETS).

6.3. Assessment of mitigation scenarios

In coming decades, newly introduced policy measures could modify an unconstrained growth trend in energy use. In terms of technology, there could be further improvements in thermal efficiency, fuel type and quality, and propulsion design. Current international legislation scenarios have already been discussed in Section 2.3. Here we show how possible improvements in technology or the use of alternative energies and fuels could impact on the future evolution of ship emissions.

The vast majority of marine propulsion and auxiliary plants onboard oceangoing ships are diesel engines. In terms of the maximum installed engine output of all civilian ships above 100 GT, 96% of this energy is produced by diesel power. These engines typically have lifetimes of 30 years and more. Because of missing alternative propulsion systems with similar power density, prime costs and fuel efficiency, it is expected that diesel engines will not be replaced in the foreseeable future. Therefore, at least for a mid-term period (around 20 years), emission reduction of existing engines will be based on effective emission reduction technologies or changes in the fuel. On the other hand, it is hard to assess which of the alternative techniques or fuels discussed in Section 6.1 are likely to be in use on the long-term, for example in 2050. However, keeping in mind that the world's oil reserves are limited (British Petrol, 2004) and that first tests with alternative fuels and energies are already underway, a shift from a diesel-only fleet to a fleet that partly uses alternative fuels and energies in 2050 is likely.

Based on these assumptions, Eyring et al. (2005b) presented 16 emission scenarios through 2050 obtained by a mid-term prognosis for 2020 and a long-term prognosis for 2050. The scenarios are a combination of four future ship traffic demand scenarios and four technology scenarios. The future ship traffic demand scenarios are mainly determined by the economic growth, which follows the IPCC SRES storylines (see Section 2.3). The resulting fuel consumption is projected through extrapolations of historical trends in economic growth, total seaborne trade and number of ships, as well as the average installed power per ship. For the future technology scenarios they assume a diesel-only fleet in 2020 resulting in fuel consumption between 382 and 409 Mt. For 2050 one technology scenario assumes that 25% of the fuel consumed by a diesel-only fleet can be saved by applying future alternative propulsion plants, resulting in a fuel consumption that varies between 402 and 543 Mt. The other scenario is a business-as-usual scenario for a diesel-only fleet even in 2050 and gives an estimate between 536 and 725 Mt. Dependent on how rapid technology improvements for diesel engines are introduced, possible technology reduction factors are applied to the today's fleet-average emission factors. The study showed that future total ship emissions, especially NO_x and SO_x emissions will be mainly determined by the technology and to a lesser extent by the future global economic development. In future scenarios this means that the calculated total emissions are dominated by the chosen technology reduction rates, and to a lesser extent by the assumed annual growth in GDP and the factor by which the fuel consumption of a diesel-only fleet in 2050 is saved through application of alternative energies and fuels. With aggressive NO_x reduction, a significant decrease from 6.52 Tg(N) in 2001 to 0.94 Tg(N) could be reached by 2050, despite a growing fleet (see Fig. 6). On the other hand, if no further reduction techniques are applied and future diesel engines will be equipped with techniques that fulfil the current IMO regulations, a further significant increase has to be expected until 2050. Future SO_x emissions will mainly be determined by the sulphur content of the fuel. In their clean scenario they assumed an average sulphur content of 1% in 2020 and 0.5% in 2050, compared to 2.4% today. This reduces SO_x emissions from 6.0 Tg (SO_2) in 2001 to 1.8 Tg(S) by 2050. Future CO_2 emissions in these scenarios are on the other hand mainly determined by the total fuel consumption, which in turn is mainly determined by the economic growth and the amount of the fuel consumption that is saved by alternative energies and fuels. The estimates suggest CO_2 emissions between 1110 and 1188 Tg (CO_2) in 2020 and between 1109 and 2001 Tg (CO_2) in 2050.

Cofala et al. (2007) used the European Monitoring and Evaluation Programme (EMEP) model to run a base year 2000 and 240 emission control cases for the year 2020. The baseline scenario in 2020 outlines the effects of current legislation on emissions from shipping. At the other end the Maximum technically feasible reductions (MFR) scenario quantifies emissions, environmental effects and costs of implementing the best available control technology on international shipping. Between the baseline and the MFR scenario, different ambition level scenarios are presented. For example, the Ambition level 2 scenario assumes a sulphur content of 0.5% in residual oil or scrubbing equivalent (2 g SO_2/kWh) in SECA, and for passenger vessels everywhere. Regarding NO_x emissions, it is assumed that HAM for all new engines post-2010 are installed. Compared to 2000, emissions of SO_2 from international shipping are expected to increase till 2020 in the baseline scenario by 42%, and NO_x and $PM_{2.5}$ emissions by 47% and 55%, respectively. This growth is mainly related to the assumed increase in traffic volume, while the additional emission control measures that are considered in the baseline (i.e. sulphur controls according to the EU Marine Fuel Directive, MARPOL standards on new vessels) show only limited impact. Maximum technically feasible emission reductions would decline SO_2 and NO_x emissions by 78 and 89%, respectively. As a side effect of using low sulphur fuel, emissions of PM decrease by 15% compared with the baseline.

Dalsøren et al. (2007) complemented existing global sea transportation emission inventories with new regional emission data-sets and scenarios for ship traffic and coastal activity in 2015. The scenarios adopted for 2015 assumed 2% yearly increase in bunker fuel consumption for the existing (year 2000) global fleet, but took into account potential reductions in emissions of components regulated by ANNEX VI of MARPOL (e.g. assumed only 15% increase 2000–2015). In the SECA of the North Sea and the Channel it was assumed that the ships adhered to the ANNEX VI demanding a maximum sulphur content of fuel oil of 1.5%. Assuming no changes in other emissions, the increases in sea transportation resulted in more than 20% increase in NO_2 from 2000 to 2015 in some coastal areas.

All these scenario calculations show that ship emissions should be recognized as a growing problem for scientists, industry and environmental policy makers. Currently ship emissions are one of the least regulated sources of anthropogenic emissions with a high reduction potential through technological improvements, alternative fuels and ship modifications. The scenario calculations further demonstrate that significant reductions are needed to offset increased emissions due to growth in seaborne trade.

7. Future impacts on atmospheric composition and climate

Most studies that are available on possible atmospheric and climate impacts in the future focused on current legislation and some emission control scenarios in the nearer future (Section 7.1). Some studies also provided projections of impacts under the assumption of changing shipping patterns due to climate change (Section 7.2).

7.1. Projected changes for current legislation and emission control scenarios

The efficiency of ozone production from NO_x emissions decreases with increasing background NO_x concentration and with the magnitude of the emissions (e.g. Lin et al., 1988). Thus the impact of shipping might be expected to depend on the land-based emission scenario chosen. This was investigated by Collins et al. (2009) who found that the shipping contribution (at 2000 shipping levels) to European surface ozone in 2030 varied from 1.1 ppb with the highest land-based emissions (2030 SRES A2) to 2.6 ppb with the lowest land-based emissions (2030 IIASA MFR). The MFR scenario considers the scope for emission reductions offered by full implementation of the presently available emission control technologies, while maintaining the projected levels of anthropogenic activities. Similarly the effect of shipping on the global tropospheric ozone budget is smallest for the A2 land-based scenario and largest for the MFR (Fig. 16). This figure also shows a small decrease in ozone production efficiency with increasing magnitude of ship emissions, confirming earlier findings by Eyring et al. (2007). While the future level of shipping NO_x emissions is very uncertain (see scenario calculations in Fig. 6), a constant growth in shipping would offset some of the expected benefits in surface ozone pollution from land-based emission control legislation.

The effects of NO_x emissions on the OH concentrations, and hence methane lifetimes, are expected to be non-linear as was found for the ozone. Fig. 16 shows that the change in methane lifetime is largest when the land-based emissions are smallest (MFR), and that the change is less than linear in the ship NO_x emissions. Again, this confirms similar findings in Eyring et al. (2007).

Eyring et al. (2007) showed that under the assumption of a constant annual growth rate for ship emissions of 2.2% per year up to 2030 (CGS), shipping would significantly counteract the benefits derived from reducing SO_2 emissions from all other anthropogenic sources under the IPCC SRES A2 scenario over the continents by 2030, for example in Europe. Globally, shipping contributes 4.5% to increases in sulphate under A2/CGS until 2030. However, if future land-based emissions follow a more stringent scenario, the relative importance of ship emissions will be even higher. Using a future scenario for both land-based and shipping emissions in 2015 Dalsøren et al. (2007) found that the SO_2 concentrations increased less than linearly due to the increased oxidants.

The EMEP model simulations by Cofala et al. (2007) suggest that, at present, emissions from ships are responsible for 10–20% of sulphur deposition in coastal areas over Europe (see Fig. 17). Until 2020 their contribution is expected to increase to more than 30% in large areas along the coast in Europe in the baseline scenario. In many coastal areas, ships will be responsible for more than 50% of sulphur deposition. Emission controls on shipping will bring down the depositions to much lower levels.

7.2. Projected changes in shipping patterns

Emissions from shipping and fisheries may change due to climate change. Mostly studied is the potential opening of the Northern Sea Route (NSR) via the Barents Sea between Europe and the north Pacific Region, but also sea level rise and changes in the location and amounts of fish stocks may be of some importance. For none of these climate induced changes there has yet been established well founded emission scenarios.

The Arctic is now experiencing some of the most rapid climate changes on Earth. On average, the rate of temperature increase has been twice as high as for the rest of the world. Observations over the past 50 years show a decline in Arctic sea-ice extent throughout the year, with the most prominent retreat in summer. The melting of Arctic sea-ice will effectively unlock the Arctic Ocean area, leaving it increasingly open to human activity – particularly shipping and oil/gas production (IPCC, 2007; Serreze et al., 2007).

The trends indicate an Arctic Ocean with longer seasons of less sea-ice cover of reduced thickness, implying improved ship accessibility around the margins of the Arctic Basin. Climate models project an acceleration of this trend and opening of new shipping routes and extension of the period during which shipping is feasible. The seaborne cargo transport in these waters has previously been very limited, and the reported ship emissions low (PAME, 2000; Corbett et al., 1999; Endresen et al., 2003). The travel along the NSR can reduce travel time by up to 50%, compared to sea routes travelled today (Fritjof Nansen Institute, 2000). Thus, if the number of navigation days increases it is expected that more traffic will pass along this route.

It is expected that increased shipping traffic will result in increased air pollution burden in this area (AMAP, 2006) and changes in regional climate forcing. Granier et al. (2006) have used a global chemical tracer model, assuming that up to 11% of total ship emissions will occur in the Arctic. They find that the Arctic may experience summer concentrations of ozone two to three times the current value and comparable with those seen in many industrialized regions in the Northern hemisphere. On the other hand the change in ship routes may imply less shipping transport globally since the new routes are shorter, thus the new routes may imply a shift in emissions from other locations and saved fuel (and less emissions) for the same amount of goods transported, and consequently influencing long-range transport of air pollution. However, this also means that emissions may be shifted from less vulnerable regions to the Arctic. Increased air pollution and deposition in the Arctic is of particular concern because of the high vulnerability, and in the case of soot deposition as a climate feedback mechanism (Flanner et al., 2007).

Dalsøren et al. (2007) included estimates and developed inventories for expected new regional emissions not previously quantified. These additional datasets were found to be of significant importance for environmental assessments and the CTM results in northern regions. By 2015, more than 1500 tankers may export oil via the Barents Sea and the Northeast Atlantic to Europe and the US. Increased oil and gas export from the Norwegian sector is also likely and gas power plants are planned along the Norwegian coast. The NSR for international transit shipping operations to Asia today is limited but could become more important if infrastructure develops and if the ice thickness and coverage decrease due to regional warming. In 2015 the
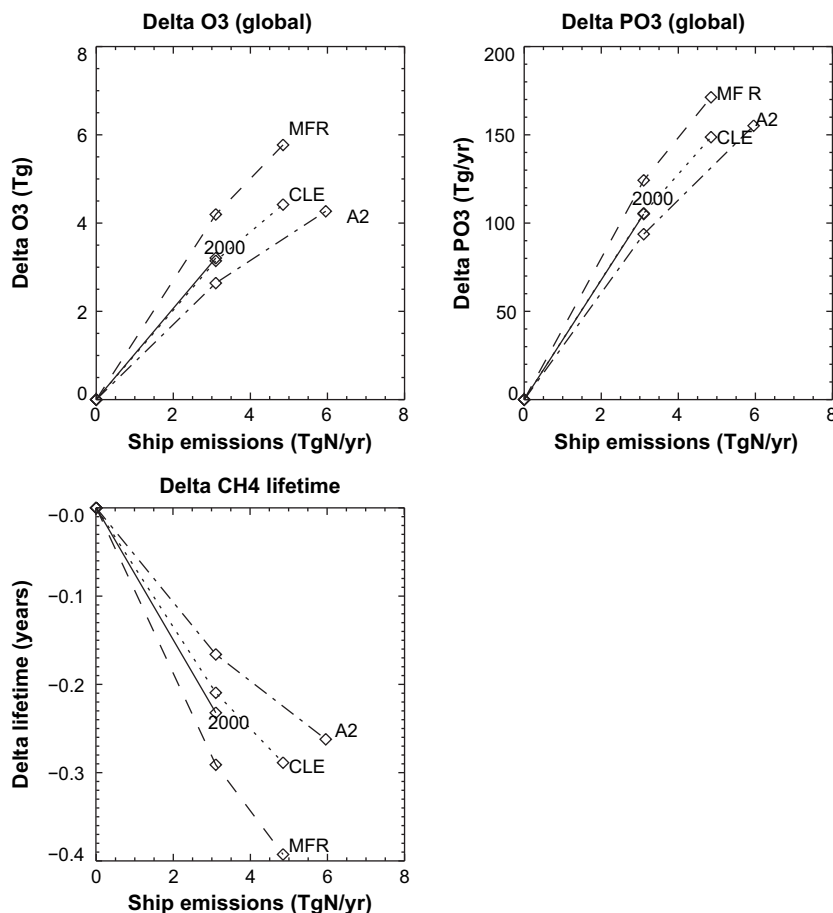
Fig. 16. Change in tropospheric ozone burden, production and methane lifetime for changes in ship emissions according to four land-based emission scenarios (from Collins et al. 2009, their Fig. 11; Reproduced by permission of Borntraeger and Cramer Science Publishers, http://www.borntraeger-cramer.de).

expected increase in activities were found to have significant effects at high-latitudes. A result of the increasing ship emissions could be an extended period where the critical loads for acidification in coastal areas are exceeded. A region suffering from high levels of sulphur is the Nikel–Passvik region located at the Norwegian–Russian border close to the expected oil and gas export areas and connected shipping routes. New coastal activities and sea transportation in 2015 increase the sulphur (and nitrate) deposition by about 4% in the region. New activity and resulting ship traffic in northern and Arctic areas may also have significant regional effects in coastal areas with low background pollution levels. Dalsøren et al. (2007) found increased particle amounts in the northern areas, and the contribution from ship traffic to Arctic haze could be increasing.

Significant changes in marine ecosystems are now observed that may partly be due to climate change (e.g. Grebmeier et al., 2006; Hobday et al., 2006). IPCC (2007) concludes: "There is high confidence, based on substantial new evidence, that observed changes in marine biological systems are associated with rising water temperatures, as well as related changes in ice cover, salinity, oxygen levels and circulation. These include shifts in ranges and changes in algal, plankton and fish abundance in high-latitude oceans". To what extent this will change emissions from the fishing fleet has not yet been estimated.

Sea level rise may leave some ports less useful and some low lying islands may become uninhabitable. Overall these changes are unlikely to cause major changes in the global emissions from shipping.

8. Summary and conclusions

Oceangoing shipping and resulting emissions produce significant impact on atmospheric composition and climate, and some impacts are dependent upon latitude and upon whether emissions occur in coastal areas or in the open oceans. We conclude that efforts to reduce CO_2 and other pollutants from ships would lead to considerable environmental benefit in light of the recent research that has identified: (1) the long-range transport and fate of these pollutants; (2) the impact of these pollutants on environment (e.g. acidification), human health, atmospheric composition and climate; and (3) the cost-effectiveness of reducing such pollutants in the context of alternative reduction options.

A variety of important results have been achieved in recent years. For example, the importance of ship emissions and the projected future increases were brought to the attention of the international community. Considering the different estimates reported, shipping moved 80–90% of world trade by volume within a bounded range of 560–1360 Tg CO_2/year. According to our best estimate, oceangoing shipping emitted around 780 Tg CO_2 in the year 2000, which corresponds to a fuel consumption of 250 Mt and a contribution of around 2.7% to all anthropogenic CO_2 emissions in 2000. In 2000, the current best estimates for the emissions released by the registered fleet for nitrogen oxides (NO_x), sulphur oxides (SO_x), and particulate matter (PM) are 5.4 Tg(N), 5.5 Tg(S), and 1.4 Tg(PM), respectively, within a bounded range of 3–10 Tg(N), 3–10 Tg(S) and 0.4–3.4 Tg(PM). Since 2000, annual growth rates in total seaborne trade have been
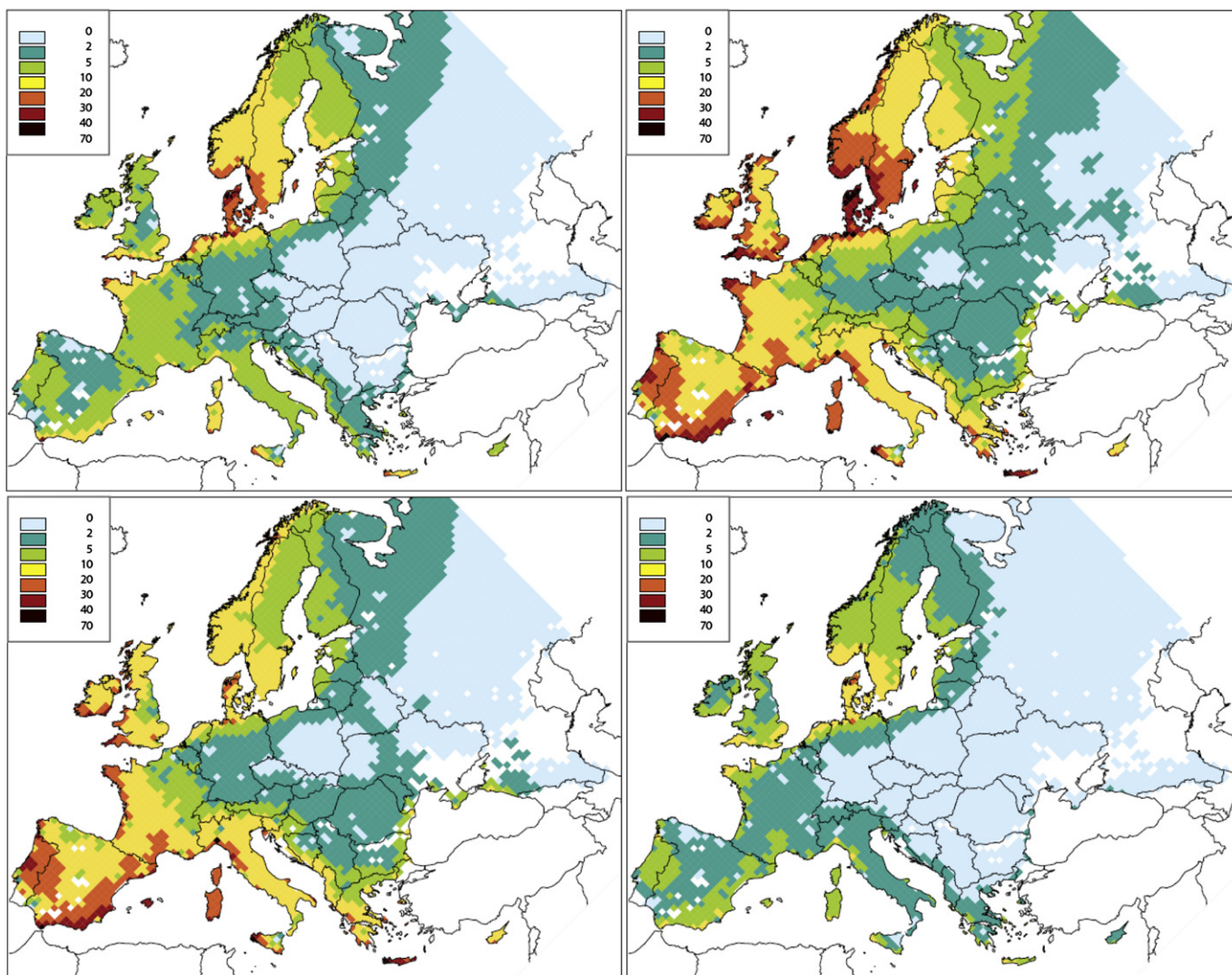
Fig. 17. Percent of sulphur deposition originating from international shipping in 2000 (upper left panel) and for the "Baseline" scenario in 2020 (upper right panel). Lower panels show the situation in 2020 for the Ambition level 2 and the Maximum technically feasible reduction scenarios (from Cofala et al., 2007, their Fig. 5.13).

higher than in the past (5.2% on average from 2002 to 2007) and accordingly the fuel consumption has increased significantly during this period as the total installed power increased by about 25%. Emission scenario calculations up to the year 2050 show that significant reductions would be needed to offset increased emissions due to the predicted growth in seaborne trade and cargo energy intensity. If no aggressive emission reduction strategies are introduced, CO_2 and SO_2 emissions from ships could double present-day values by 2050, and NO_x emissions could exceed the value of present-day global road transport.

Multiple studies and independent representations of shipping routes show that some 70% or more of emissions by oceangoing ships occurs within 400 km of land. Modelling and measurements of shipping emissions and their fate confirm that they may be transported hundreds of kilometres inland, and thus can contribute to air quality problems on land, even if they are emitted at sea. The long-range transport of ship emissions motivated the Task Force on Hemispheric Transport of Air Pollution (TF HTAP) working under the UNECE Convention on Long-range Transboundary Air Pollution (CLRTAP) to include ship emissions among sources relevant for the intercontinental transport of air pollution. Global models simulate NO_x increases over the northern Pacific,

Atlantic and Indian Oceans by 100–500 ppt, depending on the distribution of shipping emissions used, and ozone enhancements of up to 12 ppb in the central North Atlantic and central North Pacific in July due to the increased NO_x.

Shipping-related PM emissions could cause between 20,000 and 104,000 premature mortalities annually from cardiopulmonary disease and lung cancer in 2000, with a best estimate of 60,000. These health impacts are particularly concentrated in areas of Southeast Asia and Europe and might increase by 40% by 2012. The model results also show that increasing emissions from shipping would significantly counteract the benefits derived from reducing SO_2 emissions from land-based anthropogenic sources in several regions by 2030, e.g. over Europe. In many coastal areas, ships will be responsible for more than 50% of sulphur deposition by 2020, but emission controls on shipping could bring down the depositions to much lower levels. The possible opening of Arctic routes, e.g. the Northern Sea Route (NSR) via the Barents Sea between Europe and the north Pacific Region, as a result of projected ice melting in the future might increased air pollution and deposition in this region, which is of particular concern because of the high vulnerability, and in the case of soot deposition as a climate feedback mechanism.

In addition to the impact on atmospheric composition and human health, ship emissions have an impact on climate. For some of the compounds emitted from ships the radiative forcing (RF) is positive (CO_2, O_3 and BC) while for others the forcing is negative (direct effect of sulphate particles, reduced methane). The particles can also have an indirect effect on climate through their ability modify the optical properties of clouds by acting as cloud condensation nuclei (CCN) or by dissolving in the cloud drops and so change their surface tension. Of all anthropogenic sources, ship-stack effluents provide the clearest demonstration of the indirect aerosol effect on cloud albedo. Curves of larger reflectance in cloud fields, so called ship tracks, can be observed in satellite imagery as a recurrent phenomenon. One of the major findings in terms of climate impact was that particle emissions and their precursors from shipping can significantly modify the microphysical and optical properties of clouds (the so called "indirect aerosol effect"). Although the associated uncertainties are still high, the model results indicate that the cooling due to altered clouds far outweighs the warming effects from greenhouse gases such as carbon dioxide (CO_2) or ozone from shipping, overall causing a negative radiative forcing today. The indirect aerosol effect of ships on climate is found to be far larger than previously estimated contributing between 17 and 39% to the total indirect effect of anthropogenic aerosols, depending on the ship emission inventory used. This contribution is high because ship emissions are released in regions with frequent low marine clouds in an otherwise clean environment and the potential impact of particulate matter on the radiation budget is larger over the dark ocean surface than in polluted regions over land. Despite the wide range of RF values reported in different investigations, all studies agree that the present-day net RF due to shipping is negative, in contrast to, for instance, estimates of RF from aircraft. However, none of the studies on RF from shipping so far investigated the positive RF that could possibly occur from the interaction of BC with snow.

As this new research has indicated, reductions in sulphur emissions could result in regional reductions in its resultant negative radiative forcing. The climatic trade-off between positive and negative radiative forcing is still a topic of scientific research, but from what is currently known, a simple cancellation of global means is potentially inappropriate and a more comprehensive assessment metric is required. We emphasize, however, that CO_2 remains in the atmosphere for a long-time and will continue to have a warming effect long after its emission. In contrast, sulphate has a residence time in the atmosphere of approximately 10 days, and the climate response from sulphate is of the order decades whilst that of CO_2 is of the order of centuries. Indeed the CO_2 equivalent emissions using the global temperature change potential (GTP) metric indicate that after 50 years the net effect of current emissions is nearly neutral through cancellation of warming by CO_2 and cooling by sulphate and NO_x. While the control of NO_x, SO_2 and particle emissions from ships will have beneficial impacts on air quality, acidification and eutrophication, CO_2 reductions from all sources, including ships and other freight modes, will give the greatest long-term reduction in global warming.

Further work is needed to reach a complete synthesis of the impact of shipping on atmospheric composition and climate. Uncertainties in the simulated ozone contributions from ships with different model approaches are found to be significantly smaller than estimated uncertainties stemming from the ship emission inventory and the neglect of plume processes. This reflects that the net ozone change from ship emissions under relatively clean conditions in global models is rather similar and suggests that the atmospheric models are suitable tools to study these effects. However, there is considerable uncertainty in the ship emission inventories, which has to be further explored. One approach is to develop bottom-up inventories based on ship movement data and compare them with activity-based top-down approaches. Both emission totals and the geographical distribution are key parameters for the simulation of atmospheric impacts. The large differences in model results obtained with different ship emission inventories imply a high uncertainty in the input data.

From the point of view of large-scale composition impacts, there is not enough observational data to confirm or refute the various emission datasets used by global models. There are sound chemical reasons why spreading shipping plumes over the size of grid squares used by global models could overestimate the NO_x, OH and ozone responses. Plume model studies have not provided a simple reduction factor for the NO_x emissions that could be applied to global models. The step from case studies to a suitable parameterisation of subgrid-scale processes in global models has to be made for both gaseous and particulate emissions. To reach this, more measurements and model studies are needed to understand plume processes. Additional in situ measurements inside single ship plumes, but also in the corridor of the shipping lanes are required for different regions of the world to evaluate the global models' response to ship emissions. Unambiguous detection of NO_x emissions from ships in satellite data is currently only available for the region of the Red Sea and the Indian Ocean where shipping routes are close to the coastal area. Reduction in measurement uncertainties through use of long-term averages and data from more instruments (e.g. OMI and GOME-2) combined with better constraints on land-based sources and higher spatial resolution in the models should facilitate such an intercomparison in the future. The model studies also need to include different approaches than the ones applied so far. More work is needed on the thermodynamical parameters in the marine boundary layer (MBL) that control transport of ship effluent into the cloud layer, including large eddy simulations of the MBL stability, ship track buoyancy affected by fuel burning, and subcloud saturation conditions.

Current uncertainties of global modelling studies on the effects of emissions from shipping on aerosols and clouds are expected to be much higher than in the case of the ozone change studies. In particular the indirect aerosol effect depends crucially on simulated key properties such as the aerosol size-distribution and the activation of aerosol particles in clouds. Minor changes of these properties can have a significant impact on the simulated indirect effect. Furthermore, changes in cloud properties such as cloud liquid water content, cloud cover and precipitation due to ship emissions impact on atmospheric chemistry via wet deposition and changes in scavenging efficiency. Changes in atmospheric chemistry, e.g. ozone and OH concentrations, may result in a feedback on aerosols, e.g. via modified oxidation rates of SO_2. Further model development in particular on the representation of aerosol size-distribution, aerosol activation, aerosol–cloud interaction and extension of feedback mechanisms is needed in addition to extended measurement data, e.g. of the size-distribution and composition of particles emitted by ships to reduce current uncertainties in global model studies.

Despite the uncertainties discussed above, with respect to local pollutants such as particulate matter and sulphur emissions, mounting evidence shows that the benefits of emission reductions of these pollutants outweigh the costs of control for many regions of the globe. The net benefit of policy action to reduce ship emissions has been convincingly demonstrated, although the choice among a diverse set of policy strategies to achieve needed reduction targets may not be simple. Policymakers need to consider issues such as technological feasibility, economic efficiency, and total fuel cycle trade-offs. However, these considerations will help determine the appropriate and necessary policy response paths given the evidence that action is needed. Ongoing research efforts

will help filling the gaps in our scientific understanding and will continue to inform policymakers to help further implementing needed emission reduction and mitigation strategies.

Appendix A. Acronyms and abbreviations

AATSR	Advanced Along-Track Scanning Radiometer
ACE-1	Southern Hemisphere Aerosol Characterization Experiment
AIS	Automatic Identification System
AMAP	Arctic Monitoring and Assessment Programme (Norway)
AMVER	Automated Mutual-assistance Vessel Rescue System
ATTICA	Assessment of Transport Impacts on Climate Change and Ozone Depletion
AVHRR	Advanced Very High Resolution Radiometer
BC	Black Carbon
CASS	Combustion Air Saturation System
CCM	Chemistry-Climate Model
CCN	Cloud Condensation Nuclei
CGS	Constant Growth Scenario
CICERO	Centre for International Climate and Environmental Research (Norway)
CLRTAP	Convention on Long-Range Transboundary Air Pollution
COADS	Comprehensive Ocean-Atmosphere Data Set
CORINAIR	European Union Emission Inventory Programme
CTM	Chemical Transport Model
DLR	Deutsches Zentrum für Luft- und Raumfahrt (Germany)
DOC	Diesel Oxidation Catalyst
EC	European Commission
EDGAR	Environmental Database for Global Atmospheric Research
EEI	Effective Emission Index
EI	Emission Index
EMEP	European Monitoring and Evaluation Programme
ENTEC	Environmental and Engineering Consultancy
EU	European Union
EPA	Environmental Protection Agency
ETS	Emission Trading Scheme
FC	Fuel Cells
FWE	Fuel Water Emulsification
GAF	Green Award Foundation
GCM	General Circulation Model
GDP	Gross Domestic Product
GHG	Greenhouse Gas
GIS	Geographic Information System
GOME	Global Ozone Monitoring Experiment
GREEN TAX	Environmental Differentiation of Fairway and Port Fees, Ship Environment Index System and Differentiated Tonnage Tax
GT	Gross Tons
GTP	Global Temperature Change Potential
GTP20	Global Temperature Change Potential with a 20 year time horizon
GTP50	Global Temperature Change Potential with a 50 year time horizon
GTP100	Global Temperature Change Potential with a 100 year time horizon
GWP	Global Warming Potential
GWP100	Global Warming Potential with a 100 year time horizon
HAM	Humid Air Motor
HFO	Heavy Fuel Oil
HTAP	Task Force on Hemispheric Transport of Air Pollution
ICART-ITOP	International Consortium for Atmospheric Research on Transport and Transformation – Intercontinental Transport of Ozone and Precursors experiment
ICCT	International Council on Clean Transportation
ICE	Internal Combustion Engine
ICOADS	International Comprehensive Ocean-Atmosphere Data Set
IEA	International Energy Agency
IIASA	International Institute for Applied Systems Analysis (Austria)
IPCC	Intergovernmental Panel on Climate Change
IMF	International Monetary Fund
IMO	International Maritime Organization
ISO	International Organization for Standardization (Switzerland)
IVL	Swedish Environmental Research Institute (Sweden)
LES	Large Eddy Simulation
LMIS	Lloyd's Maritime Information System
LMIU	Lloyd's Marine Intelligence Unit
LOSU	Level Of Scientific Understanding
LRIT	Long-Range Identification and Tracking
LWP	Liquid Water Path
MARPOL	International Convention for the Prevention of Pollution from Ships
MARINTEK	Norwegian Marine Technology Research Institute
MAST	Monterey Area Ship Track
MBL	Marine Boundary Layer
MDO	Marine Distillate Oil
MFR	Maximum technically Feasible Reductions
Mt	Million metric tons
NAMBLEX	North Atlantic Marine Boundary Layer Experiment
NMVOC	Non Methane Volatile Organic Carbon
NOAA	National Oceanic and Atmospheric Administration (USA)
NSR	Northern Sea Route
OCD	Offshore and Coastal Dispersion Model
OECD	Organisation for Economic Co-operation and Development
OMI	Ozone Monitoring Instrument
PF	Purple Finder
PM	Particulate Matter
POM	Particulate Organic Matter
QUANTIFY	Quantifying the Climate Impact of Global and European Transport System
RF	Radiative Forcing
SCIAMACHY	SCanning Imaging Absorption SpectroMeter for Atmospheric CHartographY
SCR	selective catalytic reduction
SEAF	Ship Emissions Allocations Factors
SECA	Sulphur Emission Control Area
SRES	Special Report on Emissions Scenarios
SST	Sea Surface Temperature
STEEM	Waterway Network Ship Traffic, Energy and Environment Model
TEAMS	Total Energy & Emissions Analysis for Marine Systems
TF	Task Force
TFCA	Total Fuel Cycle Analysis
TREMOVE	Transport and Emissions Simulation Model
TST	Total Seaborne Trade
UNCTAD	United Nations Conference on Trade and Development
UNECE	United Nations Economic Commission for Europe
UNEP	United Nations Environment Programme
UNFCCC	United Nations Framework Convention on Climate Change
USCG	United Coast States Guard
USEPA	United States Environmental Protection Agency
VOC	Volatile Organic Carbon
WMO	World Meteorological Organization

References

Ackerman, A.S., Toon, O.B., Hobbs, P.V., 1995. Numerical modeling of ship tracks produced by injections of cloud condensation nuclei into marine stratiform clouds. Journal of Geophysical Research 100, 7121–7133. doi:10.1029/95JD00026.

Ahlqvist, I., 1999. The Future for the Diesel-electric Mode in Cruise Ship and Ferry Propulsion Paper Presented at Cruise + Ferry 1999 Conference, London, 11–13 May.

Albrecht, B.A., 1989. Aerosols, cloud microphysics, and fractional cloudiness. Science 245, 1227–1230.

AMAP, 2006. AMAP Assessment 2006: Acidifying Pollutants, Arctic Haze, and Acidification in the Arctic. Arctic Monitoring and Assessment Programme (AMAP), Oslo, Norway, xii + 112 pp.

Arya, S.P., 1988. Introduction to Micrometeorology. In: International Geophysics Series, 42. Academic Press, 307 pp.

Ashmore, M., 2005. Assessing the future global impacts of ozone on vegetation. Plant, Cell and Environment 28, 949–964.

Beirle, S., Platt, U., von Glasow, R., Wenig, M., Wagner, T., 2004. Estimate of nitrogen oxide emissions from shipping by satellite remote sensing. Geophysical Research Letters 31, L18102. doi:10.1029/2004GL020312.

Berntsen, T., Fuglestvedt, J., 2008. Global temperature responses to current emissions from the transport sectors. Proceedings of the National Academy of Sciences USA 105, 19154–19159.

Buhaug, Ø., Corbett, J.J., Endresen, Ø., Eyring, V., Faber, J., Hanayama, S., Lee, D.S., Lindstad, H., Mjelde, A., Pålsson, C., Wanquing, W., Winebrake, J.J., Yoshida, K., 2008. Updated Study on Greenhouse Gas Emissions from Ships: Phase I Report. International Maritime Organization (IMO), London, UK, 1 September, p. 129.

California Air Resources Board, 2006. Appendix A: Quantification of the Health Impacts and Economic Valuation of Air Pollution from Ports and Goods Movement in California. California Air Resources Board. 3/22/2006.

Campmany, E., Grainger, R.G., Dean, S.M., Sayer, A.M., 2009. Automatic detection of ship tracks in ATSR-2 satellite imagery. Atmospheric Chemistry and Physics 9 (6), 1899–1905.

Canepa, E., Georgieva, E. (Eds.), 2005. Proc. of the 1st Int. Conference on Harbours & Air Quality, ISBN 88-89884-00-2 Genoa, Italy, June 15–17, 2005.

Capaldo, K., Corbett, J.J., Kasibhatla, P., Fischbeck, P.S., Pandis, S.N., 1999. Effects of ship emissions on sulphur cycling and radiative climate forcing over the ocean. Nature 400, 743–746.

Carlton, J.S., Danton, S.D., et al., 1995. Marine Exhaust Emissions Research Programme. Lloyd's Register Engineering Services, London, U.K.

Carpenter, L.J., Liss, P.S., Penkett, S.A., 2003. Marine organohalogens in the atmosphere over the Atlantic and Southern Oceans. Journal of Geophysical Research 108 (D9), 4256. doi:10.1029/2002JD002769.

Ceuster, G.D., v. Herbruggen, B., Logghe, S., 2006. TREMOVE: Description of Model and Baseline Version 2.41. Transport & Mobility Leuven, European Commission, Brussels, Belgium.

Charlson, R.J., Lovelock, J.E., Andreae, M.O., Warren, S.G., 1987. Oceanic phytoplancton, atmospheric sulphur, cloud albedo and climate. Nature 326, 655–661.

Charnock, H., 1955. Wind stress on a water surface. Quarterly Journal of the Royal Meteorological Society 81, 639–640.

Chen, G., Huey, L.G., Trainer, M., Nicks, D., Corbett, J.J., Ryerson, T., Parrish, D., Neuman, J.A., Nowak, J., Tanner, D., Holloway, J., Brock, C., Crawford, J., Olson, J.R., Sullivan, A., Weber, R., Schauffler, S., Donnelly, S., Atlas, E., Roberts, J., Flocke, F., Hubler, G., Fehsenfeld, F., 2005. An investigation of the chemistry of ship emission plumes during ITCT 2002. Journal of Geophysical Research 110, D10S90. doi:10.1029/2004JD005236.

Clarkson, 2004. Shipping Review & Outlook, Clarkson Research Studies. Spring.

Climate Mitigation Services, 2006. In: Report Commissioned by Environmental Defense Center (Ed.), LNG Supply Chain GHG Emissions: Australia to California. Climate Mitigation Services, Snowmass, CO, 48 pp.

Coakley Jr., J.A., Borstein, R.L., Durkee, P.A., 1987. Effect of ship-stack effluents on cloud reflectivity. Science 237, 1020–1022.

Coalition Clean Baltic, WWF Baltic Programme, et al., 2001. NGO Stockholm Declaration. Second Conference on Sustainable Transport Solutions in the Baltic Sea Area II – Focus on Maritime Transport. Naturskyddsföreningen i Stockholms län, Stockholm.

Cofala, J., Amann, M., Heyes, C., Klimont, Z., Posch, M., Schöpp, W., Tarasson, L., Jonson, J., Whall, C., Stavrakaki, A., 2007. Final Report: Analysis of Policy Measures to Reduce Ship Emissions in the Context of the Revision of the National Emissions Ceilings Directive. March 2007. International Institute for Applied Systems Analysis, Laxenburg, Austria, , p. 74.

Cohen, A.J., Anderson, H.R., Ostro, B., Pandey, K.D., Krzyzanowski, M., Künzli, N., Gutschmidt, K., Pope, A., Romieu, I., Samet, J.M., Smith, K., 2005. The global burden of disease due to outdoor air pollution. J. Toxicol. Environ. Health, Part. A 68, 1301–1307.

Collins, W.J., Sanderson, M.G., Johnson, C.E., 2009. Impact of increasing ship emissions on air quality and deposition over Europe by 2030. Meteorologische Zeitschrift, Meteorologische Zeitschrift 18 (1), pp. 25–39(15).

Conover, J.H., 1966. Anomalous cloud lines. Journal of Atmospheric Science 23, 778–785.

Cooper, D., 2002. Representative Emission Factors for Use in Quantification of Emissions from Ships Associated with Ship Movements between Port in the European Community. IVL Swedish Environmental Research Institute Ltd (ENV.C.1/ETU/2001/0090), May.

Corbett, J.J., Fischbeck, P.S., 1997. Emissions from ships. Science 278 (5339), 823–824.

Corbett, J.J., Fischbeck, P.S., 2002. Commercial marine emissions and life-cycle analysis of retrofit controls in a changing science and policy environment. Naval Engineers Journal, 93–106.

Corbett, J.J., Köhler, H.W., 2003. Updated emissions from ocean shipping. Journal of Geophysical Research 108. doi:10.1029/2003JD003751.

Corbett, J.J., Köhler, H.W., 2004. Considering alternative input parameters in an activity-based ship fuel consumption and emissions model: reply to comment by Øyvind Endresen et al. on "Updated emissions from ocean shipping". Journal of Geophysical Research 109, D23303. doi:10.1029/2004JD005030.

Corbett, J.J., Winebrake, J.J., 2008. Emissions tradeoffs among alternate marine fuels: total fuel cycle analysis of residual oil, marine gas oil and marine diesel oil. Journal of the Air and Waste Management Association 58 (4), 538–542.

Corbett, J.J., Fischbeck, P.S., Pandis, S.N., 1999. Global nitrogen and sulphur inventories for oceangoing ships. Journal of Geophysical Research 104 (3), 3457–3470.

Corbett, J.J., Firestone, J., Wang, C., 2007a. Estimation, Validation, and Forecasts of Regional Commercial Marine Vessel Inventories, Final Report for the California Air Resources Board and the California Environmental Protection Agency and for the Commission for Environmental Cooperation in North America, ARB Contract Number 04–346.

Corbett, J.J., Winebrake, J.J., Green, E.H., Kasibhatla, P., Eyring, V., Lauer, A., 2007b. Mortality from ship emissions: a global assessment. Environmental Science & Technology 41 (24), 8512–8518. doi: 10.1021/es071686z.

Cotton, W., Alexander, G., Hertenstein, R., McAnelly, Walko, R., Nicholls, M., 1995. Cloud venting – a review and some new global annual estimates. Earth Science Reviews 39, 169–206.

Dalsøren, S.B., Endresen, Ø., Isaksen, I.S.A., Gravir, G., Sørgård, E., 2007. Environmental impacts of the expected increase in sea transportation, with a particular focus on oil and gas scenarios for Norway and northwest Russia. Journal of Geophysical Research 112, D02310. doi:10.1029/2005JD006927.

Davis, D.D., Grodzinsky, G., Kasibhatla, P., Crawford, J., Chen, G., Liu, S., Bandy, A., Thornton, D., Guan, H., Sandholm, S., 2001. Impact of ship emissions on marine boundary layer NO_x and SO_2 distributions over the Pacific Basin. Geophysical Research Letters 28, 235–238.

Denman, K.L., Brasseur, G., Chidthaisong, A., Ciais, P., Cox, P.M., Dickinson, R.E., Hauglustaine, D., Heinze, C., Holland, E., Jacob, D., Lohmann, U., Ramachandran, S., da Silva Dias, P.L., Wofsy, S.C., Zhang, X., 2007. Couplings between changes in the climate system and biogeochemistry. In: Solomon, S., Qin, D., Manning, M., Chen, Z., Marquis, M., Averyt, K.B., Tignor, M., Miller, H.L. (Eds.), Climate Change 2007: the Physical Science Basis. Contribution of Working Group I to the Fourth Assessment Report of the Intergovernmental Panel on Climate Change. Cambridge University Press, Cambridge, United Kingdom and New York, NY, USA.

Dentener, F., Kinne, S., Bond, T., Boucher, O., Cofala, J., Generoso, S., Ginoux, P., Gong, S., Hoelzemann, J.J., Ito, A., Marelli, L., Penner, J.E., Putaud, J.P., Textor, C., Schulz, M., van der Werf, G.R., Wilson, J., 2006. Emissions of primary aerosol and precursor gases in the years 2000 and 1750, prescribed data-sets for AeroCom. Atmospheric Chemistry and Physics 6, 4321–4344.

Derwent, R.G., Stevenson, D.S., Doherty, R.M., Collins, W.J., Sanderson, M.G., Johnson, C.E., Cofala, J., Mechler, R., Amann, M., Dentener, F.J., 2005. The contribution from ship emissions to air quality and acid deposition in Europe. Ambio 34 (1), 54–59.

Derwent, R.G., Stevenson, D.S., Doherty, R.M., Collins, W.J., Sanderson, M.G., Johnson, C.E., 2008. Radiative forcing from surface NO_x emissions: spatial and seasonal variation. Climatic Change DOI: 10.1007/s10584-007-9383-8.

Devasthale, A., Krüger, O., Graßl, H., 2006. Impact of ship emissions on cloud properties over coastal areas. Geophysical Research Letters 33, L02811. doi:10.1029/2005GL024470.

Devotta, S., et al., 2006. IPCC/TEAP Special Report "Safeguarding the Ozone Layer and the Global Climate System: Issues Related to Hydrofluorocarbons and Perfluorocarbons" (Chapter 4): Refrigeration.

Dickerson, R.R., Rhoads, K.P., Carsey, T.P., Oltmans, S.J., Burrows, J.P., Crutzen, P.J., 1999. Ozone in the remote marine boundary layer: a possible role for halogens. Journal of Geophysical Research 104, 21385–21395.

Doney, S.C., Mahowald, N., Lima, I., Feely, R.A., Mackenzie, F.T., Lamarque, J.-F., Rasch, P.J., 2007. Impact of anthropogenic atmospheric nitrogen and sulfur deposition on ocean acidification and the inorganic carbon system. Proceedings of the National Academy of Sciences USA 104 (37), 14580–14585.

Dore, A.J., Vieno, M., Tang, Y.S., Dragosits, U., Dosio, A., Weston, K.J., Sutton, M.A., 2006. Modelling the atmospheric transport and deposition of sulphur and nitrogen over the United Kingdom and assessment of the influence of SO_2 emissions from international shipping. Atmospheric Environment 41, 2355–2367.

Durkee, P.A., Chartier, R.E., Brown, A., Trehubenko, E.J., Rogerson, S.D., Skupniewicz, C., Nielsen, K.E., Platnick, S., King, M.D., 2000a. Composite ship track characteristics. Journal of Atmospheric Science 57, 2542–2553.

Durkee, P.A., Noone, K.J., Bluth, R.T., 2000b. The Monterey ship track experiment. Journal of Atmospheric Science 57, 2523–2541.

Durkee, P.A., Noone, K.J., Ferek, R.J., Johnson, D.W., Taylor, J.P., Garrett, T.J., Hobbs, P.V., Hudson, J.G., Bretherton, C.S., Innis, G., Frick, G.M., Hoppel, W.A., O'Dowd, C.D., Russel, L.M., Gasparovic, R., Nielsen, K.E., Tessmer, S.A., Öström, E., Osbourne, S.R., Flagan, R.C., Seinfeld, J.H., Rand, H., 2000c. The impact of ship-produced aerosols on the microstructure and albedo of warm marine stratocumulus clouds: a test of MAST hypothesis 1i and 1ii. Journal of Atmospheric Science 57, 2554–2569.

Edson, J.B., Fairall, C.W., 1998. Similarity relationships in the marine atmospheric surface layer for terms in the TKE and scalar variance budgets. Journal of Atmospheric Science 55, 2311–2328.

EMEP/CORINAIR, 2002. Emission Inventory Guidebook – 3rd Edition October 2002 UPDATE. European Environment Agency, Copenhagen, Denmark. Technical Report No 30, Shipping Activities – Sub Sector 0804.

Emmons, L.K., Hauglustaine, D.A., Muller, J.F., Carroll, M.A., Brasseur, G.P., Brunner, D., Staehelin, J., Thouret, V., Marenco, A., 2000. Data composites of airborne observations of tropospheric ozone and its precursors. Journal of Geophysical Research 105, 20,497–20,538.

Endresen, Ø., Sørgård, E., Sundet, J.K., Dalsøren, S.B., Isaksen, I.S.A., Berglen, T.F., Gravir, G., 2003. Emission from international sea transportation and environmental impact. Journal of Geophysical Research 108, 4560. doi:10.1029/2002JD002898.

Endresen, Ø., Sørgård, E., Bakke, J., Isaksen, I.S.A., 2004. Substantiation of a lower estimate for the bunker inventory: comment on "Updated emissions from ocean shipping" by James J. Corbett and Horst W. Köhler. Journal of Geophysical Research 109, D23302. doi:10.1029/2004JD004853.

Endresen, Ø., Bakke, J., Sørgård, E., Berglen, T.F., Holmvang, P., 2005. Improved modelling of ship SO_2 emissions – a fuel based approach. Atmospheric Environment 39, 3621–3628.

Endresen, Ø., Sørgård, E., Behrens, H.L., Brett, P.O., Isaksen, I.S.A., 2007. A historical reconstruction of ships fuel consumption and emissions. Journal of Geophysical Research 112, D12301. doi:10.1029/2006JD007630.

EPA (Environmental Protection Agency, U.S.A.), 2000. Analysis of Commercial Marine Vessels Emission and Fuel Consumption Data. Rep. EPA420-R-00–002, February 2000, web site:. Office of Transportation and Air Quality http://www.epa.gov/otaq/models/nonrdmdl/c-marine/r00002.pdf.

EPA (Environmental Protection Agency), 2002. Control of emissions of air pollution from new marine compression–ignition engines at or above 30 liters/cylinder; proposed rule. In: 40 CFR Part 94, vol. 67. U.S. Environmental Protection Agency, Washington, DC. 37548–37608.

EPA (Environmental Protection Agency, U.S.A.), 2006. SPECIATE 3.2, Profiles of Total Organic Compounds and Particulate Matter. http://www.epa.gov/ttn/chief/software/speciate/index.html.

Esler, J.G., 2003. An integrated approach to mixing sensitivities in tropospheric chemistry: a basis for the parameterization of subgrid-scale emissions for chemistry transport models. Journal of Geophysical Research 108 (D20), 4632. doi:10.1029/2003JD003627.

European Commission and ENTEC UK Limited, 2002. Quantification of Emissions from Ships Associated with Ship Movements between Ports in the European Community. European Commission. DG ENV.C1, Rue de la Loi, 200, B-1049: Brussels, Belgium.

European Commission and Entec UK Limited, 2005. Service Contract on Ship Emissions: Assignment, Abatement and Market-based Instruments Task 2b and C – NO_x and SO_2 Abatement.

Eyring, V., Köhler, H.W., van Aardenne, J., Lauer, A., 2005a. Emissions from international shipping: 1. The last 50 years. J. Geophys. Res. 110, D17305. doi:10.1029/2004JD005619.

Eyring, V., Köhler, H.W., Lauer, A., Lemper, B., 2005b. Emissions from international shipping: 2. Impact of future technologies on scenarios until 2050. Journal of Geophysical Research 110, D17306. doi:10.1029/2004JD005620.

Eyring, V., Stevenson, D.S., Lauer, A., Dentener, F.J., Butler, T., Collins, W.J., Ellingsen, K., Gauss, M., Hauglustaine, D.A., Isaksen, I.S.A., Lawrence, M.G., Richter, A., Rodriguez, J.M., Sanderson, M., Strahan, S.E., Sudo, K., Szopa, S., van Noije, T.P.C., Wild, O., 2007. Multi-model simulations of the impact of international shipping on atmospheric chemistry and climate in 2000 and 2030. Atmospheric Chemistry and Physics 7, 757–780.

Fairall, C.W., Helmig, D., Ganzeveld, L., Hare, J., 2007. Water-side turbulence enhancement of ozone deposition to the ocean. Atmospheric Chemistry and Physics 7, 443–451.

Farrell, A., Redman, D.H., Corbett, J.J., Winebrake, J.J., 2003. Comparing air pollution from ferry and landside commuting. Transportation Research D: Energy and Environment 8 (5), 343–360.

Fearnleys, 2003. Fearnleys World Bulk Trades 2003 An Analysis of 2002 With 2003 Update, Oslo.

Fearnleys, 2004. Fearnleys Review 2003. The Tanker and Bulk Markets and Fleets, Oslo.

Fearnleys, 2007. Fearnleys Review 2007. The Tanker and Bulk Markets and Fleets, Oslo.

Ferek, R.J., Garrett, T., Hobbs, P.V., Strader, S., Johnson, D., Taylor, J.P., Nielsen, K., Ackermann, A.S., Kogan, Y., Liu, Q., Albrecht, B.A., Babb, D., 2000. Drizzle suppression in ship tracks. Journal of Atmospheric Science 57, 2707–2728.

Flanner, M.G., Zender, C.S., Randerson, J.T., Rasch, P.J., 2007. Present day climate forcing and response from black carbon in snow. Journal of Geophysical Research 112, D11202. doi:10.1029/2006JD008003.

Fleming, Z.L., Monks, P.S., Rickard, A.R., Heard, D.E., Bloss, W.J., Seakins, P.W., Still, T.J., Sommariva, R., Pilling, M.J., Morgan, R., Green, T.J., Brough, N., Mills, G.P., Penkett, S.A., Lewis, A.C., Lee, J.D., Saiz-Lopez, A., Plane, J.M.C., 2006. Peroxy radical chemistry and the control of ozone photochemistry at Mace Head, Ireland during the summer of 2002. Atmospheric Chemistry and Physics 6, 2193–2214.

Forster, P., Ramaswamy, V., Artaxo, P., Berntsen, T., Betts, R., Fahey, D.W., Haywood, J., Lean, J., Lowe, D.C., Myhre, G., Nganga, J., Prinn, R., Raga, G., Schulz, M., Van Dorland, R., 2007. Changes in atmospheric constituents and in radiative forcing. In: Solomon, S., Qin, D., Manning, M., Chen, Z., Marquis, M., Averyt, K.B., Tignor, M., Miller, H.L. (Eds.), Climate Change 2007: the Physical Science Basis. Contribution of Working Group I to the Fourth Assessment Report of the Intergovernmental Panel on Climate Change. Cambridge University Press, Cambridge, United Kingdom and New York, NY, USA.

Franke, K., Eyring, V., Sander, R., Hendricks, J., Lauer, A., Sausen, R., 2008. Toward effective emissions of ships in global models. Meteorologische Zeitschrift 17 (2), pp. 117–129(13).

Fridell, E., Norrman, J., Sternhufvud C., 2006. Formulation of Environmental Legislation for Transports – How the Expansion Possibility of Enterprises Would Be Affected, Report B1707, www.ivl.se, publicationservice@ivl.se.

Fritjof Nansen Institute (FNI), 2000. Northern Sea Route Cargo Flows and Infrastructure-Present State and Future Potential. FNI REPORT 13/2000. Fritjof Nansen Institute, Pbox 326, N-1326, Norway, ISBN 82-7613-400-9.

Fuglestvedt, J.S., Berntsen, T., Myhre, G., Rypdal, K., Bieltvedt Skeie, R., 2007. Climate forcing from the transport sectors. Proceedings of the National Academy of Sciences USA 105, 454–458.

Fuglestvedt, J.S., Shine, K.P., Berntsen, T., Cook, J., Lee, D.S., Stenke, A., Skeie, R.B., Velders, G.J.M., Waitz, I.A. Transport impacts on atmosphere and climate: metrics. Atmospheric Environment, in this issue.

Galloway, J.N., Aber, J.D., Erisman, J.W., Seitzinger, S.P., Howarth, R.W., Cowling, E.B., Cosby, B.J., 2003. The nitrogen cascade. BioScience 53, 341–356.

Garratt, J.R.D., 1977. Review of drag coefficients over oceans and continents. Monthly Weather Review 105, 915–929.

von Glasow, R., Lawrence, M.G., Sander, R., Crutzen, P.J., 2003. Modeling the chemical effects of ship exhaust in the cloud-free marine boundary layer. Atmospheric Chemistry and Physics 3, 233–250.

Granier, C., Niemeier, U., Jungclaus, J.H., Emmons, L., Hess, P., Lamarque, J.F., Walters, S., Brasseur, G.P., 2006. Ozone pollution from future ship traffic in the Arctic northern passages. Geophysical Research Letters 33, L13807. doi:10.1029/2006GL026180.

Grebmeier, J.M., Overland, J.E., Moore, S.E., Farley, E.V., Carmack, E.C., Cooper, L.W., Frey, K.E., Helle, J.H., McLaughlin, F.A., McNutt, S.L., 2006. A major ecosystem shift in the northern Bering Sea. Science 311 (5766), 1461–1464. doi: 10.1126/science.1121365.

Gros, V., 2002. Bio-oils for diesel engines. Wärtsilä Energy News 15, December.

Gunner, T., 2007. Shipping, CO2 and Other Air Emissions. http://www.eionet.europa.eu/training/bunkerfuelemissions Technical workshop meeting on emissions from aviation and maritime transport, Oslo, October 2007.

Hanna, S.R., Schulman, L.L., Paine, R.J., Pleim, J.E., Baer, M., 1985. Development and evaluation of the offshore and coastal dispersion model. Journal of Air Pollution Control Association 35, 1039–1047.

Hansen, J., et al., 2005. Efficacy of climate forcings. Journal of Geophysical Research 110, D18104. doi:10.1029/2005JD005776.

Hansen, J., Nazarenko, L., 2004. Soot climate forcing via snow and ice albedos. Proceedings of the National Academy of Sciences USA 101, 423–428. doi:10.1073/pnas.2237157100.

Harrington, R.L. (Ed.), 1992. Marine Engineering. Society of Naval Architects and Marine Engineers, Jersey City, NJ.

Harrington, W., Morgenstern, R.D., 2004. Choosing environmental policy: comparing instruments and outcomes in the United States and Europe. In: Harrington, Winston, Morgenstern, Richard D., Sterner, Thomas (Eds.). Resources for the Future, Washington, DC, p. 283.

Heywood, J.B., 1988. Internal Combustion Engine Fundamentals. McGraw-Hill, Inc, New York, NY.

Hobbs, P.V., Garrett, T.J., Ferek, R.J., Strader, S.R., Hegg, D.A., Frick, G.M., Hoppel, W.A., Gasparovic, R.F., Russell, L.M., Johnson, D.W., O'Dowd, C., Durkee, P.A., Nielsen, K.E., Innis, G., 2000. Emissions from ships with their respect to clouds. Journal of Atmospheric Science 57, 2570–2590.

Hobday, A.J., Okey, T.A., Poloczanska, E.S., Kunz, T.J., Richardson, A.J. (Eds.), 2006. Impacts of Climate Change on Australian Marine Life: Part A. Executive Summary Report to the Australian Greenhouse Office, Canberra, Australia. September, 2006.

Hooper, W.P., James, E.J., 2000. Lidar observations of ship plumes. Journal of Atmospheric Science 57, pp. 2649–2566.

Hoor, P. et al. The effects of traffic emissions on the current state of the atmosphere: results from QUANTIFY. Atmospheric Chemistry and Physics Discussion, in preparation.

ICCT (The International Council on Clean Transportation), 2007. Air pollution and greenhouse gas emissions from ocean-going ships: impacts. Mitigation Options and Opportunities for Managing Growth.

ICF Consulting, 2005. Best Practices in Preparing Port Emission Inventories: Draft for Review, Prepared for Office of Policy, Economics and Innovation. United States Environmental Protection Agency, Fairfax, Virginia. 39.

IEA (International Energy Agency), 2003. World Energy Statistics and Balances, 2003 ed..

IEA (International Energy Agency), 2006. World Energy Statistics and Balances, 2006 ed..

IMF, 2004. International Monetary Fund, World Economic Outlook. http://www.imf.org.

International Maritime Organization (IMO), 1992. IMO sub-Committee on Bulk Materials, 22nd Session, Agenda Item 7, Ref.code IMO, BCH 22/INF.10. IMO, London.

International Maritime Organization (IMO), 1998. Regulations for the Prevention of Air Pollution from Ships and NO_x Technical Code, ANNEX VI of MARPOL 73/78 London.

IPCC, 2007. Climate change 2007: impacts, adaptation and vulnerability. Contribution of Working Group II to the Fourth Assessment Report of the Intergovernmental Panel on Climate Change. In: Parry, M.L., Canziani, O.F., Palutikof, J.P., van der Linden, P.J., Hanson, C.E. (Eds.). Cambridge University Press, Cambridge, UK, p. 976.

ISL, 1994. Shipping Statistics Yearbook 1994. Institute of Shipping Economics and Logistics, Bremen, Germany (December).

ISO, 1987. International Standard, Petroleum Products – Fuels (Class F) – Specifications of Marine Fuels. International Organization for Standardization, Geneva, Switzerland.

Johnsson, H.K., Höjstrup, J., Vested, H.J., Larsen, S.E., 1998. On the dependence of sea surface roughness on wind waves. Journal of Physical Oceanography 28, 1702–1716.

Jonson, J.E., Tarason, L., Bartnicki, J., 2000. Effects of International Shipping on European Pollution Levels, EMEP/MSC-W, Note 5/2000. Norwegian Meteorological Institute, Oslo, Norway.

Kågeson, P., 1999. Economic Instruments for Reducing Emissions from Sea Transport. Swedish NGO Secretariat on Acid Rain, The European Federation for

Transport and Environment (T&E) and the European Environmental Bureau (EEB), Göteborg, Sweden and Brussels, Belgium.

Kasibhatla, P., Levy II, H., Moxim, W.J., Pandis, S.N., Corbett, J.J., Peterson, M.C., Honrath, R.E., Frost, G.J., Knapp, K., Parrish, D.D., Ryerson, T.B., 2000. Do emissions from ships have a significant impact on concentration of nitrogen oxides in the marine boundary layer? Geophysical Research Letters 27 (15), 2229–2233.

Keuken, M., Wesseling, J., Van den Elshout, S., Hermans, L., 2005. Impact of shipping and harbour activities on air quality – a case study in the Rijmond Area (Rotterdam). In: Canepa, E., Georgieva, E. (Eds.), Proc. of the 1st Int. Conference on Habours & Air Quality, ISBN 88-89884-00-2 Genova, Italy, June 15–17, 2005.

Koch, D., Hansen, J., 2005. Distant origins of Arctic black carbon: a Goddard Institute for space studies model experiment. Journal of Geophysical Research 110, D04204. doi:10.1029/2004JD005296.

Kvalevåg, M.M., Myhre, G., 2007. Human impact on direct and diffuse solar radiation during the industrial era. Journal of Climate 20, 4874–4883.

Lack, D., Lerner, B., Granier, C., Baynard, T., Lovejoy, E., Massoli, P., Ravishankara, A.R., Williams, E., 2008. Light absorbing carbon emissions from commercial shipping. Geophysical Research Letters 35, L13815. doi:10.1029/2008GL033906.

Lauer, A., Eyring, V., Hendricks, J., Jöckel, P., Lohmann, U., 2007. Effects of oceangoing shipping on aerosols and clouds. Atmospheric Chemistry and Physics 7, 5061–5079.

Lawrence, M.G., Crutzen, P.J., 1999. Influence of NO_x emissions from ships on tropospheric photochemistry and climate. Nature 402, 167–170.

Lee, D.S., Lim, L.L., Eyring, V., Sausen, R., Endresen, Ø., Behrens, H.L., 2007. Radiative forcing and temperature response from shipping. In: Proceedings of the International Conference on Transport, Atmosphere and Climate (TAC). Oxford, UK, pp. 208–213.

Lee, D.S., Pitari, G., Grewe, V., Gierens, K., Penner, J.E., Petzold, A., Prather, M., Schumann, U., Bais, A., Iachetti, D., Berntsen, T., Lim L.L., Sausen, R. Transport impacts on atmosphere and climate: aviation. Atmospheric Environment, in this issue.

Levelton Consultants Ltd, 2006. Marine Emission Inventory Study Eastern Canada and Great Lakes – Interim Report 4: Gridding Results Prepared for: Transportation Development Centre Transport Canada.

Lin, X., Trainer, M., Liu, S.C., 1988. On the nonlinearity of the tropospheric ozone production. Journal of Geophysical Research 93 (D12), 15879–15888. doi:10.1029/88JD03750.

Liu, S.C., Trainer, M., Fehsenfeld, F.C., Parrish, D.D., Williams, E.J., Fahey, D.W., Hübler, G., Murphy, P.C., 1987. Ozone production in the rural troposphere and the implications for regional and global ozone distributions. Journal of Geophysical Research 92 (D4), 4191–4207.

Lloyd's Register of Shipping (LR), 1995. Marine Exhaust Emissions Research Programme. Lloyd's Register Engineering Services, UK, London.

Lloyd's Maritime Information System (LMIS), 2002. The Lloyd's Maritime Database (CD-ROM). Lloyd's Register–Fairplay Ltd., London.

Lloyd's Register Fairplay (LRF), 2006. Extracts from the World Merchant Fleet Database for 2001 to 2006 (All Civil Oceangoing Cargo and Passenger Ships above or Equal To 100 GT). provided by Lloyd's, UK.

Maeda, K., Matsuhita, H., Kanaoka, H., Suetsugu, T., 1998. Reduction methods of NOx emissions from ships. Bulletin of the Marine Engineering Society in Japan 26, 1.

MARINTEK, 2000. Study of Greenhouse Gas Emissions from Ships – Final Report to the International Maritime Organization. Norwegian Marine Technology Research Institute, MARINTEK, Trondheim, Norway (March).

Marmer, E., Langmann, B., 2005. Impact of ship emissions on the Mediterranean summertime pollution and climate: a regional model study. Atmospheric Environment 39, 4659–4669.

McCulloch, A., Lindley, A.A., 2003. From mine to refrigeration: a life cycle inventory analysis of the production of HFC-134a. International Journal of Refrigeration 26 (8), 865.

National Research Council, 1980. U.S. Commission on Sociotechnical Systems, and Maritime Transportation Research Board, Alternative Fuels for Maritime Use. National Academy of Sciences, Washington, D.C, 191 pp.

O'Dowd, C.D., Hämeri, K., Mäkelä, J.M., Pirjola, L., Kulmala, M., Jennings, S.G., Berresheim, H., Hansson, H.C., de Leeuw, G., Allen, A.G., Hewitt, C.N., Jackson, A., Viisanen, Y., Hoffmann, T., 2002. A dedicated study of new particle formation and fate in the coastal environment (PARFORCE): overview of objectives and initial achievements. Journal of Geophysical Research 107, 8108. doi:10.1029/2001000555.

Olivier, J.G.J., Peters, J.A.H.W., 1999. International Marine and Aviation Bunker Fuel: Trends, Ranking of Countries and Comparison with National CO2 Emissions. RIVM.

Olivier, J.G.J., Bloos, J.P.J., Berdowski, J.J.M., Visschedijk, A.J.H., Bouwman, A.F., 1999. A 1990 global emission inventory of anthropogenic sources of carbon monoxide on 1×1 degree developed in the framework of EDGAR/GEIA. Chemosphere: Global Change Science 1, 1–17.

Olivier, J.G.J., Berdowski, J.J.M., Peters, J.A.H.W., Bakker, J., Visschedijk, A.J.H., Bloos, J.P.J., 2001. Applications of EDGAR. Including a Description of EDGAR 3.0: Reference Database with Trend Data for 1970–1995. RIVM, Bilthoven. RIVM report no. 773301 001/ NOP report no. 410200 051.

PAME, 2000. The Norwegian Maritime Directorate and the Norwegian Ministry of Environment, PAME – Snap Shot Analysis of Maritime Activities in the Arctic, 2000 REPORT NO. 2000–3220.

Panayotou, T., 1994. Economic Instrument for Environmental Management and Sustainable Development. United Nations Environment Programme (UNEP) Environment and Economics Unit (EEU).

Petry, H., Hendricks, J., Mollhoff, M., Lippert, E., Meier, A., Ebel, A., Sausen, R., 1998. Chemical conversion of subsonic aircraft emissions in the dispersing plume:

calculation of effective emission indices. Journal of Geophysical Research 103, 5759–5772.

Petzold, A., Weinzierl, B., Huntrieser, H., Stohl, A., Real, E., Cozic, J., Fiebig, M., Hendricks, J., Lauer, A., Law, K., Roiger, A., Schlager, H., Weingartner, E., 2007. Experimental studies on particle emissions from cruising ship, their characteristic properties, transformation and atmospheric lifetime in the marine boundary layer. Atmospheric Chemistry and Physics Discussion 7, 15105–15154.

Piccot, S.D., Beck, L., Srinivasan, S., Kersteter, S.L., 1996. Global methane emissions from minor anthropogenic sources and biofuel combustion in residential stoves. Journal of Geophysical Research 101 (D17), pp. 22757–22276.

Pszenny, A.A.P., Moldanova, J., Keene, W.C., Sander, R., Maben, J.R., Martinez, M., Crutzen, P.J., Perner, D., Prinn, R.G., 2004. Halogen cycling and aerosol pH in the Hawaiian marine boundary layer. Atmospheric Chemistry and Physics 4, 147–168.

Radke, L.F., Coakley Jr., J.A., King, M.D., 1989. Direct and remote sensing observations of the effects of ships on clouds. Science 346, 1146–1149.

Ramana, M.V., Krishnan, P., Nair, S.M., Kunhikrishnan, P.K., 2004. Thermodynamic structure of the atmospheric boundary layer over the Arabian sea and the Indian ocean during pre-INDOEX and INDOEX-FFP campaigns. Annales Geophysicae 22, 2679–2691.

Reynolds, G., Endresen, Ø, 2002. Ship emission and discharge inventories, marine science and technology for environmental Sustainability. ENSUS 2002, 16–18 (December).

Richter, A., Eyring, V., Burrows, J.P., Bovensmann, H., Lauer, A., Sierk, B., Crutzen, P.J., 2004. Satellite measurements of NO_2 from international shipping emissions. Geophysical Research Letters 31, L23110. doi:10.1029/2004GL020822.

Rogers, R.R., Yau, M.K., 1989. A Short Course in Cloud Physics. Pergamon Press, 293 pp.

Russell, L., Lenschow, D., Laursen, K., Krummel, P., Siems, S., Bandy, A., Thornton, D., Bates, T., 1998. Bidirectional mixing in an ACE 1 marine boundary layer overlain by a second turbulent layer. Journal of Geophysical Research 103 (D13), 16411–16432.

Sausen, R., Isaksen, I.S.A., Grewe, V., Hauglustaine, D.A., Lee, D.S., Myhre, G., Köhler, M.O., Pitari, G., Schumann, U., Stordal, F., Zerefos, C., 2005. Aviation radiative forcing in 2000: an update on IPCC (1999). Meteorologische Zeitschrift 14, 555–561.

Schlager, H., Baumann, R., Lichtenstern, M., Petzold, A., Arnold, F., Speidel, M., Gurk, C., Fischer, H., 2008. Aircraft-based trace gas measurements in a primary European ship corridor. In: Proceedings of the International Conference on Transport. Atmosphere and Climate (TAC), Oxford, UK, pp. 83–88.

Schlager, H., Pacyna, J., 2004. International conventions on aviation, shipping and coastal pollution Chapter 4 of the GMES-GATO Strategy Report, European Commission Air Pollution Series No.82, EUR 21154, ISBN: 92-894-4734-6.

Schreier, M., Kokhanovsky, A.A., Eyring, V., Bugliaro, L., Mannstein, H., Mayer, B., Bovensmann, H., Burrows, J.P., 2006. Impact of ship emissions on the microphysical, optical and radiative properties of marine stratus: a case study. Atmospheric Chemistry and Physics 6, 4925–4942.

Schreier, M., Mannstein, H., Eyring, V., Bovensmann, H., 2007. Global ship track distribution and radiative forcing from 1-year of AATSR-data. Geophysical Research Letters 34, L17814. doi:10.1029/2007GL030664.

Segrin, M.S., Coakley Jr., J.A., Tahnk, W.R., 2007. MODIS observations of ship tracks in summertime stratus off the west coast of the United States. Journal of Atmospheric Sciences doi: 10.1175/2007JAS2308.1.

Seik, F.T., 1996. Urban environmental policy – the use of regulatory and economic instruments in Singapore. Habitat International 20 (1), 5–22.

Seinfeld, J.H., Pandis, S.N., 1998. Atmospheric Chemistry and Physics – from Air Pollution to Climate Change. John Wiley & Sons, Inc., New York.

Serreze, M.C., Holland, M.M., Stroeve, J., 2007. Perspectives on the Arctic's shrinking sea-ice cover. 16 March 2007. Science 315 (5818), 1533–1536. doi: 10.1126/science.1139426.

Shindell, D.T., Faluvegi, G., Bell, N., Schmidt, G., 2005. An emissions-based view of climate forcing by methane and tropospheric ozone. Geophysical Research Letters 32, L04803. doi:10.1029/2004GL021900.

Shine, K.P., Berntsen, T.K., Fuglestvedt, J.S., Sausen, R., 2005. Scientific issues in the design of metrics for inclusion of oxides of nitrogen in global climate agreements. Proceedings of the National Academy of Sciences USA 102, 15768–15773.

Shine, K.P., Berntsen, T.K., Fuglestvedt, J.S., Bieltvedt Skeie, R., Stuber, N., 2007. Comparing the climate effect of emissions of short- and long-lived climate agents. Philosophical Transactions of the Royal Society A 365, 1903–1914.

Sinha, P., Hobbs, P.V., Yokelson, R.J., Christian, T.J., Kirchstetter, T.W., Bruintjes, R., 2003. Emissions of trace gases and particles from two ships in the southern Atlantic Ocean. Atmospheric Environment 37, 2139–2148.

Skjølsvik, K.O., Andersen, A.B., Corbett, J.J., Skjelvik, J.M., 2000. Study of Greenhouse Gas Emissions from Ships. MEPC 45/8 Report to International Maritime Organization on the Outcome of the IMO Study on Greenhouse Gas Emissions from Ships. MARINTEK Sintef Group, Carnegie Mellon University, Center for Economic Analysis, and Det Norske Veritas, Trondheim, Norway.

Song, C.H., Chen, G., Hanna, S.R., Crawford, J., Davis, D.D., 2003. Dispersion and chemical evolution of ship plumes in the marine boundary layer: investigation of $O_3/NO_y/HO_x$ chemistry version. Journal of Geophysical Research 108, 4143. doi:10.1029/2002JD002216.

Stavins, R.N., 2002. Experience with Market-Based Environmental Policy Instruments. Resources for the Future.

Stevens, C.J., Dise, N.B., Mountford, J.O., Gowing, D.J., 2004. Impact of nitrogen deposition on the species richness of grasslands. Science 303, 1876–1879.

Stopford, M., 1997. Maritime Economics. CRC Press. ISBN 0203442660, 9780203442661.

Sullivan, P.P., McWilliams, J.C., Melville, W.K., 2004. The oceanic boundary layer driven by wave breaking with stochastic variability. I: direct numerical simulations. Journal of Fluid Mechanics 507, 143–174.

Swedish Shipowners' Association, 2002. Proposal of emissions trading scheme of sulphur dioxide and nitrogen, Swedish Shipowners' Association.

Taylor, J.P., Glew, M.D., Coakley Jr., J.A., Tahnk, W.R., Platnick, S., Hobbs, P.V., Ferek, R.J., 2000. Effects of aerosols on the radiative properties of clouds. Journal of Atmospheric Science 57, 2656–2670.

Thomas, R., Lauretis, R.D., Fontelle, J.P., Hill, N., Kilde, N., Rypdal, K., 2002. Shipping activities, Chapter B842. In: Lavender, K., Reynolds, G., Webster, A., Rypdal, K. (Eds.), EMEP/CORINAIR Emission Inventory Guidebook – October 2002 UPDATE. European Environment Agency, Copenhagen, Denmark.

Times Books, 1992. The Times Atlas of the World Comprehensive, nineth ed. London.

Twomey, S., Howell, H.B., Wojciechowski, T.A., 1968. Comments on Anomalous cloud lines. Journal of Atmospheric Science 25, 333–334.

Uherek, E., Halenka, T., Balkanski, Y., Berntsen, T., Borken-Kleefeld, J., Borrego, C., Gauss, M., Hoor, P., Juda-Rezler, K., Lelieveld, J., Melas, D., Rypdal, K., Schmid, S. Transport impacts on atmosphere and climate: land transport, Atmospheric Environment, in this issue.

UNCTAD, 2007. Review of Maritime Transport, 2006. United Nations, New York and Geneva. http://www.unctad.org/Templates/Page.asp?intItemID=2618&lang=1.

UNEP, 2002. Economic Instruments for Environmental Protection. UNEP Briefs on Economics, Trade and Sustainable Development, 2004. http://www.unep.ch/etu/publications/UNEP_Econ_Inst.PDF From.

UNFCCC and Subsidiary Body for Scientific and Technological Advice, Methodological Issues Relating to Emissions from International Aviation and Maritime Transport; Note by the Secretariat, 2004. United Nations Framework Convention on Climate Change. Subsidiary Body for Scientific and Technological Advice, Bonn, Germany, p. 11.

U.S. Department of Transportation, Bureau of Transportation Statistics, 2003. U.S. International Trade and Freight Transportation Trends BTS03-02, Washington, DC.

U.S. Environmental Protection Agency, 2001. The United States Experience with Economic Incentives for Protecting the Environment. EPA, Office of Policy, Economics, and Innovation, Office of the Administrator, Washington, DC, U.S. 230.

Vogel, C., 1999. Hydrogen diesel engine with direct injection, high power density and low exhaust gas emissions. Motortechnische Zeitschrift 60 (10).

Vogt, R., Crutzen, P.J., Sander, R., 1996. A mechanism for halogen release from sea-salt aerosol in the remote marine boundary layer. Nature 383, 327–330.

Volk, B., Hader, G.A., Zachcial, M., 2000. Incentive-based Instruments for Environmentally Acceptable Sea Transportation. Institute of Shipping Economics and Logistics, Bremen.

Wang, C., Corbett, J.J., 2005. Geographical characterization of ship traffic and emissions. Transportation research record. Journal of the Transportation Research Board 1909, 90–99.

Wang, C., Corbett, J.J., Firestone, J., 2007. Improving spatial representation of global ship emissions inventories. Environmental Science & Technology doi: 10.1021/es0700799.

Wang, C., Corbett, J.J., Firestone, J., 2008. Modeling energy use and emissions from north American shipping: application of ship traffic, energy and environment model. Environmental Science & Technology 42 (1), 193–199.

Wild, O., Prather, M.J., Akimoto, H., 2001. Indirect long-term global radiative cooling from NO_x emissions. Geophysical Research Letters 28 (9), 1719–1722.

Williams, E., Lerner, B., Quinn, P., Bates, T., 2005. Measurements of Gas and Particle Emissions from Commercial Marine Vessels. American Geophysical Union. Fall Meeting 2005, Abstract A51E-0130.

Winebrake, J.J., Corbett, J.J., Meyer, P.E., 2007. Energy use and emissions from marine vessels: a total fuel cycle approach. Journal of Air and Waste Management 57, 102–110.

Wismann, T., Oxbol, A., 2005. Emissions from ships in port. In: Canepa, E., Georgieva, E. (Eds.), Proc. of the 1st Int. Conference on Habours & Air Quality Genova, Italy, June 15–17, 2005, ISBN: 88-89884-00-2.

Woodfield, M., Rypdal, K., 2003. Atmospheric Emission Inventory Guidebook. European Environmental Agency, Copenhagen, Denmark.

Wu, J., 1980. Wind-stress coefficients over sea surface near neutral conditions – a revisit. Journal of Physical Oceanography 10, 727–740.

Zeebroeck, B.V., Ceuster, G.D., Herbruggen, B.V., 2006. TREMOVE 2: maritime model and runs. In: TRANSPORT & MOBILITY LEUVEN (Ed.). European Commission, Brussels, Belgium.